Engineering LuxR-type Quorum Sensing Proteins For New Functions

by

Nicholas Andrew DeLateur

B.S. Chemistry, Northeastern University (2012)
M.S. Chemistry, Northeastern University (2013)

Submitted to the Department of Chemistry
in partial fulfillment of the requirements for the degree of

Doctor of Philosophy in Chemistry

at the

MASSACHUSETTS INSTITUTE OF TECHNOLOGY

September 2019

Signature redacted

Author .....
Department of Chemistry
August 16, 2019

Certified by... Signature redacted .....
Ron Weiss, PhD
Professor of Biological Engineering and EECS
Signature redacted Thesis Supervisor

Accepted by ....
Robert W. Field, PhD
Haslam and Dewey Professor of Chemistry
Chairman, Department Committee on Graduate Theses

Engineering LuxR-type Quorum Sensing Proteins For New Functions

by

Nicholas Andrew DeLateur

Submitted to the Department of Chemistry
on August 16, 2019, in partial fulfillment of the
requirements for the degree of
Doctor of Philosophy in Chemistry

Abstract

Bacteria communicate information in a process known as quorum sensing, actuating downstream gene expression based on cell-cell signalling. Cell-cell signalling allows for complex and multi-cellular behavior otherwise impossible with unicellular logic. However, building complex cell-cell signalling genetic circuits is currently challenged by a lack of tools for the fine-tuning and control of quorum sensing systems.

Although derived from distinct biochemical entities, the diffusion rate and expression profile of a given LuxR-family module are not modular. Here, we develop chimeric proteins that can accept the small molecule cognate belonging to the *las* operon from *Pseudomonas aeruginosa* while activating the cognate promoter of other quorum sensing systems. The ability to swap in a modular fashion the ligand-binding domain and DNA-binding domain of transcription factors allows precise control of diffusion rates and expression profiles independently.

Methods to control quorum sensing by transcriptional repression can be slow because they rely on dilution and degradation, require promoter engineering, or lack specificity against only a single signalling pathway. Here, we develop proteins to knock down expression from LuxR-type quorum sensing transcription factors utilizing molecular sequestration for fast, tunable, and specific control. Natural sequesters and engineered truncation proteins are successfully applied against 5 of the most prevalent LuxR-type transcription factors (LasR, LuxR, RhlR, RpaR, and TraR) as well as the chimeric transcription factors developed in this work.

Chimeric LuxR-type quorum sensing proteins and proteins for the sequestration of LuxR-type quorum sensing proteins provide powerful new parts to facilitate building sophisticated gene circuitry.

Thesis Supervisor: Ron Weiss, PhD
Title: Professor of Biological Engineering and EECS

Acknowledgments

I am blessed and beyond privileged to live a life full of people who have helped me reach where I am now, and I wish to acknowledge a non-exhaustive list of those people below[1].

There are many things I could acknowledge about Ron, but for the sake of brevity I wish to highlight 3 (an arbitrarily chosen number). First, Ron accepts all those who come to his lab hoping to engage in synthetic biology regardless of background. The Weiss lab includes those from biology, biological engineering, chemical engineering, chemistry, medicine, computer science, mechanical engineering, and architecture. This philosophy allowed me to join the lab and additionally surrounded me with others who could provide different viewpoints from myself which enriched my experience here, and for that I am grateful. Second, the priority has always been whether a project is scientifically interesting more than it was scientifically publishable, a sentiment that I share and appreciate. The question is always "what interesting constructs can we build with this" rather than "where can we publish this" and I can't imagine being in a lab where that is inverted, so for that I am grateful. Third, with apologies to gatekeeping, Ron loves data like a true scientist. Nothing brings more joy to a meeting than a fresh set of plots to scrutinize and the never ending sense of drive and appreciation for fresh data creates an environment that encourages exploration and a sense of purpose, and for that I am grateful.

I wish to thank my other committee members Brad Pentelute, Alex Shalek, and Jim Collins for their selfless time and feedback. One of my largest regrets of my time here was not engaging with my committee more, all of which was on me. My committee has always had nothing but my best interests at heart and in deed and for that I am grateful. Brad Pentelute I must single out for always pushing me to be better than the previous time we met since my first week at MIT and asking not only about research but me as a person during each annual check-in.

Bureaucracy is not exactly my strong suit and it is by the grace of the Department

[1]In addition to these acknowledgements, whatever the opposite of an acknowledgement is I bestow upon Chipotle for giving me food poisoning in 2018.

of Chemistry Education Office that I am still here. In particular Jennifer Weisman has been an unending fount of wisdom, suggestions, solutions, and help from everything from TA assignments, RA assignments, qualifying exams, thesis defense, room reservations, consulting conflicts, and general graduate school solutions.

Kristine, Olga, and Cammie made everything run in the Weiss lab which cannot be overstated as a feat. I wish to thank Ky for both scientific and career discussions as well as allowing me to use much of the Lu Lab instrumentation when needed (one of the perils of being the sole bacteria researcher in a mammalian lab).

My first year at MIT was made possible in no small part by being surrounded by an exclusively excellent group of people: the biological division entering class of 2013. Without listing each person, I do wish to thank each person, and I am grateful for their companionship and camaraderie, especially during the first year where the program front-loads all the courses both taking and teaching.

As alluded to above, the Weiss Lab is full of people from all walks of life and they have all helped me grow as a scientist and as a person. Blake Elias is always a source of amazing ideas and conversation and it was my pleasure to work with him. The graduate students are particularly close-knit; Jake, Bre, Ross, Jesse, Casper, and Noreen are all a second family to me. No matter the trials or tribulations I can count on them and that is a beautiful thing. Our friendship was and is the most important thing to me from my time here and I cannot express it more simply.

Over the last 5 years there have been two postdocs in the Weiss lab who have suffered the fate of working closely with me. Brian Teague has given me infinite wisdom, friendship, and forgiveness. Christian Cuba is the person who introduced me to molecular sequestration and the very first anti-lasR protein, QslA, so really this entire thesis is his fault, which is no small feat and which I hope you do not hold against him.

Beyond the Weiss Lab I am blessed with many people who have left an indelible mark and are gems of human beings: Jon Teo, Mark Mimee, Rob Citorik, Kevin Yehl, Isaak Muller, ZJ, Thomas Segall-Shapiro, Adam Meyer, Yongjin Park, Prashant Vaidyanathan, Curtis Madsen, Tim Jones, Kevin Yang, Felix Moser and John Sexton.

3000 miles away from home I have been welcomed with open arms by many. Dan and Julie Pollock, Dana Xu and Teague Bick, Natasha Seelam and Dariusz Murakowski, I can't thank enough for letting me into their homes and lives as family.

Everything I know about research and mentorship I learned from Penny Beuning, Mary Jo Ondrechen, and Srinivas Somarowthu. It can never be stated enough how much I owe my career to them.

Finally the most important people in my life are Mom, Dad, and Matt. Their infinite fount of love and forgiveness is what keeps me going.

This doctoral thesis has been examined by a Committee of the Department of Chemistry as follows:

Signature redacted

Professor Bradley L. Pentelute .....
Chairman, Thesis Committee
Associate Professor of Chemistry

Signature redacted

Professor James J. Collins .....
Member, Thesis Committee
Termeer Professor of Medical Engineering and Science

Signature redacted

Professor Alex K. Shalek ... .
Member, Thesis Committee
Pfizer-Laubach Career Development Assistant Professor of Chemistry

Signature redacted

Professor Ron Weiss . .....
Thesis Supervisor
Professor of Biological Engineering
Professor of Electrical Engineering and Computer Science

Contents

List of Figures

List of Tables

Chapter 1

Introduction

What I cannot create,

I do not understand

Richard Feynman

1.1 Synthetic Biology

Synthetic biology is the pursuit to build new biological systems. These new biological systems include artificial life[1, 2], minimal genomes[3, 4], cells that can perform industrial processes[5, 6], synthesize therapeutics[7], act as therapeutics themselves[8, 9, 10] or perform complex computations[11, 12, 13].

A useful approach to building new biological systems capable of performing complex computations is leveraging the terminology and principles behind electrical circuit engineering[14, 15]. Parts, such as promoters, ribosome binding sites, ribozymes, coding sequences, and terminators, can be composed into transcription units[16]. These transcription untis can then be composed into modules akin to "gates" that represent an input-output relationship. Module inputs can be chemicals or another gene-product such as miRNA or proteins. When the input of a module is of the same form as the output of another module, these modules can be composed to form "circuits"[16, 17, 18, 19].

Parts to build modules to compose circuits initially were adapted from natural

Molecule	Abbreviation	Organism	Genetic System
N-(3-Oxododecanoyl)-L-homoserine lactone	3OC12HSL	*Pseudomonas aeruginosa*	*las*
N-(3-Oxohexanoyl)-L-homoserine lactone	3OC6HSL	*Vibrio fischeri*	*lux*
N-Butanoyl-L-homoserine lactone	C4HSL	*Pseudomonas aeruginosa*	*rhl*
N-(p-Coumaroyl)-L-homoserine lactone	pC-HSL	*Rhodopseudomonas palustris*	*rpa*
N-(3-Oxooctanoyl)-L-homoserine lactone	3OC8HSL	*Agrobacterium tumefaciens*	*tra*

Table 1.1: Most commonly utilized quorum sensing systems and their signalling molecule.

systems known to sense inputs and then regulate genes, such as the *ara*, *tet*, λ proteins from bacteria and phage[16]. Engineered parts with novel properties, kinetics, or functions further expand the toolbox available to synthetic biologists. These new parts have been mined with bioinformatics, rationally designed, or evolved[20, 21, 22, 23].

Even with advanced and improved parts, single-cell circuits are limited in their capacity for complex functions such as organ development, communication, patterning, or synchronization. To coordinate behavior across many cells, cell-cell signalling is one of the most valuable tools in synthetic biology for programming advanced behaviors into new biological systems[24, 25, 26, 22, 27, 28, 29].

1.2 Quorum Sensing

To perform complex computations and build genetic circuits capable of decentralized behavior, synthetic biologists often turn to natural cell-cell communication paradigms[24]. One such natural cell-cell communication system exists in *Vibrio Fisheri*, which is a gram-negative bacterium that forms a commensal relationship within a specialized light organ of the Hawaiian Bobtail Squid (*Euprymna scolopes*)[30]. In exchange for protection and a ready source of food, *V. Fisheri* produces light. The genetic system responsible for the production of bioluminesence was found to be the *lux* operon; *luxA*, *luxB*, *luxC*, *luxD*, and *luxE* encode enzymes for light production and *luxR* and *luxI* encode regulatory functions[31].

This bioluminesence provides valuable camouflage to the squid, but is metabolically costly to the bacteria[32]. For a single bacterium in isolation (in sea water

on the order of 10^2 cells/mL[33]) the expression of the *luxABCDE* operon would be burdensome and wasteful. However, when there is a sufficient density of the bacteria inside *E. scolopes*, (on the order of 10^{10} cells/mL[33]) expression of the *lux* operon becomes advantageous.

To decide optimal gene expression, each cells needs to know the overall density of fellow bacteria in the surrounding environment. Without communication, each individual cell is incapable of sensing far-neighbors. In order to approximate the density of *V. Fisheri*, a computation must be made intracellularly based on an intercellular chemical signal. Three components and one assumption are required to build such a system capable of expressing genes if and only if a certain density is met:

1. Each cell emits a small amount of signal

2. Each cell has some way to sense the signal

3. Once a threshold of signal is sensed, it triggers downstream gene regulation

Finally we assume that the signalling molecule can diffuse freely in and out of each cell to and from the surrounding media and that this means that effectively [intracellular] $\approx$ [extracellular] for signalling molecules.

This phenomenon of individual cells coordinating their behavior based on sensing their overall density is known as quorum sensing. Quorum sensing exists across kingdoms and includes archaea[34], fungi[35, 36], both gram-negative bacteria and gram-positive bacteria[37], and can even be hijacked by phage[38].

In gram-negative bacteria, quorum sensing controls aggregation, antibiotic resistance, biofilm formation and maturation, bioluminesence, motility, competence/conjugation, exopolysaccharides production, nodulation/symbiosis, sporulation, and virulence[39, 40, 41]. By regulating genes that are density-dependent each cell conserves resources and shares information with those around it.

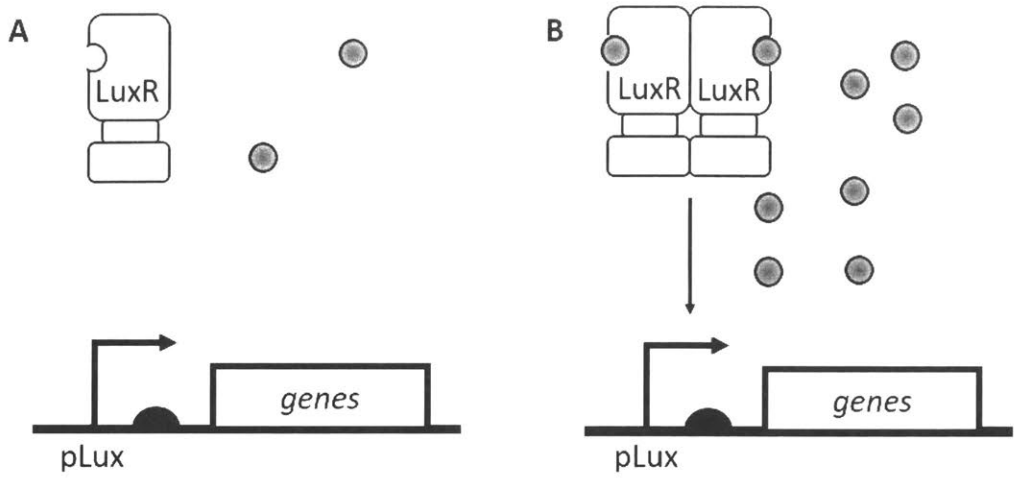

Figure 1-1: Because AHL (circles) freely diffuses in and out of gram-negative bacteria, its concentration approximates the density of bacteria in a given confined system. **A.** At low densities AHL concentrations are insuffecient to form active LuxR complexes and there is minimal, basal gene expression from the pLux promoter. **B.** At high AHL densities LuxR forms a complex with AHL, forms a homodimer, and this active complex drives expression of genes downstream from pLux.

1.2.1 Las, Lux, Rhl, Rpa, and Tra, Oh My!

In the world of synthetic biology, genetic clocks[42], edge detection[43], spatial band-pass filters[44], communicating across physical barriers[45] or spaces[46], and creation of stable microbial consortia[47, 48] all utilize LuxR-type quorum sensing (Figure 1-1). Much critical work of the field of synthetic biology, such as building sets of biosensors[49] or building integral controllers[50], utilizes LuxR-family transcription factors even when there is no cell-cell signalling function of the genetic circuit, solely for its robust expression profile and orthogonality to other transcription factors.

In this work, we utilize 5 of the most well-studied quorum sensing systems, LasR, LuxR, RhlR, RpaR, and TraR (Table 1.1), to demonstrate the universality of the design principles in Chapters 3 and 4 and characterize possible cross-reactivity.

1.2.2 AHL Structure Allows For Diffusion and Signalling

When the synthesis of a signalling molecule stimulates additional synthesis of itself in a positive feedback loop it is deemed an "autoinducer"[51]. The structure of the *lux* autoinducer was solved in 1981[52] and discovered to be a molecule of both a head

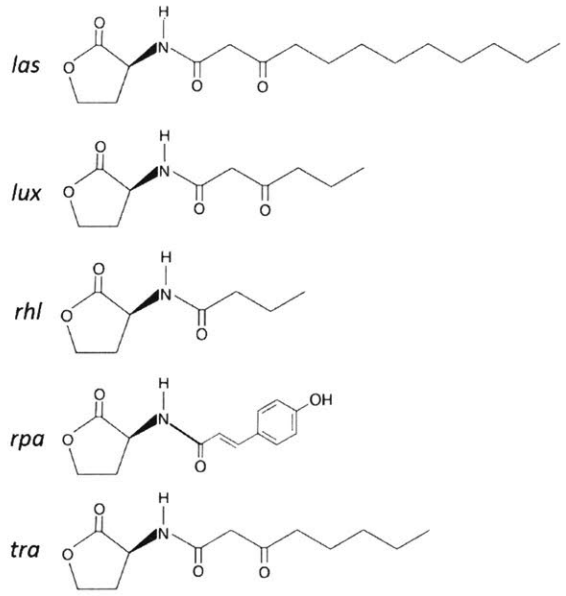

Figure 1-2: Chemical structure of AHL molecules used in this study.

and a tail, akin to a lipid. The head consists of a homoserine lactone and the tail an acyl-chain, sometimes with an additional carbonyl at the 3 position. This lipid-like chemical structure allows AHL molecules to diffuse freely across the cell-wall[53].

3OC8HSL and C4HSL are analogous to 3OC6HSL with different carbon length tails. Due to it's long acyl chain 3OC12HSL does not rely entirely on passive diffusion across the membrane but is also facilitated by active transport[54]. The *rpa* system has a unique signalling molecule, pC-HSL, without an acyl chain tail. Attached to the homoserine lactone head is a *p*-coumaroyl group[55] which results in drastically reduced cross-talk with other quorum sensing systems due to its unique structure[56, 57].

The hydrophobic moiety binds deep in the ligand-binding domain hydrophobic cavity[58]. The differences in steric hindrance based on the length of the acyl chain as well as the electrostatics of having an additional carbonyl at the 3 position determine specificity[59]. Signalling molecules with similar physical properties due to similar chemical structure, such as 3OC6HSL and 3OC8HSL (which differ only in a methylene group, can present a difficulty known as "cross-talk", where the signalling molecules are indistinguishable to the ligand receptors[60, 27, 56, 57].

1.2.3 QS Promoter's Design Allows for Low Basal Expression

Bacterial promoters utilize two hexamer DNA recognition sequences to recruit transcriptional machinery and initiate transcription[16]. These hexamers are known as the "-35" and "-10", located with their midpoint at the respective position relative to the transcriptional start site (known as the TSS or "+1"). In addition to the -35 and -10 sites there can be additional operator sequences that allow further regulation of transcription. For example, pBAD has binding sites for the transcription factor AraC to activate gene expression in the presence of sugar[61]. Repressible promoters can be kept in the off state by operator sequences that overlap between the -35 and -10. For example, TetR binds the operator sequence *tetO* between the -35 and -10 of the pTet promoter, occluding transcriptional machinery from engaging with the promoter[62].

In *V. Fisheri* pLuxI is bidirectional controlling the *luxICDABEG* operon and *luxI* gene on the opposite diverging strand[33]. Unlike most bacterial promoters, pLuxI has no -35 hexamer. Instead, centered at the -42.5 position, is a 20 base pair operator sequence "ACCTGTAGGATCGTACAGGT". This *lux* operator sequence (also known as the "*lux* box") serves as a recognition site for active LuxR complexes to bind and then recruit transcriptional machinery. This lack of -35 hexamer helps keep the basal expression of pLuxI low in the off state and the (reverse complement) palindromic nature of the operator sequence gives rise to the bidirectional expression.

The pLux promoter used in this work has been engineered for unidirectional expression[18]. Many natural promoters of other quorum sensing systems provide very low expression[60, 63]. To engineer stronger responses for the pRpa and pTra promoters, we replace the *lux* operator sequence in pLux with the *rpa* or *tra* recognition site[56]. The pLas promoter used in this work is derived from the *P. aeruginosa* genomic *qscrsaL* promoter and the pRhl promoter from *P. aeruginosa* genomic *qsc119* promoter[63].

1.2.4 QS Transcription Factors Are Built Similarly

Quorum sensing transcription factors in the LuxR-family all share similar sequence and structure[59]. The N-terminal ~180 amino acids comprise the ligand-binding domain and C-terminal ~65 amino acids are the DNA-binding domain with an ~11 amino acid linker between each domain[64].

The ligand-binding domain consists of α-helix with a 5-strand β-sheet forming the ligand binding pocket. The ligand binding pocket is buried within the protein and extensively hydrophobic allowing the acyl (or *p*-coumaroyl) moiety to be completely protected from solvent. The fact that the AHL ligand is buried so deeply into the three dimensional structure of the protein provides partial evidence for a theory that the protein folds around the ligand[65, 59]. The DNA-binding domain is a canonical four α-helix Helix-Turn-Helix (HTH) motif common to many other microbial transcription factors that make contact with DNA[59, 66, 67].

At a high level all LuxR-family transcription factors have the same input-output relationship: the presence of AHL in sufficient concentration leads to activation of the cognate promoter. However, not all LuxR-family transcription factors bind their ligand by identical mechanism[68, 69]. There have been multiple proposed mechanisms for the action of AHL facilitating downstream gene expression at a biochemical level which include[65]

1. The presence of the AHL molecule allows the nascent LuxR polypeptide to properly fold

2. The presence of the AHL molecule causes a conformational change in LuxR that hides the sequence of the protein that causes it to be marked for proteolysis. This protects LuxR, increasing the protein's half-life and allows LuxR to find and activate the cognate promoter

3. The presence of the AHL molecule causes a conformation change that facilitates dimerization, which is required for DNA binding

Connections between *in vivo* and *in vitro* studies on LuxR mechanisms can be chal-

lenging. Multiple reports have shown that it can be impossible for a purified LuxR-type protein *in vitro* to release its cognate acyl homoserine lactone[70, 71], but when cells are exchanged from saturating conditions of signalling molecule to media without signalling molecule, transcription falls precipitously[65]. Precise mechanistic details for LuxR-family proteins transition between their low-ligand and high-ligand functions is still an active area of research[65, 59, 72].

1.2.5 A Dearth of Purification and Crystal Structures

Despite attempts, LuxR and its homologues have been, and mostly still remain, incredibly recalcitrant to purification and subsequent structural characterization in the absence of saturating ligand[59]. An AHL-free purification of full length LasR was reported in 2016[73]. However subsequently the authors acknowledged difficulty reproducing the results, and even in their own hands reported puzzling results(specifically, similar K_D values for all AHLs cognate or not)[74]. *In vivo* LasR shows a preference for 3OC12HSL with a 1000-fold more sensitivity than C4HSL [56, 63, 60].Lixa et al. were able to express insoluble RhlR C-terminal DNA-binding domain (amino acids 177-241) and refold it to purify substantial amounts of this fractional protein[75] that retained DNA-binding activity. This represented the first report of purified RhlR, albeit severely truncated. A new approach using mBTL (*meta*-bromo-thiolactone) as a ligand has shown success[76] for full-length RhlR stability.

There are no Protein Data Bank[77] (PDB) crystal structures for LuxR, RhlR, or RpaR. LasR has many ligand-stabilized, ligand-binding domain-only solved crystal structures, in complex with 3OC12HSL in the ligand-binding pocket[78, 79], non-cognate AHLs[80, 81], or synthetic agonist homologs[82], but none that include the full-length protein. Full-length structures have been solved for QscR[83] and TraR[84, 85, 86].

The unparalleled usefulness of LuxR and quorum sensing systems when building new genetic systems, paired with the lack of detailed biophysical or structural data of the proteins, make LuxR an optimal target for rational design of new and improved functions.

1.3 Thesis Organization and Scope

In the following chapters, I describe the contributions I have made to the field of synthetic biology and protein engineering during my time here in Prof. Ron Weiss's research group at MIT. The overarching theme of this thesis is the development of protein design principles that allow for new interactions in genetic circuit construction with LuxR-type quorum sensing systems. It is my sincere desire and expectation that this greatly expanded toolbox of biomolecular interactions and wires will be useful for the field of synthetic biology and protein engineering writ large.

In Chapter 2, I describe the Turing Pattern project and its design, constraints, and results. This work was initially done by Ting Lu and David Karig. After additional control experiments, the addition of advanced mathematical analysis by K. Michael Martini and Nigel Goldenfeld at UIUC, and extensive narrative revisions, we published this work in PNAS in 2018. the conditions Turing proposed are disappointingly hard to achieve in nature, but recent stochastic extension of the theory predicts pattern formation without such strong conditions. We have forward-engineered bacterial populations with signaling molecules that form a stochastic activator-inhibitor system that does not satisfy the classic Turing conditions but exhibits disordered patterns with a defined length scale and spatial correlations that agree quantitatively with stochastic Turing theory. The genetic design constraints on this system inspire tools to overcome them, which present in Chapters 3 and 4.

In Chapter 3, I describe my work to create "chimera" proteins consisting of a ligand-binding domain from a protein different than that of its DNA-binding domain. Biochemical characterization and sequence alignments offer delineations between the ligand-binding domain, DNA-binding domain, and the linker sequence that connects them. LasR from *P. aeruginosa* is chosen as the DNA-binding domain for its useful properties and expression profile. We explore multiple sites of domain swapping in an initial rhl-las case study, and then expand this to each other quorum sensing protein in this work (lux, rpa, and tra). These chimeras show robust activity, similar cross-talk profiles as the wild-type proteins, and excellent on-off expression behavior.

In Chapter 4, I describe my work to design proteins to sequester LuxR-type transcription factors. First, I examine the known proteins that serve such a function in the literature and discuss their advantages/disadvantages. Second, I utilize a natural sequester protein of TraR from *A. tumefaciens*, TrlR, as the basis for further design. After validating that removal of extraneous C-terminal amino acids still results in full activity, I implement analogous construction of TrlR to each other LuxR-family transcription factor of this work (LasR, LuxR, RhlR, and RpaR). We show that these truncation products can knock down gene expression of their cognate full-length transcription factor by sequestration, that expression can be recovered by competition of the active monomer, and that, with the exception of RhlR's truncation, they are specific to their respective parent protein. In addition, these truncation sequester proteins successfully knock down activity of the chimera proteins developed in Chapter 3 allowing both protein design paradigms to be combined for even more expansive control and design of quorum sensing genetic circuits.

In Chapter 5, I describe work done in collaboration with many others in the NIST Synthetic Biology Working Group on Flow Cytometry to perform an interlab study of instrument variation in the quantification of fluorescent proteins in bacteria. While there will always be biological variability to contend with in the characterization, much less engineering, of biological systems, instrument and protocol variability themselves represent a threat to standardization and characterization. I developed a protocol for loss-free stasis of bacterial samples, sent them to 15 different labs across the country, and examined the distribution of results.

Chapter 2

Stochastic Turing Patterns

> It is suggested that a system of chemical substances,
> called morphogens, reacting together and diffusing through a tissue,
> is adequate to account for the main phenomena of morphogenesis
>
> A. M. Turing[87]

The following is adapted from our manuscript published in PNAS[88]. The main body of work for the stochastic Turing Patterns was done by David Karig, Ting Lu, and K. Michael Martini. Here I focus on the design and the constraints on the genetic circuit and experimental work, which provides background for the motivation in Chapters 3 and 4.

2.1 Motivation

A fundamental challenge in developmental biology is understanding how global spatial patterns emerge from local interactions in isogenic cell populations. Synthetic systems can be forward engineered to include relatively simple circuits that are loosely coupled to the larger natural system into which they are embedded, making it easier to design and control the molecular underpinnings of a biological pattern phenomenon[89, 90, 91, 92, 93, 94, 95, 96].

Motivated by classical theoretical studies of Turing, Gierer, and Meinhardt[97, 98],

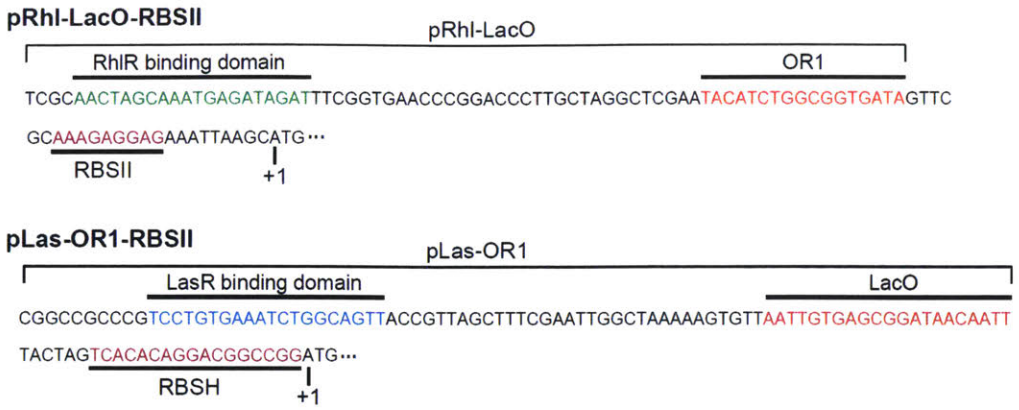

Figure 2-1: New hybrid promoters designed for the Turing Pattern genetic circuit. (Top) $P_{Las-OR1}$is activated by RhlR and repressed by lambda repressor CI. (Bottom) $P_{Rhl-lacO}$is activated by LasR and repressed by LacI.

as well as recent extensions to stochastic patterning[99, 100], we created an emergent patterning system in *E. coli*. Previous pattern formation efforts in synthetic biology have focused on oscillations in time[92, 101, 102, 103], or requiring an initial template[90, 104, 105, 95], or an expanding population of cells[106]. Programming a synthetic biological system with none of these limitations in a forward engineered manner[107] allows us to probe stochastic Turing Patterns where many of the natural Turing Pattern systems are difficult to precisely manipulate and the underlying chemical mechanisms still an active area of research[96, 108, 109, 110, 111, 112].

2.2 Design of a Turing Pattern Gene Circuit

In our synthetic gene network design we use two artificial diffusible morphogens: 3OC12HSL and C4HSL, from the *las* and *rhl* quorum sensing pathways respectively in *P. aeruginosa* [113]. 3OC12HSL serves as an activator of both its own synthesis and that of C4HSL, while C4HSL serves as an inhibitor of both signals (Figure 2-2a-b). 3OC12HSL activates its own synthesis by binding regulatory protein LasR to form a complex that activates the hybrid promoter $P_{Las-OR1}$2-1. This promoter regulates expression of LasI, a 3OC12HSL synthase, and *rhlI*, a C4HSL synthase. To increase the sensitivity of 3OC12HSL self-activation, LasR is regulated by a second copy of $P_{Las-OR1}$. C4HSL inhibits synthesis of 3OC12HSL and itself by forming a

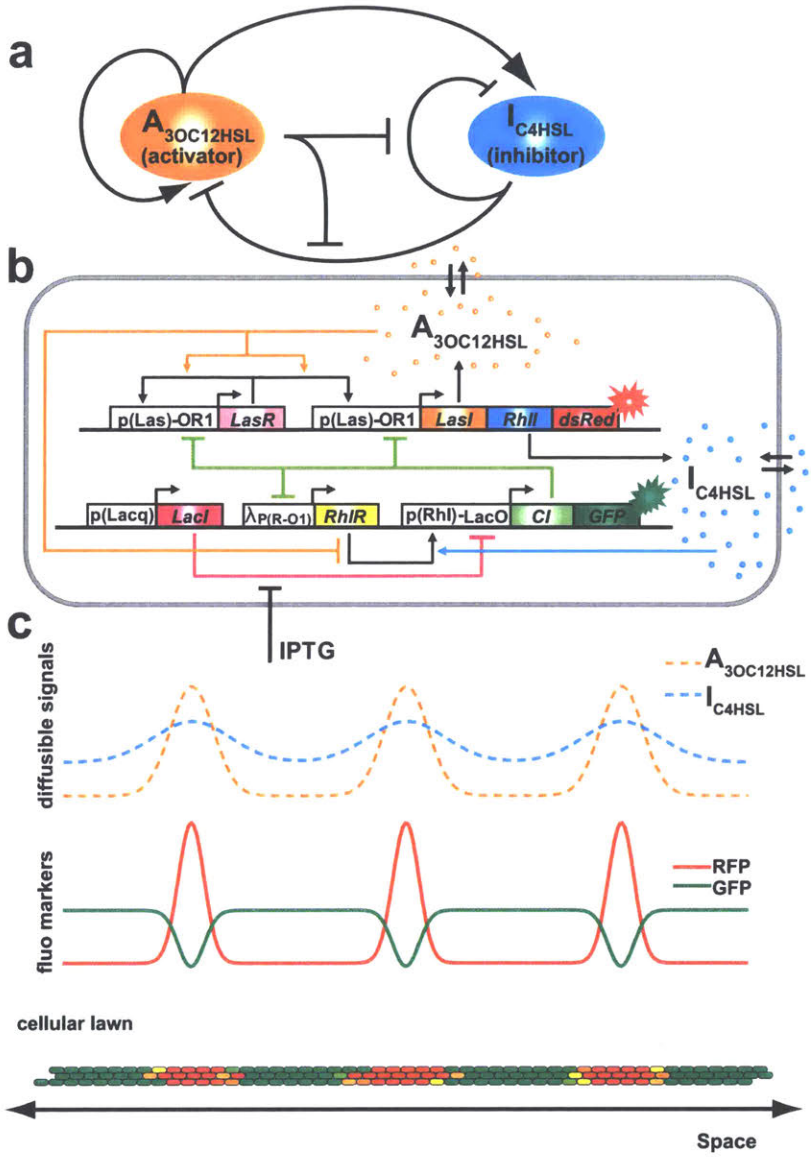

Figure 2-2: Design of a synthetic multicellular system for emergent pattern formation. **a**, Abstractly, the system consists of two signaling species 3OC12HSL and C4HSL: 3OC12HSL is an activator catalyzing synthesis of both species while C4HSL is an inhibitor repressing their synthesis, with additional repression by 3OC12HSL by cross-talk with RhlR. **b**, Genetic circuit implementation. Promoter regions are indicated by white boxes, while protein coding sequences are indicated by colored boxes. IPTG is an external inducer modulating system dynamics. **c**, Top: Illustration of signaling species concentrations in one-dimensional space. The dashed orange and blue lines correspond to 3OC12HSL and C4HSL respectively. Middle: Spatial profiles of reporter proteins. RFP expression (red line) correlates with 3OC12HSL concentrations, while GFP expression (green line) roughly mirrors RFP expression. Bottom: A vertical slice of cell lawn. Cells express fluorescence proteins according to the profiles above and produce a global multicellular pattern.

complex with regulatory protein RhlR. This complex activates expression of lambda repressor CI which, in turn, represses transcription of LasI, RhlI, LasR and RhlR. Pattern formation in our system can be modulated by altering the concentration of isopropyl β-D-1-thiogalactopyranoside (IPTG), a small molecule inducer that binds LacI and alleviates repression of $P_{Rhl-lacO}$. Green and red fluorescent proteins (GFP and RFP) are expressed from the *rhl* and *las* hybrid promoters respectively to aide in experimental observation (Figure 2-2).

2.3 Results

In our experimental setup, the 3OC12HSL activator diffuses more slowly than the C4HSL inhibitor (SI 2-5). The estimated diffusion coefficient for 3OC12HSL is $83\,\mu m^2/s$ and for C4HSL is $1810\,\mu m^2/s$. The slower diffusion rate of 3OC12HSL, coupled with positive feedback regulating its synthesis, allows 3OC12HSL to aggregate in local domains, leading to formation of visible red fluorescent spots (cellular lawn illustration shown in Figure 2-2c). Within these red domains, both 3OC12HSL and C4HSL are found in high concentrations, but because 3OC12HSL competitively binds RhlR, GFP is attenuated[114]. The faster diffusion rate of C4HSL allows it to diffuse into regions outside of the red fluorescent domains. Here, C4HSL is free to bind RhlR, activating GFP expression. Collectively, these processes lead to green regions between red spots.

To study pattern forming behavior, engineered cells are first cultured in liquid media, then concentrated and plated on a Petri dish to form an initially homogeneous 'lawn' of cells (see Experimental Details). After plating, the Petri dish is incubated for 24 hours at 30°C and microscope fluorescence images are captured as needed. Prior to the self-activation of the 3OC12HSL synthase positive feedback loop, the cell lawn exhibits no fluorescence. However, over time red fluorescent spots emerge with sizes much larger than that of a single cell (10-1000x). Simultaneously, green fluorescence develops in a honeycomb-like pattern with dark voids positioned precisely in the locations of the intense red fluorescence (Figure 2-3a). Time-series microscopy

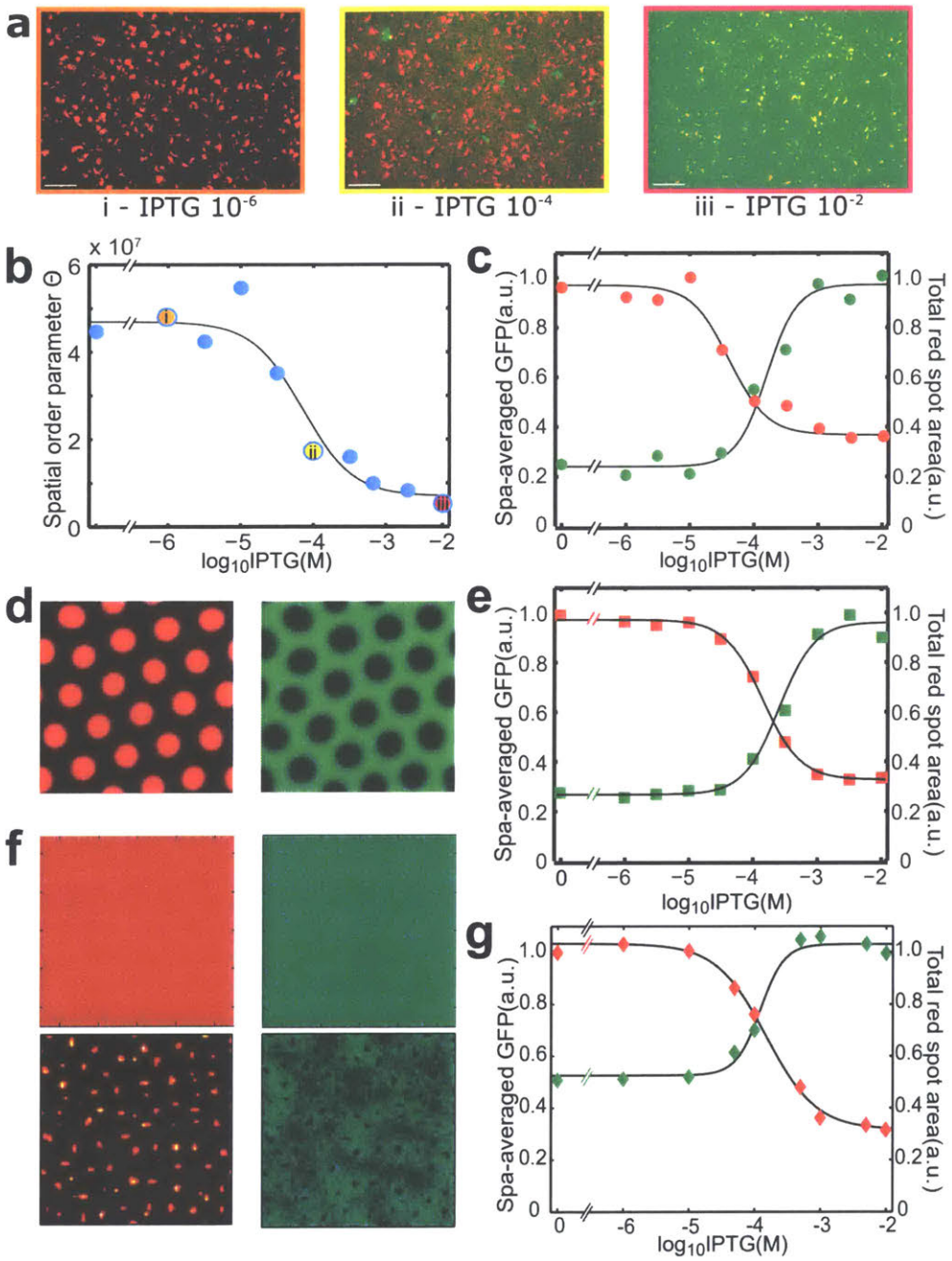

Figure 2-3: **Experimental observations of emergent pattern formation. a**, Representative (6 technical replicates) microscope images of a typical field of view showing a fluorescent pattern formed by an initially homogeneous isogenic lawn of cells harboring the Turing circuit with no IPTG. Spots and voids appear in the red and green fluorescence channels, respectively. Scale bar, 100 µm. **b**, Microscope images of cell lawns with constitutive expression of fluorescent proteins. Left: cells expressing RFP; Middle: cells expressing GFP; Right: mixed population of red and green cells. **c**, Fluorescence density plots computed from the images above (left-to-right: red, green, red/green, and Turing). Color intensity is in log scale.

reveals that patterns begin to emerge after approximately 16 hours.

We then conducted experiments to ensure that the diffusion of I_{C4HSL} and $A_{3OC12HSL}$ did not drastically change due to potential differences in biofilm characteristics over many hours of incubation. Specifically, the diffusion experiment was again carried out, varying the initial incubation time before AHL addition. Images were then captured following 0, 2.5, 5, and 8 hours of AHL exposure (Figure 2-6).

By parameter estimation using the fluorescence intensities of cells far away from the center in the model with the experimental setup, we obtained a cellular growth rate of $\alpha_n = 0.15$ hr^{-1} and saturation cell density of $N_l = 5.0$ ($N_0 = 1.0$). Then, by parameter estimation of the fluorescence wave profile over time, we estimate the diffusion coefficients to be $D_{c_{12}} = 0.003$ cm^2/hr for $A_{3OC12HSL}$ and $D_{c_4} = 0.065$ cm^2/hr for I_{C4HSL}. The corresponding simulation results are shown in Figure 2-5c-d. These experiments suggest that the diffusion coefficient for the activator is approximately 21.6 fold slower than that of the inhibitor, qualitatively consistent with a previous study [115]. One possible explanation for why the ratio of diffusion rates is higher than expected based on molecular weight differences alone is that the hydrophobic nature of $A_{3OC12HSL}$ causes it to partition in the cell membrane, thus essentially slowing down its diffusion from cell to cell [115].

2.3.1 The Formation of Stochastic Turing Patterns

In control experiments, we show that our patterns are not simply a result of the outward growth of clusters of differentially colored cells (Figure 2-4). We also test whether observable patterns would emerge if individual cells autonomously made cell-fate decisions at some point after plating. The fluorescence fields after 24 hours of incubation at 30°C in both experiments are uniform, showing no emergence of patterns. We further tested additional ratios of constitutively fluorescent green and red cells and again observed relatively uniform fields of fluorescence (Figure 2-4). These experiments demonstrate that, in our experimental setup, neither cell growth nor initial spatial heterogeneity of cell density give rise to the large scale spatial patterns observed with the Turing cells.

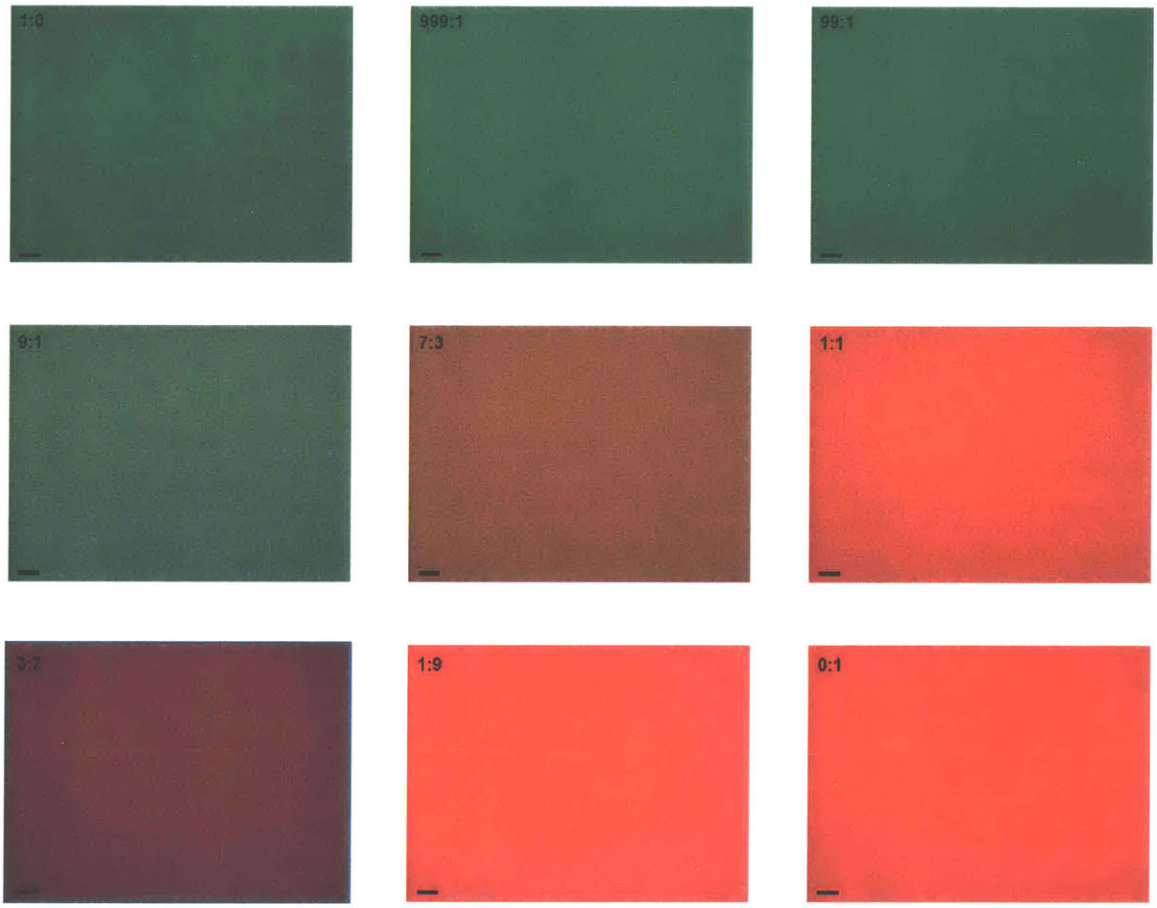

Figure 2-4: Populations of *E. coli* expressing constitutive fluorescent reporter proteins GFP or mCherry were mixed in various ratios of [Green:Red] on M9 supplemented minimal media and then imaged by microscopy. Scale bar, 200 µm.

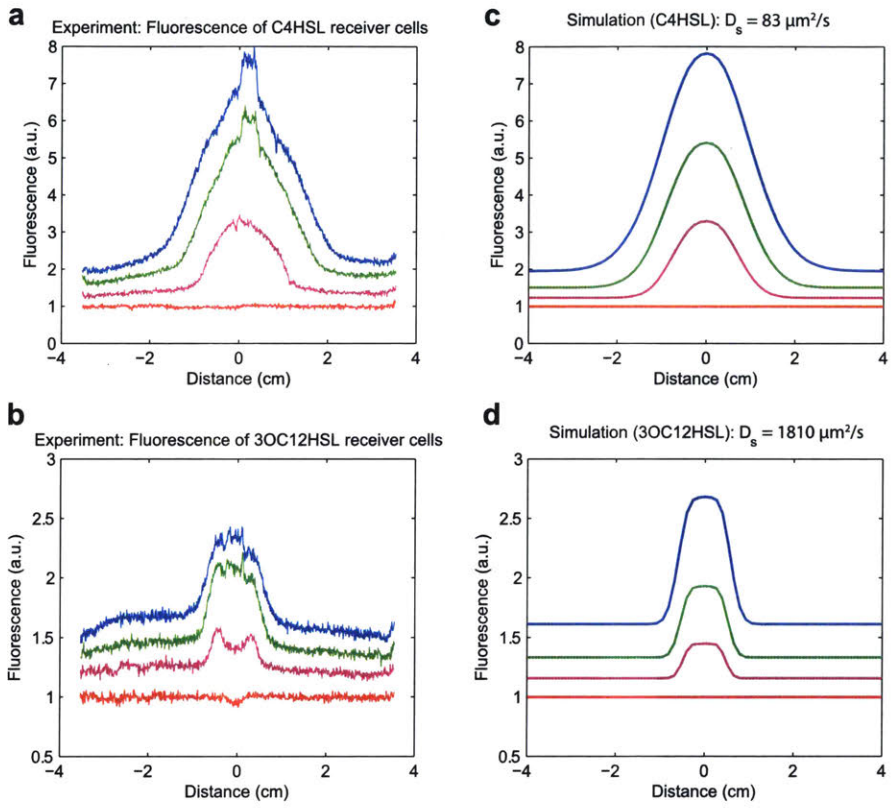

Figure 2-5: **a-b**, Fluorescence intensity of receiver cells in response to AHL gradients in 2% M9 agar plates. In both panels, the four curves correspond to hours 0, 2.5, 5, and 8.75. **c-d**, For simulations, fluorescence intensity simulation results were obtained using our mathematical model. The estimated diffusion coefficient for $A_{3OC12HSL}$ is $83\,\mu m^2/s$ and for I_{C4HSL} is $1810\,\mu m^2/s$.

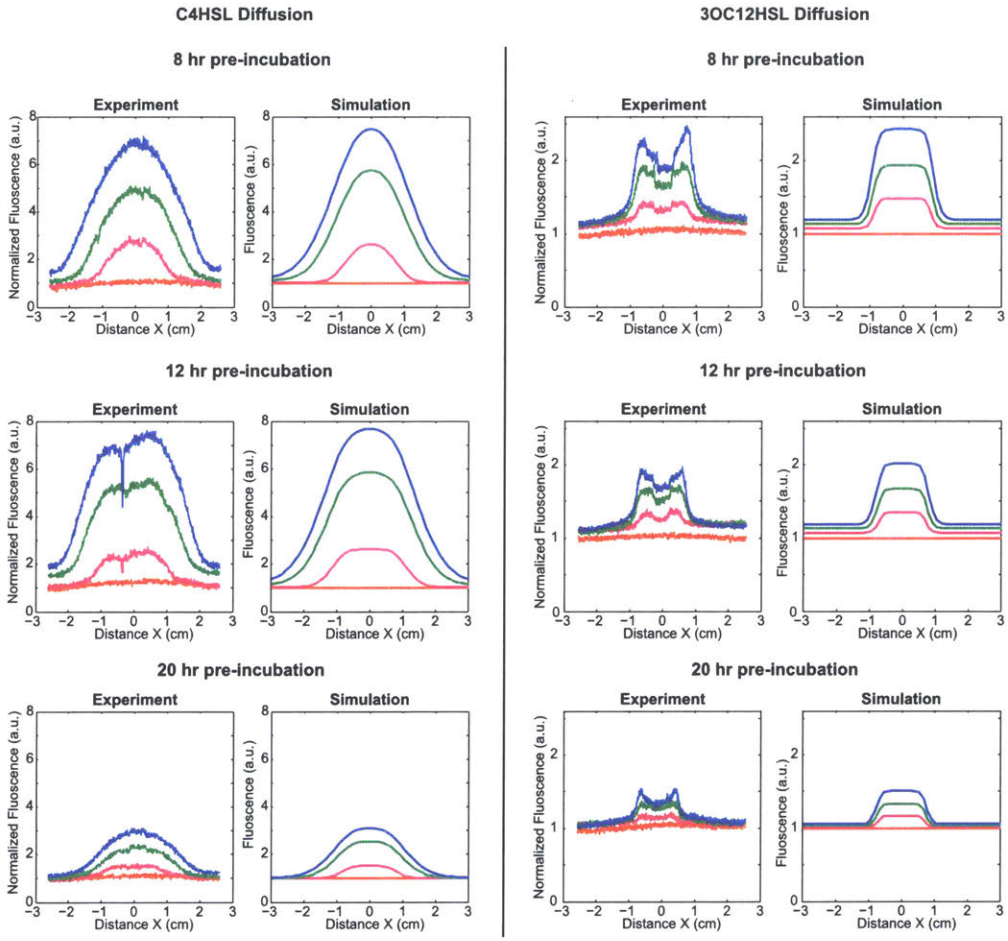

Figure 2-6: Additional experiments to verify that diffusion rate calculations are reasonably robust to changing biofilm characteristics over time. Fluorescence intensity of receiver cells in response to AHL gradients in 2% M9 agar plates.The four curves correspond to hours 0, 2.5, 5, and 8.

Next, we examine how changes in the levels of localized interactions lead to different global outcomes in our pattern forming gene circuit. In our system, IPTG can be used to modulate the inhibitory efficiency of C4HSL in individual cells by affecting CI expression from $P_{Rhl-lacO}$. Specifically, IPTG relieves LacI repression of CI and GFP reporter. The increased range of CI ultimately increases inhibition of both morphogens. This increased inhibition is expected to decrease activator spot sizes, while the field of CI and GFP reporter are more strongly expressed.

Our data show that mean GFP levels increase sigmoidally with inducer concentration while the overall area of red spots decreases (Figure 2-3a-d). In addition to offering further support that our gene circuit gives rise to emergent patterns, these results show how pattern formation characteristics can potentially be tuned to fit future application needs.

2.4 Conclusions and Future Directions

Our engineered system provides a platform for quantitatively exploring the general features of pattern formation in other spatially extended collective systems such as biofilms. Many biofilms exhibit patterning at scales much larger than the individual bacteria involved, and this can be associated with resistance of the biofilm to environmental insult or antibiotics[116]. From a bioengineering perspective[89], our work offers a method for rational design of patterning systems. Future extensions may focus on approaches for achieving more regular patterns, such as those associated with the Nodal/Lefty2[111], HetR/PatS[117], Notch/Delta[118], and FGF/Shh signals[110], and additional nodes such as Bmp/Sox9/Wnt[112]. Future extensions may also consider modifications to achieve different types of patterns.

Nonetheless, our demonstration of large-scale global patterning using a small gene circuit is an important step towards realizing programmed structures for biomaterial fabrication, whereby fluorescent reporters may be replaced by genes to functionalize cells[119], or for tissue engineering – one of the most ambitious yet important objectives of systems and synthetic biology.

2.5 Experimental Details

2.5.1 Plasmids

Our patterning system was constructed using two plasmids that correspond to the upper and lower portions of the circuit diagram in Figure 1b; pFNK512 and pFNK806 in Figure 2-3a and pFNK512 and pFNK804lacOlacI for Figure 2-3. The two-color bistable toggle switch plasmid pTOG-1 was constructed from plasmid pIKE-107. All plasmids were constructed using standard cloning and DNA recombination techniques. *E. coli* strain MG1655 was used for all experiments.

2.5.2 Patterning

Cells harboring appropriate plasmids were initially grown in LB liquid media with corresponding antibiotics at 30°C until optical density at 600 nm reached $0.1 - 0.3$. Cells were then concentrated and re-suspended in M9 media with appropriate antibiotics[120]. 0.5 mL of concentrated cell solutions ($OD_{600} = 2.0$) were poured onto a 2% M9 agar plate (60×15 mm Petri dish) to form a cellular lawn. Plates were incubated at 30 °C and fluorescence images were captured periodically. To examine the single cell fluorescence evolution of toggle switch cell populations, we performed flow cytometry at the beginning of the experiment (0 h) and the end of the experiment (24 h).

2.5.3 Diffusion of AHL Through LB-Agar

We performed solid-phase diffusion experiments in 2% M9 agar plates as described in Experimental Details. Reporter cells picked from single colonies were cultured in liquid LB media overnight and diluted 1000:1 into fresh media the next day. When culture OD's reached $0.1 - 0.3$, cells were concentrated and resuspended in M9 media to final OD of 2.0. 1.5 mL of the concentrated cells were plated onto 80×15 mm M9 agar Petri dishes for the diffusion experiments. To correspond with the environmental conditions of our patterning experiments, plates with the cells were first incubated at

30 °C for 12 hours. Afterwards, 3 μL AHL droplets with an appropriate concentration (10 mM for I_{C4HSL}, and 0.01 mM for $A_{3OC12HSL}$) were added at the center of the plates for each type of reporter cell. We chose these concentrations based on the AHL's half activation thresholds so that the AHL's activate cells around the center but not close to the edge of the Petri dishes. Fluorescence images were taken at hours 0, 2.5, 5, and 8.75 using a Bio-rad Molecular Imager ChemiDoc XRS+ System. An XcitaBlue conversion screen was used for capturing GFP intensities.

Every image obtained from this experiment has a fluorescence radial gradient centered around the position where the AHL droplet was added. Figure 2-5a-b shows representative fluorescence intensity lines crossing the image centers for different time points for the two AHL diffusion experiments. The image exposure times for I_{C4HSL} and $A_{3OC12HSL}$ are 0.1 s and 0.2 s respectively. Raw images were processed to remove exposure bias in the field of view by background subtraction of reference frames.

Chapter 3

Chimeric Quorum Sensing Transcription Factors

Hydra bore Chimaira, who breathes fire not to be resisted,
a dreadful, great thing, swift of foot and powerful.
She has three heads. One is that of a fierce lion,
another of a goat, and the last of a mighty serpent snake

Hesiod, *Theogony*

Christian Cuba collaborated with the experimental design and theory for this project. Parts of this chapter have been adapted for a prepared manuscript *Engineering Molecular Sequestration of Quorum Sensing Proteins* Nicholas A DeLateur, Christian S. Cuba, Ron Weiss.

3.1 Motivation

For the design and implementation of genetic circuits that function by cell-cell communication for spatial patterning, the signalling molecule represents the central factor for choice of quorum sensing system[88]. In an aqueous media such as LB-agar, the diffusion rate of an acyl-homoserine lactone is defined by the hydrophobicity of its tail moiety, and acyl chains of too great a length require active transport in addition

to passive transport[115]. Much as each signalling molecule has its own proprieties of diffusion, each transcription factor and cognate promoter have their own proprieties of basal expression (leakiness), maximal expression, and threshold (K_D of the overall system composed of K_D of ligand-protein interaction and K_D active transcription factor-DNA interaction)[49]. The expression levels, activation threshold, and cross-talk are not modular, and require extensive efforts to improve or change[121, 49].

In quorum sensing these properties of activation threshold, basal expression, and maximal expression, vary between each system[56, 57]. For example, although the *rpa* system has the least cross-talk interactions[56] with its unconventional side-chain[55], it however suffers from low fold-changes[56, 57]. Similarly, among well-studied quorum sensing transcription factors used in genetic circuits, TraR has the lowest expression when maximally induced[57]. This poor transcription profile is balanced by 3OC8HSL having many useful properties such as minimal cross-talk with C4HSL while retaining moderate diffusion due to its shorter acyl chain than 3OC12HSL.

Modular domain swapping allows for transcriptional logic gates that can be multi-input and orthogonal[122, 123, 124, 125]. Chimeras composed from a selection of swappable ligand-binding domain and DNA-binding domain (or general downstream activation domains) have been used with sugar-sensing transcription factors[126, 127, 128], Two-Component Systems (TCS)[129], T7 RNA Polymerases[130], allosteric regulators[131, 132], mammalian signalling pathways such as VEGF[133], and chimeric antigen receptor (CAR)-expressing T cells[134, 135].

We chose LasR as the transcription factor for the DNA-binding domain. LasR's DNA-binding domain is well characterized[70] as well as its promoter[137]. The LasR-pLas expression profile has low leakiness and high maximal expression with an activation threshold on the order of 1 nM 3OC12HSL (Figure 3-6). Thus the *las* DNA-binding domain and promoter combined with the ligand-binding domain of LuxR, RhlR, RpaR, or TraR would provide optimal parameters from each respective domain for new chimeric proteins.

There are previous reports of quorum sensing chimeras that utilize lasR DNA-binding domain. The DNA-binding domain of LasR has successfully been combined

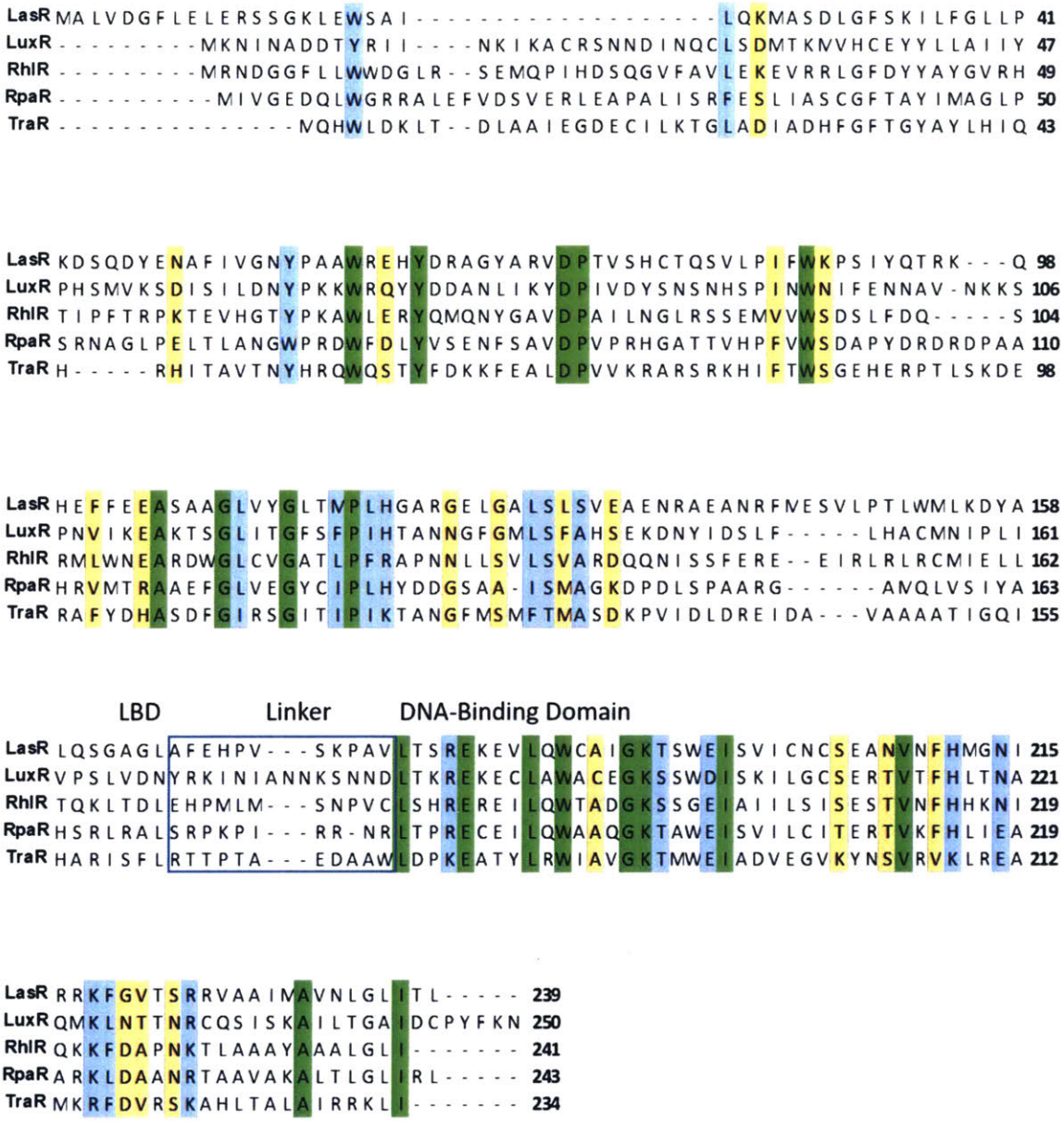

Figure 3-1: CLUSTAL O(1.2.4)[136] multiple sequence alignment of the five transcription factors used in this work. Fully conserved positions in green, mostly conserved positions in blue, and partially conserved positions in yellow. The linker region is boxed with all upstream residues comprising the ligand-binding domain and all downstream residues comrpising the DNA-binding domain. The ligand-binding domain of LuxR-family transcription factors on average shares only 21% identity with fellow homologes among LasR, LuxR, RhlR, RpaR, and TraR, in contrast to an average of 41% identity conserved for any given pairwise comparison of the DNA-Binding Domains.

with the ligand-binding domain of RhlR as well as the ligand-binding domain of OyhR resulting in a 2- to 3-fold induction between vehicle and the respective ligand-binding domain cognate signalling molecule being added to the media[138]. Perhaps most interestingly it is possible to create a chimeric transcription factor with **two** ligand-binding domain attached to a DNA-binding domain and retain response to either ligand, although the design principles of the order of the ligand-binding domain utilized is much more complex[138].

Activating silent Bacterial Gene Clusters (BGC) is a compelling use of chimeric transcription factors since they are often flanked by quorum sensing operons that may have unknown or hard-to-synthesize ligands to activate downstream expression[139]. By swapping the ligand-binding domain of MupR onto the DNA-binding domain of LasR expression of the *mup* operon reached wild-type levels in response to 3OC12HSL [140].

3.2 Design and Nomenclature Of LasR Chimeras

Since here we focus on making fusion sites across the linker domain, the sequence and name of each chimera is defined by three attributes:

1. The parent protein ligand-binding domain
2. The amount of nucleotides from the parent ligand-binding domain the linker retains
3. The parent protein DNA-binding domain

For example, "rhl12lasR" would refer to a protein composed of the RhlR ligand-binding domain, 12 nucleotides coding the RhlR linker, the remaining portion of the lasR linker, and the DNA-binding domain of LasR. Using the nucleotide position rather than amino acid position helps for programmatic design and removing ambiguity of where each codon comes from for chimeric genes. Some linker fusion sets result in identical amino acids at a given position (even though the codons used are

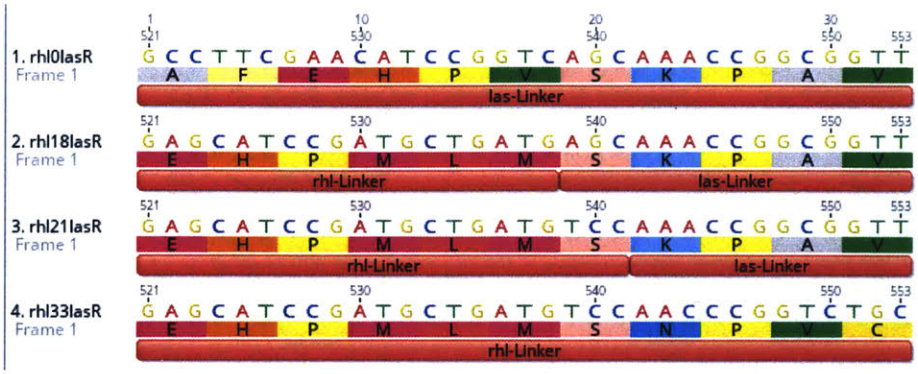

Figure 3-2: Examples of chimera linker sequences, a subset for rhl-X-lasR proteins. rhl18lasR and rhl21lasR fusions result in identical protein products due to overlap in identical amino acids at the same position along the linker for the parent proteins RhlR and LasR.

not necessarily identical) such as rhl18lasR to rhl21lasR where a serine using codon AGC is replaced by a serine using codon TCC as shown in Figure 3-2. LasR, RhlR, RpaR, and TraR linkers are 11 amino acids, defined as those contained within two conserved leucine residues at position 165 (LasR numbering).

3.3 Results

3.3.1 Determining Optimal Fusion Site For Rhl-Las Chimera

We initially chose the rhl-las chimera to interrogate the best fusion site to make hybrid transcription factors. The coding sequence was put under constitutive control of pLacIq-RBS31, and reporter proteins mCherry driven from the pLas promoter, GFP driven from the pRhl promoter.

Figure 3-3 shows the successful response to C4HSL to activate the las promoter. Full length wild-type rhlR results in the lowest absolute expression as well as highest K_D. The fold changes between 0 nM C4HSL and 2000 nM C4HSL reveal a non-monotonic distribution peaking at rhl24lasR. Starting at the N-terminal side of the linker junction, a greater identity from the ligand-binding domain continues to improve expression and sensitivity until rhl30lasR and subsequent designs where the increase in basal expression overcomes the increase in maximal expression. These ini-

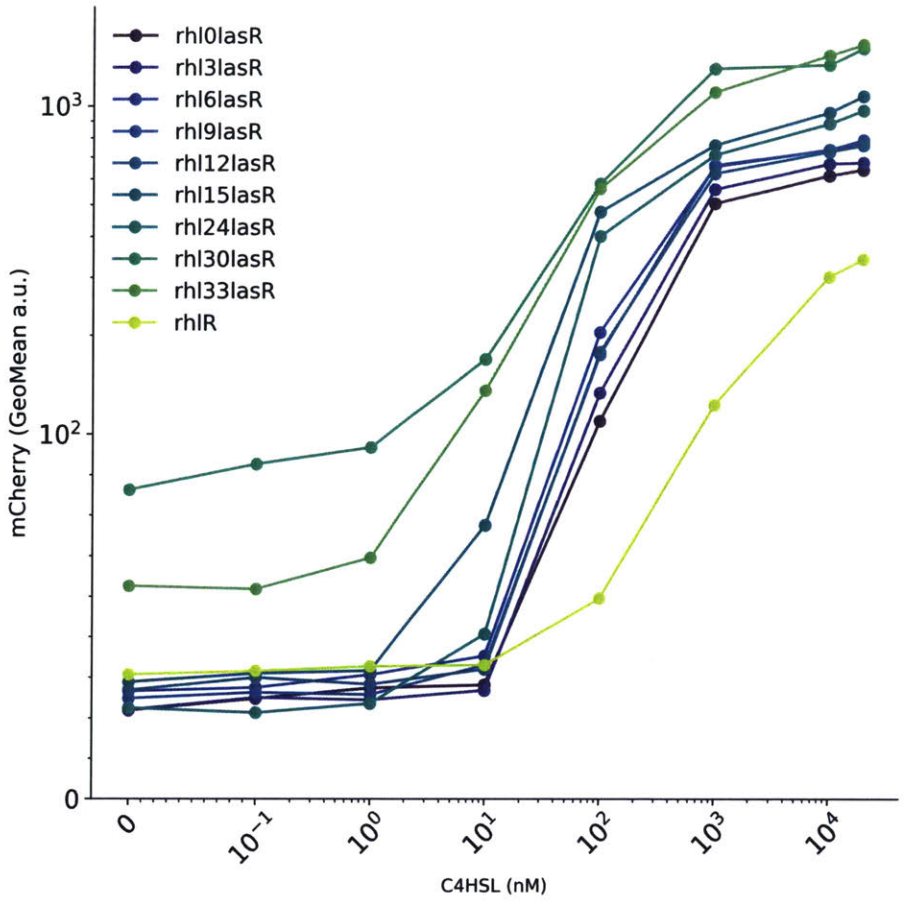

Figure 3-3: Initial fusion site scan of rhl-X-lasR for las DNA-binding function. mCherry is driven by pLas-RBS31.

tial results suggested that leaving 8 amino acids of the linker from the ligand-binding domain of the parent protein was optimal.

Most quorum sensing systems have off-target activity resulting in cross-talk at multiple levels[56] that increases with expression. Figure 3-4 shows the rhl-las chimeric proteins would activate the pRhl promoter at lower levels and with less sensitivity than full length wild-type RhlR.

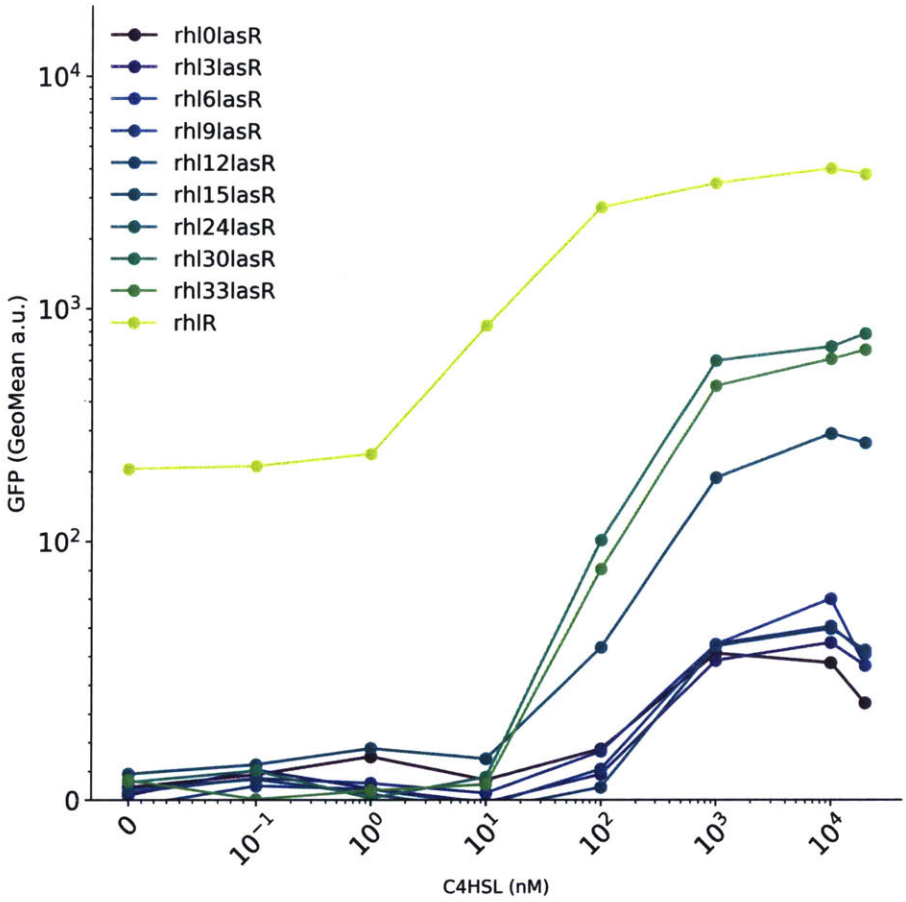

Figure 3-4: Initial fusion site scan of rhl-X-lasR for lack of rhl DNA-binding function. GFP is driven by pRhl-RBS31.

Gene	Fold Change
rhl0lasR	26.3
rhl3lasR	27.5
rhl6lasR	26.2
rhl9lasR	28.5
rhl12lasR	25.4
rhl15lasR	33.4
rhl24lasR	38.8
rhl30lasR	17.6
rhl33lasR	26.3
rhlR	10.0

Table 3.1: Fold changes for fusion sites of rhl-X-lasR chimeras, calculated as expression at maximal C4HSL divided by expression at vehicle control.

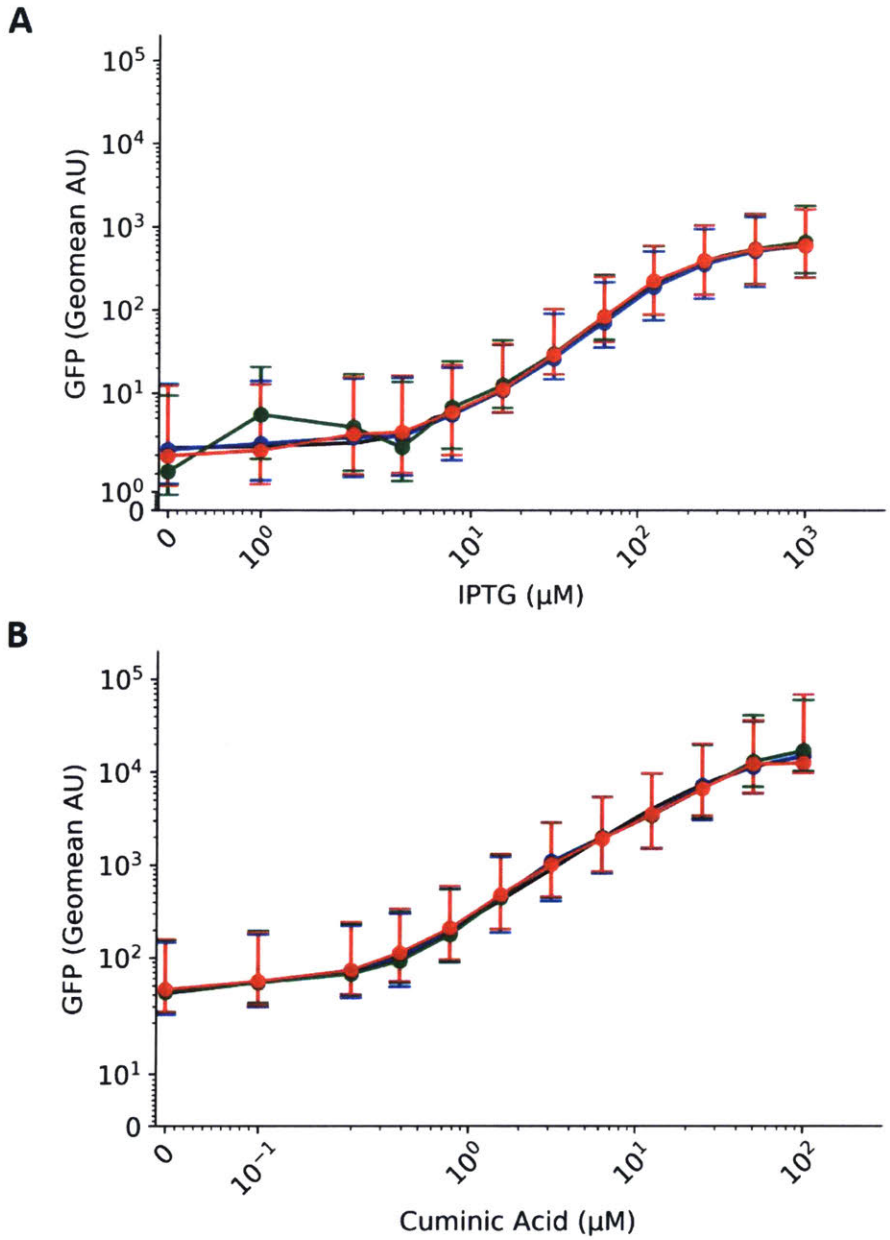

Figure 3-5: (**A**) IPTG and (**B**) Cuminic Acid reference inducer profiles. Circle: data, line: fit. Results are of triplicates performed on the same day (color) and error bars represent the geometric standard deviation within each population.

3.3.2 Control of Expression Levels for Transcription Factors

pLacIq-RBS31 constitutive expression of the chimera proteins confirmed a change in cognate promoter for the new DNA-binding domain with the same ligand-binding domain of RhlR. To further examine the expression profile of our chimeric transcription factors we adopted two orthogonal inducible systems from the Marionette collection[49]. The IPTG reference inducer (Figure 3-5A) allows for expression of an output of GFP between 5-50 AU and the cuminic acid reference inducer (Figure 3-5B) allows for expression of an output of GFP 50-15000 AU, covering an extended range.

Figure 3-7A shows the schematic for testing expression profiles of our chimeric transcription factors. IPTG relieves repression by constitutively expressed lacI using the genomic pLacI-RBS[49] allowing expression of the chimera. In the presence of AHL the chimera then activates downstream pLas promoter driving GFP. Figure 3-7B shows the 4 expression profiles for each chimera, following the characteristic Hill Function sigmoidal response to the cognate AHL signalling molecule. Rpa24lasR and Tra24lasR show basal levels comprable to empty vector. Lux24lasR, and to a lesser extent Rhl24lasR, increasingly has leaky expression as the expression of transcription factor increases.

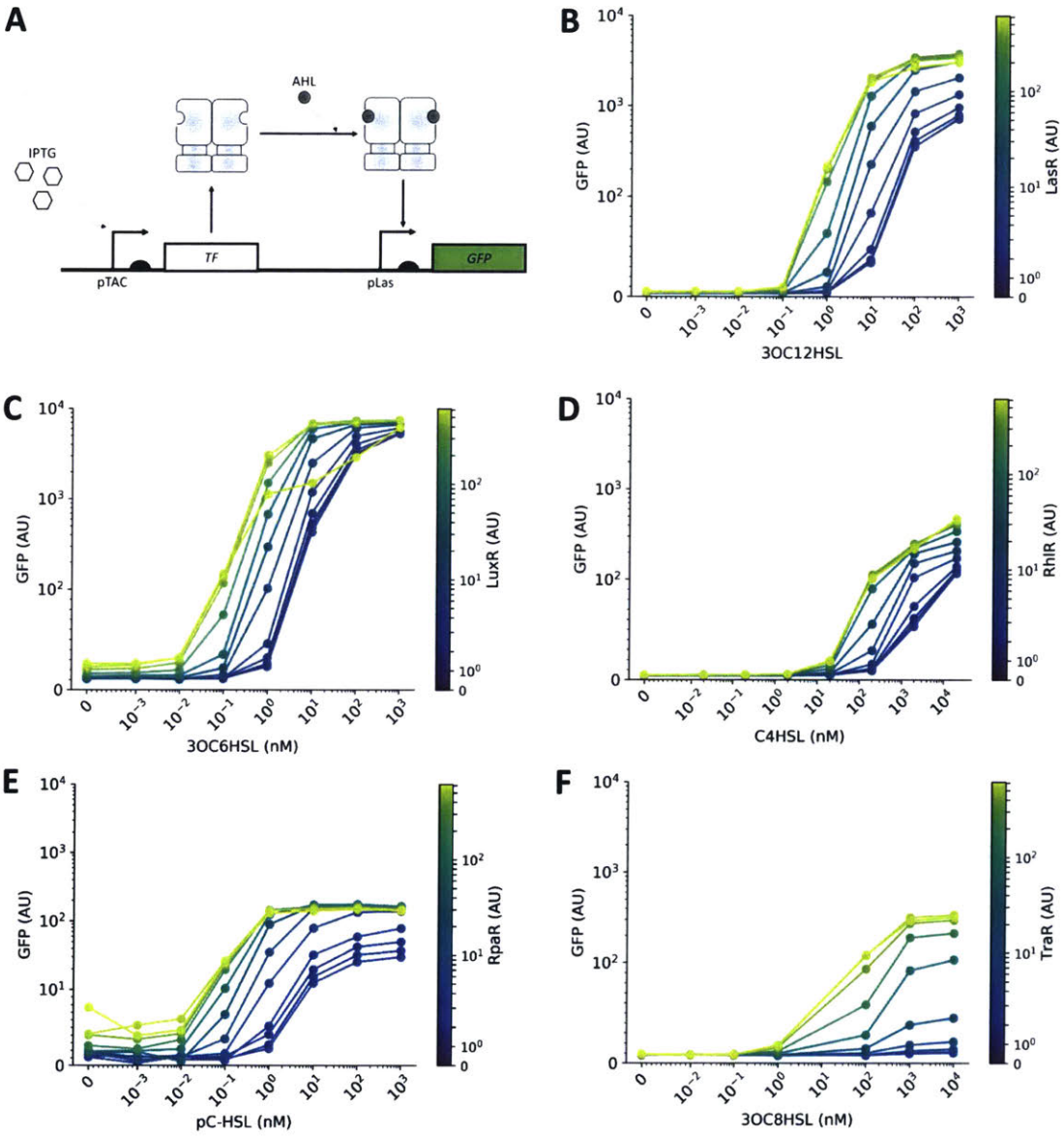

Figure 3-6: (**A**) Schematic for the induction circuit. (**B-F**) Full expression profile to each wild-type transcription factor (**B**) LasR, (**C**) RhlR, (**E**) RpaR, (**F**) TraR

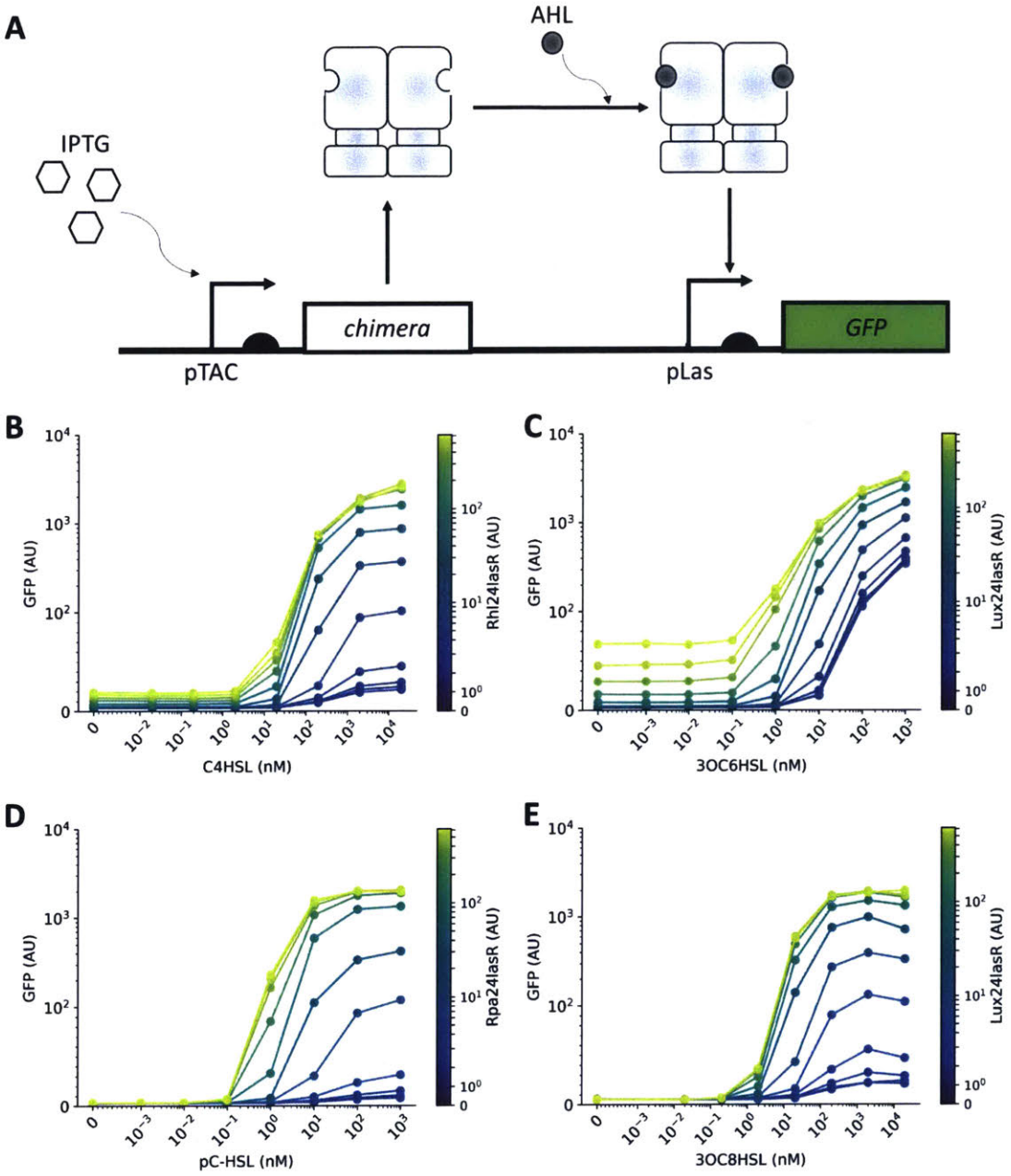

Figure 3-7: (**A.**) Schematic for the induction circuit. (**B-E**) Full expression profile to each chimeric transcription factor ((**B.**) Rhl24lasR, (**C.**) Lux24lasR, (**D.**) Rpa24lasR, (**E.**) Tra24lasR

3.3.3 Ligand Specificity of WT and Chimera Proteins

Ligand specificity in quorum sensing system is of considerable interest[56, 57, 49] and the characterization of cross-talk is essential for building robust genetic circuits[141]. Rewiring ligand-to-promoter interactions with chimeras changes the cognate AHL molecule for a transcription factor, but it is still susceptible to activation by non-cognate signalling molecules. To examine the extent our chimeras cross-talk at an AHL-protein interaction, we took each construct and examined its induction at maximal AHL (20,000 nM for 3OC8HSL and C4HSL, 1,000 nM for 3OC12HSL, 3OC6HSL, and pC-HSL).

Figure 3-8A shows that the wild-type transcription factors are mostly orthogonal with the exception of 3OC8HSL-LuxR and the reciprocal 3OC6HSL-TraR interactions. The TraR-LuxR crosstalk is expected since 3OC8HSL and 3OC6HSL share almost identical structures, differing only by two carbons in the acyl chain. Recently a mutant of LuxR was evolved to be specific to 3OC8HSL (I58N)[142], but efforts to increase specificity to its cognate 3OC6HSL were not nearly as successful. The chimeras share the same cross-talk profile for maximal AHL induction, including the off-target effects by those containing the Lux and Tra ligand-binding domain (Figure 3-8B).

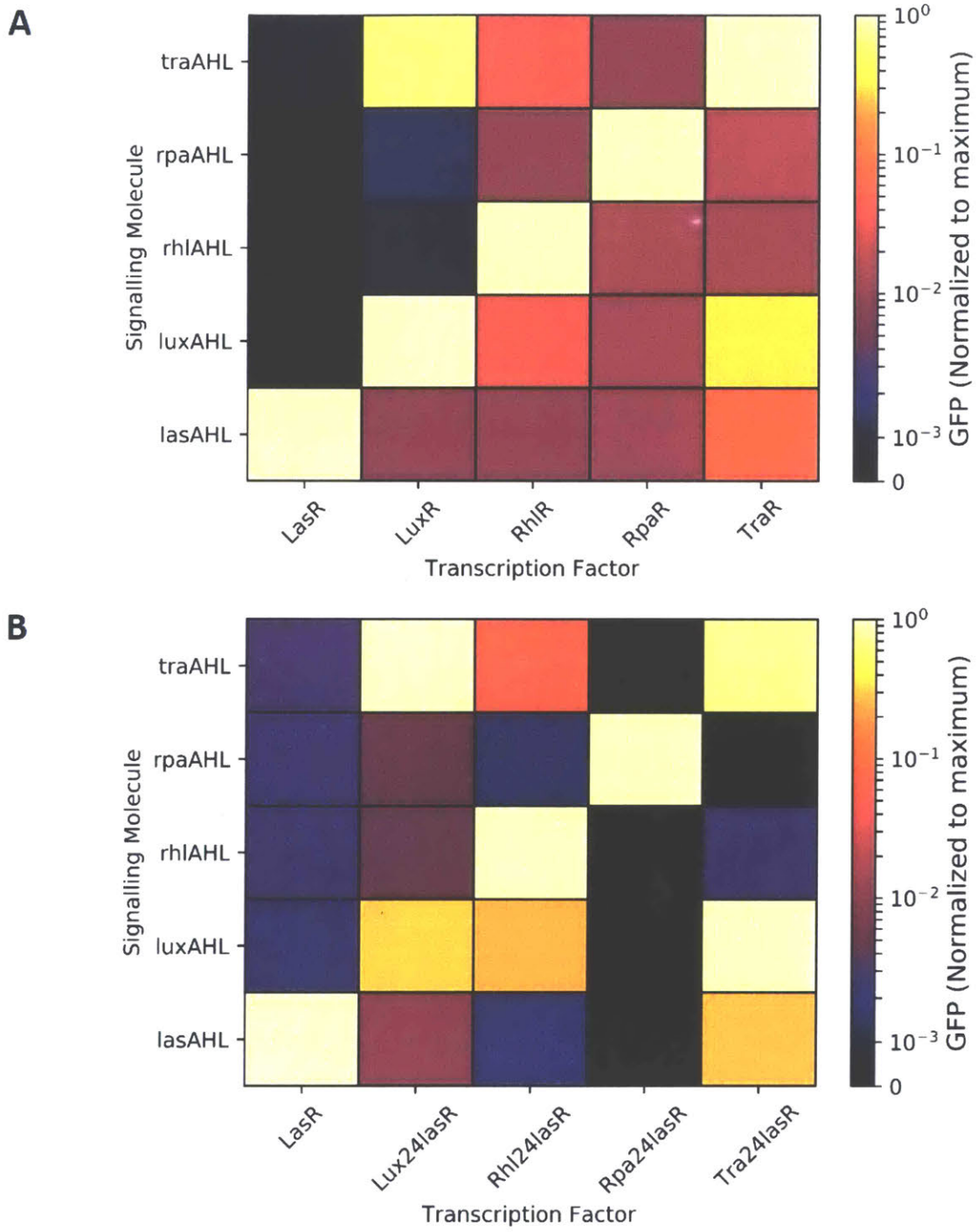

Figure 3-8: AHL Orthogonality of wild-type and chimera proteins. Expression for each transcription factor induced with each signalling molecule at its maximal induction concentration (20,000 nM for 3OC8HSL and C4HSL, 1,000 nM for 3OC12HSL, 3OC6HSL, and pC-HSL). (**A.**) Wild-type proteins were induced with 0 µM for LasR, LuxR, RhlR, RpaR, and 500 µM for TraR. (**B.**) Chimeric proteins were induced with 0 µM for LasR, Lux24lasR, and 500 µM for Rhl24lasR, Rpa24lasR, and Tra24lasR.

3.4 Conclusions and Future Directions

The diffusion kinetics of each AHL molecule determine whether usefulness for cell-cell signalling circuits concerning spatial patterning and other complex multi-cellular functions. These diffusion kinetics cannot be altered as they are intrinsic to the chemical structure of the signalling molecule. While we cannot change the structure of C4HSL or others, we can change the structure of the protein which responds to them. By creating chimeric proteins that consist of the ligand-binding domain of one protein and the DNA-binding domain of another homolog, we show that these transcription factors combine the best gene expression parameters combined with the user's choice of signalling molecule. The ability to re-wire responses widens the available useful AHL systems. An additional direction in the future may look at other DNA-binding domain such as those from *rpa*, *rhl*, or *tra*, which would open up even more possibilities for chimeras.

3.5 Experimental Details

3.5.1 Primer Design and Cloning

All genetic circuits in this work were constructed by GoldenGate [143] construction using MoClo empty vectors [144]. Full circuits were generated into one of two level 2 expression vectors. pL2f1A is the canonical pL2f1 with the pVS1 origin of replication[144](Addgene kit #1000000044) removed. pL2F was assembled by InFusion (Takara #638920) fusing a lacZ negative selection marker from pL1f1[144](Addgene kit #1000000044), p15a origin of replication from pTHSS1025 (A gift from Thomas Segall-Shapiro), and chloramphenicol resistance marker from pFNK512[88].

For chimeric proteins, designed primers amplify the ligand-binding domain and DNA-binding domain with additional BbsI restriction enzyme recognition sites at the 3' and 5' respectively. Since the standard MoClo overhangs for a level 0 coding sequence empty vector are AATG at the 5' and GCTT at the 3', so the scarless junction connecting the LBD and DBD must be orthogonal. These 2 sub-level-0 amplicons were then inserted into the pL0SC entry vector by goldengate with BbsI.

3.5.2 Steady State Induction and Flow Cytometry

M9 media was prepared as 1X M9 Salts (6.78 g/L Na_2HPO_4, 3 g/L KH2PO4, 1 g/L NH_4Cl, 0.5 g/L NaCl (Sigma-Aldrich #M6030), 0.34 g/L thiamine hydrochloride (Sigma-Aldrich #T4625), 0.2% casamino acids (Acros #61204), 2 mM $MgSO_4$ (Sigma-Aldrich #63138), 0.1 mM $CaCl_2$ (Sigma-Aldrich #3000-OP), 0.4% D-glucose (Sigma-Aldrich #G8270), with 50 µg/mL kanamycin (IBI Scientific #IBI2120) and/or 20 µg/mL chloramphenicol (IBI Scientific #IBI2080) and sterile filtered.

AHL was prepared by dissolving in DMSO, diluted to 0.5 µg/mL in DMSO (Sigma-Aldrich #D8418), and then further diluted to a working concentration in M9 media. Cuminic acid (Sigma-Aldrich #268402) was prepared by dissolving to 100 mM in ethanol. IPTG (TermoFisher #R1171) and cuminic acid were then diluted to a working concentration in M9 media.

Plasmids were transformed into NEB10-beta commercial competent cells ((New England BioLabs #C3019I)) according to manufacture's recommendations on selective LB-Agar. A single colony was picked and used to inoculate 200 uL of M9 media with antibiotics overnight in a 96-well U-bottom microplate (ELMI North America #DTS-4) at 900 RPM and 37 °C. Samples were then diluted 10 µL into 190 µL M9 media, and subsequently 10 µL into 190 µL M9 media. Following 3 hours of subculture at 900 RPM and 37 °C each well was diluted 180 µL into 1620 µL M9 media and then distributed 10 µL into a well of total 200 µL containing M9 media and inducer chemical, and then were induced for 5 hours at 900 RPM and 37 °C.

Samples were stored in 2 mg/mL Kanamycin until ran on a BD LSR Fortessa flow cytometer with HTS attachment (BD, Franklin Lakes, NJ, USA). Raw .fcs data were processed with Cytoflow[145]. Morphology gating to remove debris was performed on FSC-A vs FSC-H, and then data reported as geometric mean FITC-A (488 nm laser, 350 V, 530/30 nm filter) or geometric mean PE-Texas-Red-A (561 nm laser, 600 V, 610/20 nm filter) of cellular events. Auto-fluorescent subtraction is performed by cells containing a corresponding empty vector plasmid.

3.5.3 Plasmids

Figure	Circuit	Plasmid
3-3	constitutive rhl0lasR	pL2f1565
3-3	constitutive rhl3lasR	pL2f1566
3-3	constitutive rhl6lasR	pL2f1567
3-3	constitutive rhl9lasR	pL2f1568
3-3	constitutive rhl12lasR	pL2f1569
3-3	constitutive rhl15lasR	pL2f1570
3-3	constitutiverhl24lasR	pL2f1572
3-3	constitutive rhl30lasR	pL2f1573
3-3	constitutive rhl33lasR	pL2f1574
3-3	constitutive rhlR	pL2f1577

3-5	IPTG reference	pL2f1768
3-5	Cuminic reference	pL2f1773
3-7, 3-8	Inducible Lux24lasR	pL2f1941
3-7, 3-8	Inducible Rhl24lasR	pL2f1942
3-7, 3-8	Inducible Rpa24lasR	pL2f1943
3-7, 3-8	Inducible Tra24lasR	pL2f1982
3-8	Inducible LasR	pL2f1787
3-8	Inducible LuxR	pL2f1826
3-8	Inducible RhlR	pL2f1829
3-8	Inducible RpaR	pL2f1817
3-8	Inducible TraR	pL2f1893

Table 3.2: Plasmids used in this chapter

Chapter 4

Molecular Sequestration of LuxR-type Transcription Factors

Christian Cuba collaborated with the experimental design and theory for this project. Parts of this chapter have been adapted for a prepared manuscript *Engineering Molecular Sequestration of Quorum Sensing Proteins* Nicholas A DeLateur, Christian S. Cuba, Ron Weiss. In addition parts of this chapter have been adapted from "Biomolecular stabilisation near the unstable equilibrium of a biological system". Christian Cuba Samaniego, Nicholas A. DeLateur, Giulia Giordano, and Elisa Franco, Accepted to IEEE 58th Annual Conference on Decision and Control, CDC 2019.

4.1 Motivation

Traditionally the regulation of genes, and therefore the phenotype of a biological system, is done at the transcriptional level[146]. Activators and repressors influence the expression of promoters and the downstream genetic components by binding to, or not binding to, the promoter elements of the DNA[147]. The biggest advantage of this genetic circuit engineering paradigm is the modularity; once a transcriptional system has been well characterized, the downstream genes can be swapped out at will or even designed in an automated fashion[146, 148].

The original design for a simple Turing Pattern genetic circuit consists of an

activator species and an inhibitor species that diffuse at different rates[132] (Figure 2-2A). However for gram-negative quorum sensing systems the presence of the signalling molecule only leads to an increase in downstream gene expression, leading to exclusively activation systems. There is a subset of LuxR-family proteins based on *esaR*[149] which have an inverted mechanism to the canonical LuxR. EsaR binds tightly to its cognate promoter until it is relieved in the presence of 3OC6HSL [150]. However, since this leads to the same input-output relationship, there are no gram-negative bacteria quorum sensing systems where an increase in AHL leads to a decrease in expression without one or more intermediate transcriptional steps.

This design constraint led to our Turing Pattern genetic circuit topology where the activation species is 3OC12HSL and our inhibiting species is C4HSL; since RhlR is an activator we have RhlR express the λ phage repressor CI which then represses transcription of all genes associated with the Turing Pattern genetic circuit (Figure 2-2B). However transcriptional control is slow compared to enzymatic or protein-protein interactions, adding another time-step to the system before it can come to equilibrium[151, 152].

Inspired to find solutions that could alleviate this gap in the field we examined possibilities for controlling quorum sensing circuits in a manner that was (1) direct and (2) fast.

Quorum quenching enzymes exist as natural defensive mechanisms in many bacteria [153, 154, 155]. The most common is AiiA, a lactonase that hydrolytically cleaves the homoserine lactone ring rendering them inert[141, 156], has also been reported in *A. tumefaciens* as AttM[157]. AiiA can be a powerful modulator of the quorum sensing threshold response and has been used or proposed in many recent advanced genetic circuits[48, 158].

However since all AHL molecules have a homoserine moiety AiiA does not discriminate in its quorum quenching[159] leaving the field with a empty space of genetically coded devices to halt quorum sensing activity in a fast and specific manner. Next, we turned to natural gene regulations architectures from the genomes of *P. aeruginosa* and *A. tumefaciens* themselves for proteins that were specific to quorum sensing

transcription factors.

4.2 Results

4.2.1 QslA and QteE

In *P. aeruginosa* there are three quorum sensing systems based on LuxR-family proteins: LasR, RhlR, and QscR[160, 161] and a large mutli-level hierarchy regulating their activity[162]. QscR[163] is an orphan (has no unique cognate signalling molecule[164, 165]) transcription factor who's function as a global regulator are still being uncovered[166].

In addition to the transcription factors there are two other proteins which directly regulate the transcription factors: QslA and QteE. QslA shares no sequence homology with LasR and is itself much smaller at 114 amino acids (compared to LasR's 239). QslA forms homodimers which then form heterotrimer quaternary structures with LasR monomers preventing dimerization and downstream gene activation[167]. QslA can insert itself into already formed LasR-AHL homodimers[167] and is AHL-independent[168]. Transcription and translation of *lasR* is unaffected by QslA levels[168].

In contrast to QslA preventing dimerization of the LasR-AHL complexes, QteE degrades both LasR and to a lessor extent RhlR proteins without affecting transcription or translation and in an AHL-independent manner[169]. There has been no further inquiry into the biochemical mechanism of QteE, although there have been some subsequent analysis of it's effect on downstream phenotypes[170, 161, 159]. QscR, QslA, and QteE have overlapping but non-identical effects on *P. aeruginosa* transcriptome consistent with their unique mechanisms[161]. To characterize the effects QslA and QteE would have on quorum sensing gene expression, we cloned both *lasR* and then either *qslA* or *qteE* as shown in Figure 4-1A under orthogonal inducible control. QslA (Figure 4-1B) monotonically decreased GFP expression with additional QslA induction in a tunable manner. QteE (Figure 4-1C) eliminated all downstream gene activation except for the lowest of cuminic acid inductions, suggesting a cat-

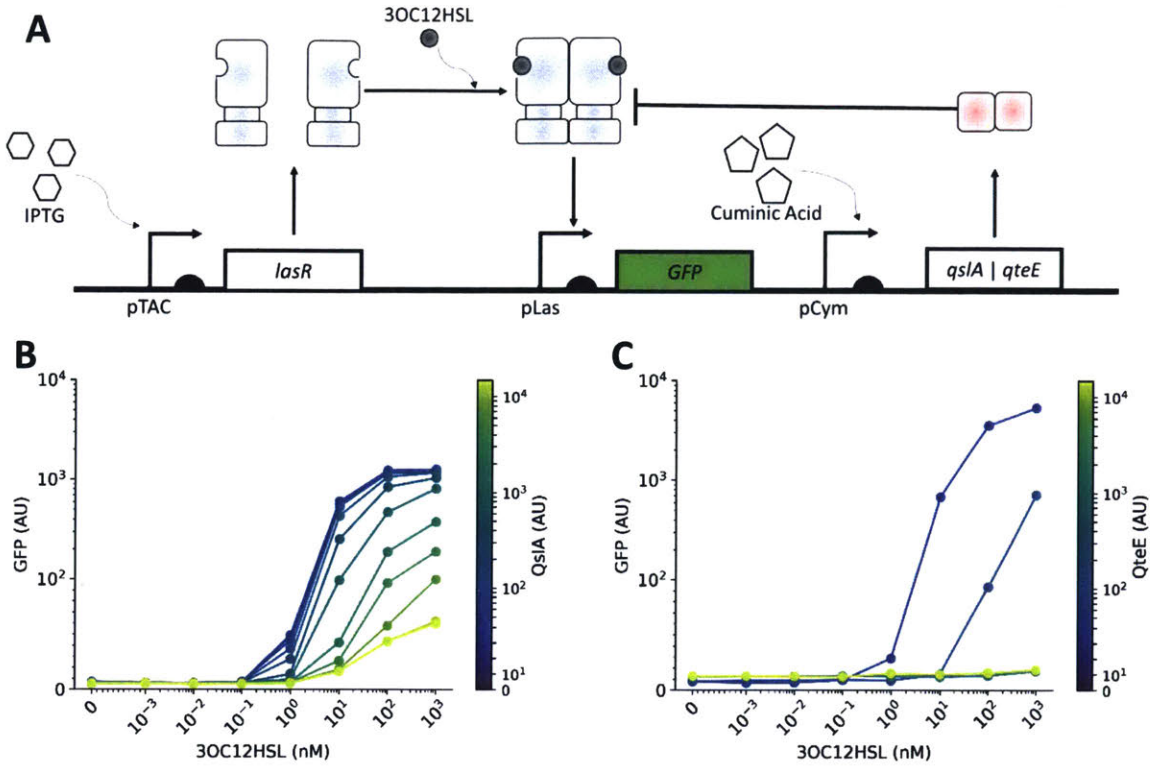

Figure 4-1: **A.** Schematic of the genetic circuit. IPTG, here held constant at 0 µM, induces expression of the transcription factor LasR, which in the presence of 3OC12HSL dimerizes and can recruit transcriptional machinery to drive expression off the pLas promoter. Cuminic acid induces the sequester protein. QslA acts as a homodimer; it is not known what quaternary structure QteE takes. **B.** QslA shows strong knockdown of GFP with increasing expression in a monotonic manner.**C.** QteE greatly knocks down LasR activity, completely ablating downstream expression at moderate or higher levels of QteE.

alytic mechanism capable of turning over multiple LasR proteins (whether monomer or dimer) per QteE active form. To completely knock down all activity of LasR, which at the minimal expression used in Figure 4-1 has a K_D of 100 nM 3OC12HSL (Figure 3-6) represents an extremely powerful sequester strategy.

4.2.2 TraM and TraM2

With rare full-length crystal structures of the LuxR-homolog TraR[84] and well-characterized inhibitors the *tra* regulatory system has the some of the richest biochemical characterization to draw upon[171] for bacterial quorum sensing systems. To control the quorum sensing response in *A. tumefaciens* TraM sets a thresholding

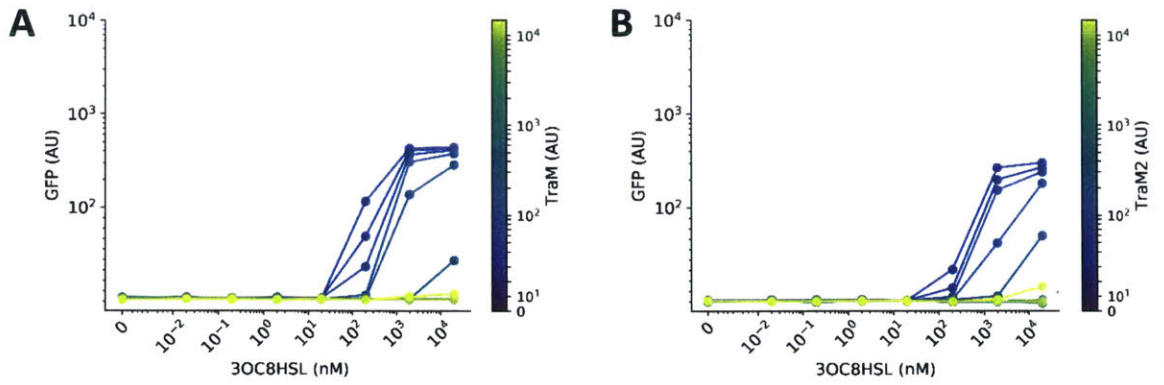

Figure 4-2: IPTG, here held constant at 500 µM, induces TraR using the same genetic circuit topology as Figure 4-1A). **A.** TraM and **B.** TraM2 show strong sequestration with minimal expression over TraR.

response controlling TraR activity[172] that is AHL-independent and affects TraR at a protein level without interference to transcription or translation[173]. TraM forms a homodimer followed by binding with the DNA-binding domain of an active TraR dimer[174, 175] to form a dimer-dimer complex occluded from DNA-binding[85, 86, 176].

Using the same circuitry motif as Figure 4-1, we tested the potential for TraM and TraM2[177] to knock down TraR expression in our genetic circuits. As expected both TraM (Figure 4-2A) and TraM2 (Figure 4-2B) showed considerable sequestration of TraR with moderate inductions of sequester protein completely ablating activity.

4.2.3 A Poor Toolkit

Since QslA, QteE, TraM, and TraM2 are extremely specific to their natural targets (Figure 4-3) this results in a gap for circuit design. LuxR and RpaR have useful properties to give reason to a synthetic biologist for use in genetic circuits, however there are no sequester proteins for these systems (Figure 4-3), much less for an arbitrary LuxR-family homolog of interest. While powerful regulators, these proteins are currently intractable for adaptation to other useful quorum sensing systems due to their highly specific tertiary structure mechanisms. While RhlR can be targeted by QteE, it comes at a significant cost of ablating all LasR activity (Figure 4-3).

As expected TraM and TraM2 have no effect on Tra24lasR chimera proteins (Figure 4-4) since they do not have the *tra* DNA-binding domain. QslA similarly has no effect on chimeras lacking it's natural target of the *las* ligand-binding domain. QteE acts as a master regulator ablating almost all downstream expression from chimeric quorum sensing proteins with a *las* DNA-binding domain. The fact that QteE targets the *las* DNA-binding domain brings us closer to understanding it's mechanism of action as while it has been proposed that the mechanism of QteE works analogously to TraM[169], however no other subsequent study has provided evidence for this conjecture.

This current toolkit for sequestration of quorum sensing transcription factors is inadequate in both breadth and specificity. It lacks tools and the design principles to build them that are capable of knocking down known (LuxR, RpaR) or future transcription factors.

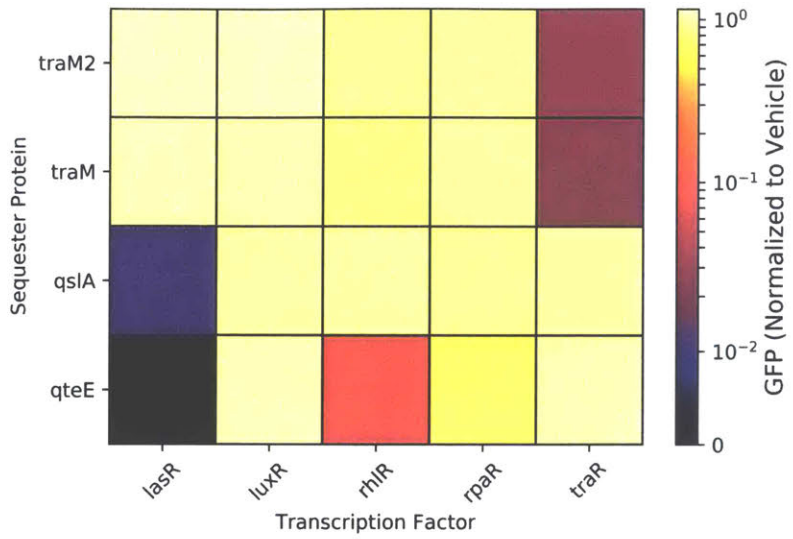

Figure 4-3: Heatmap for knockdown by natural sequester proteins co-expressed with wild-type five LuxR-family transcription factors with maximal AHL induction. Values are normalized to GFP expression when sequester proteins is completely uninduced. AHL concentrations are 20,000 nM for 3OC8HSL and C4HSL, 1,000 nM for 3OC12HSL, 3OC6HSL, and pC-HSL. LasR, LuxR, RhlR, RpaR: 0 µM IPTG, TraR: 500 µM IPTG.

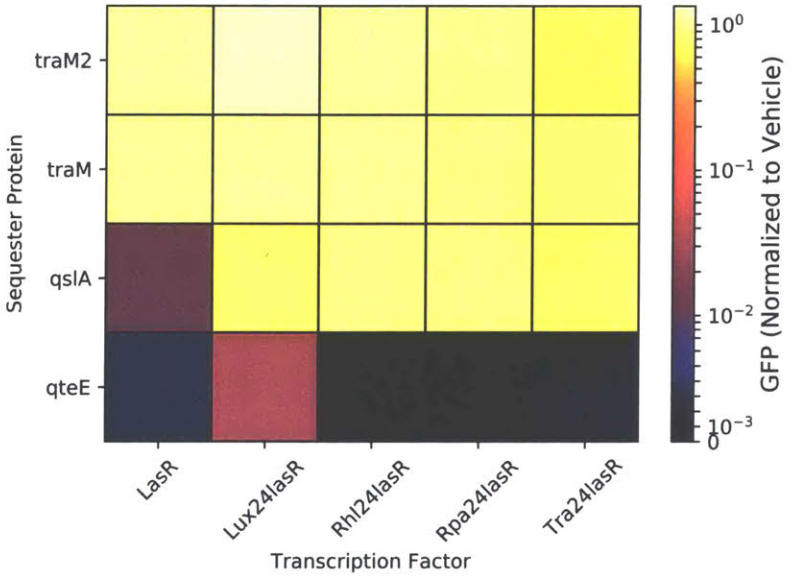

Figure 4-4: Heatmap for knockdown by natural sequester proteins co-expressed with chimeric LuxR-family transcription factors with maximal AHL induction. Values are normalized to GFP expression when sequester proteins is completely uninduced. AHL concentrations are 20,000 nM for 3OC8HSL and C4HSL, 1,000 nM for 3OC12HSL, 3OC6HSL, and pC-HSL. Lux24lasR: 0 µM IPTG, Rhl24lasR, Rpa24lasR, Tra24lasR: 500 µM IPTG.

Figure 4-5: Pairwise alignment between *traR* and *trlR* using ClustalW algorithm[136] with amino acids coded by color.

4.2.4 TrlR

In *A. tumefaciens* there was a duplication and then deletion event of the *traR* gene resulting in the gene *trlR* [178]. TrlR is 89% identical and 95% similar to TraR for the 181 N-terminal amino acid sequence. Figure 4-5 shows that after a "KEATY" sequence at positions 176-181, there is no similarity between the resulting residues. TrlR then has a premature stop codon following an additional 31 amino acids following the KEATY sequence. This leads to a natural proposed mechanism: TrlR forms heterodimers with TraR that are incompetent for binding to the *tra* box and activating downstream expression[178] which was later validated biochemically[179].

TrlR is the weakest natural sequester protein tested to date (Figure 4-6), compared to QslA, QteE, TraM, or TraM2, and does little to fix the inadequacy of the current toolkit's breadth by being the 3rd protein to sequester TraR when many other homologs have none. However TrlR is tractable in the design principles that allow us to design sequester proteins for other homologes. *trlR* suggests an easy heuristic:

- Express a truncated protein product identical to the first the transcription factor of interest that terminates once it reaches the equivalent "KEATY" sequence.

This strategy is extremely compelling not only due to the ease of implementation, but the proposed mechanism of action. TrlR creates incompetent heterodimers with TraR, sequestering away what would otherwise be active monomer molecules[179].

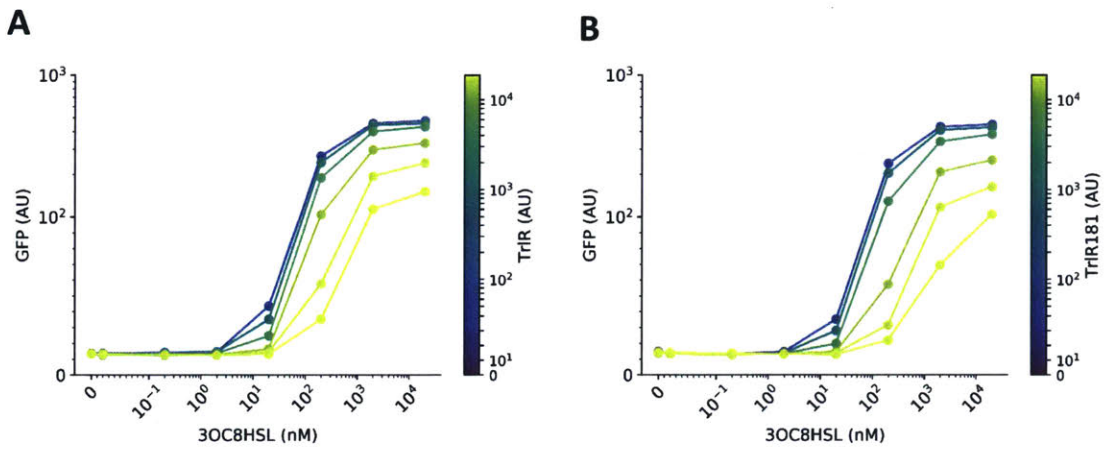

Figure 4-6: TrlR compared to TrlR181 for sequestration profile. TraR: 500 µM IPTG. TrlR181, afterwards abbreviated to TrlRt, contains only the first 181 amino acids of the full length TrlR.

An essential initial question however is whether the additional 31 amino acids found after the KEATY sequence in trlR are necessary for sequestration function.

To answer this question, we truncated TrlR (denoted throughout as TrlRt) at position 181 where it no longer matched TraR, and compared the knockdown effects. Figure 4-6 shows that TrlR and TrlRt have similar molecular sequestration properties. We then hypothesized that this approach would allow us to design sequestration proteins for our 4 other major quorum sensing transcription factors: LasR, LuxR, RhlR, and RpaR. Importantly, this approach would require

1. No structural knowledge of the LuxR protein
2. No biochemical knowledge of the LuxR protein
3. **Only** the sequence of interest

making it as useful as possible to the broader community and newly-discovered quorum sensing systems with minimal engineering required.

Parent Protein	Truncation Position	Remaining DBD
LasR	184	LTSREKEV
LuxR	190	LTKREKEC
RhlR	188	LSHREREI
TrlR	181	LDPKEATY
RpaR	188	LTPRECEI

Table 4.1: Truncation positions for LasRt, LuxRt, RhlRt, TrlRt, and RpaRt. The remaining DBD portion is highly conserved.

4.2.5 Sequestration of WT transcription factors

To test our hypothesis we created truncated versions of each of the 4 other major LuxR-family transcription factors (LasR, LuxR, RhlR, and Rpar). These genes are denoted as the parent gene with a suffix of "t" (LasRt is the truncated form of LasR for example). The end of homology between TrlR and TraR resides directly at an ultra-conserved leucine 9 residues into the DNA-binding domain (Figure 3-1). The specific truncation positions are listed in Table 4.1 for reference; while all LuxR-proteins have similar post-linker sequences to initiate the DNA-binding domain, not all proteins have identical lengths to their ligand-binding domain.

LuxR-family transcription factors are incredibly sensitive (Figure 3-6)[18, 156] so for all but TraR initial knockdown was performed using minimal expression by basal activity of the LacIAM-pTAC system[49] with the exception of TraR who requires much higher expression levels for full dynamic range (Figure 3-6)[56]. Figure 4-7 shows that for all 5 wild-type transcription factors increasing expression of the corresponding truncation product results in a monotonic decrease in downstream gene expression. These results are with no additional engineering of the truncation products. Effective K_D values of each system are shifted right to require higher concentrations of AHL as more sequester protein enters the system, as well as lower maximal expressions.

A unique behavior for LasRt is having a pronounced effect at the highest AHL concentration that turns the classic Hill Function response curve downwards at the highest levels. This is a consistent phenomenon with LasRt (Figure 4-8B). At this time we don't have clear mechanistic evidence for why this happens with LasRt, but

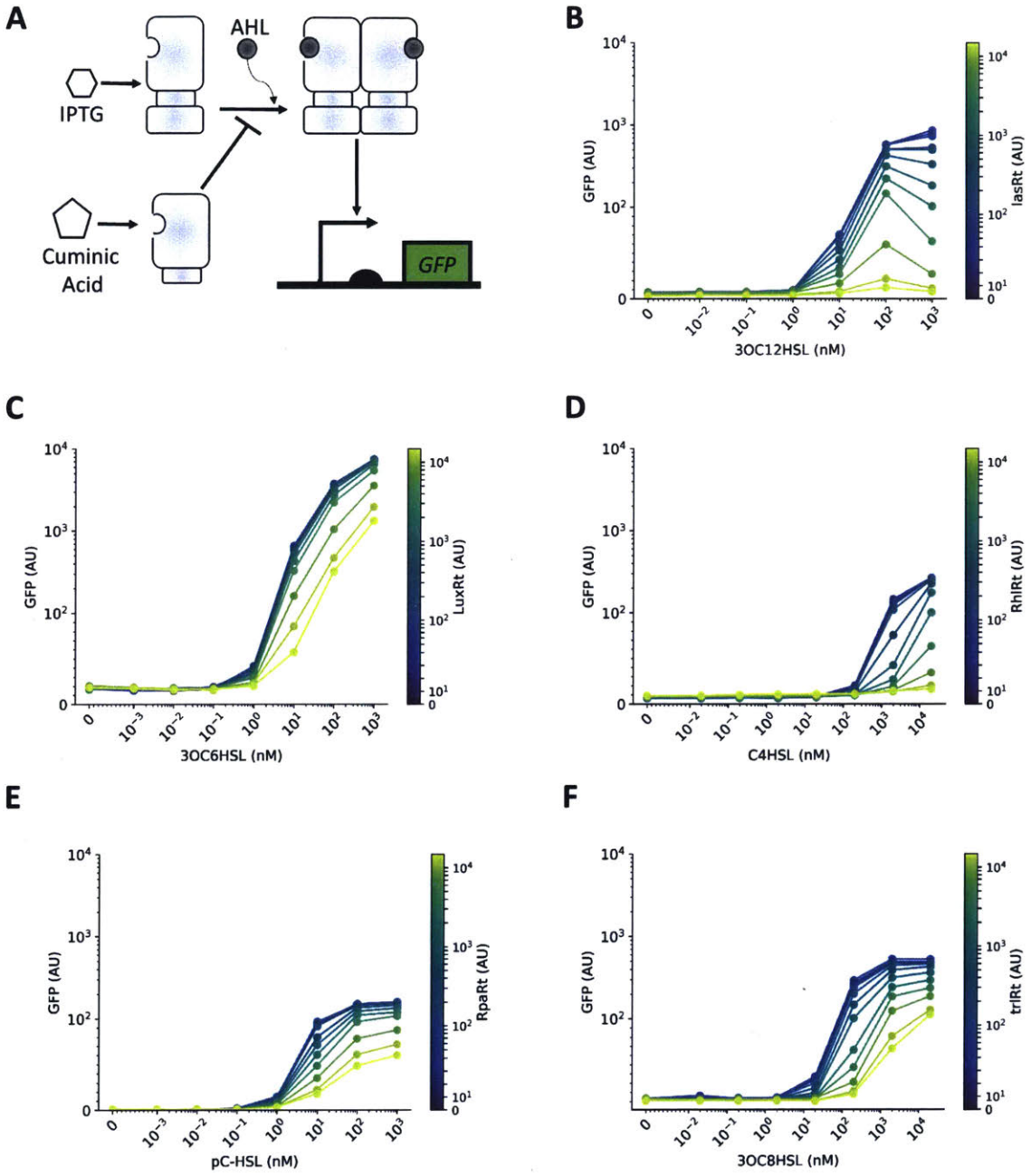

Figure 4-7: Sequestration of wild-type transcription factors by truncation protein products. **A.** Schematic representation of the gene circuit. **B.** LasR, **C.** LuxR, **D.** RhlR, **E.** RpaR, **F.** TraR expression profiles with constant transcription factor and titrated sequester protein. LasR, LuxR, RhlR, RpaR: 0 µM IPTG, TraR: 500 µM IPTG.

it represents another facet that future modeling might be able to help uncover. This behavior is absent from all other systems tested, but also notably QslA which targets the same transcription factor (Figure 4-1A), suggesting that QslA and LasRt may have subtle differences in when during the folding and ligand-binding processes they sequester LasR monomers.

After showing our truncation proteins can sequester wild-type transcription factors in a dose-dependent manner we asked whether GFP levels could be restored by dosing additional full-length protein. Figure 4-8 shows GFP levels when truncation protein is fully induced with 500 µM cuminic acid and the transcription factor is titrated. At full expression of full length protein (~500 AU) for LasR, LuxR, and RpaR sequestration can be completely overcome while RhlR and TraR are still repressed.

Leakiness from a promoter is almost invariably an undesired trait in genetic systems, especially for those being used to build genetic circuits[49]. In the absence of sequester proteins the *lux* and *rpa* systems can show basal expression that increases proportionally to the levels of transcription factor in the system (Figure 3-6C, E). In the presence of sequester proteins (Figure 4-7C, E) this basal expression is eliminated back to minimal levels. It has been proposed that in quorum sensing systems natural sequester proteins are used for this function as a sink to create absolute control over leaky expression which would otherwise allow quorum sensing systems to activate prematurely[166, 171].

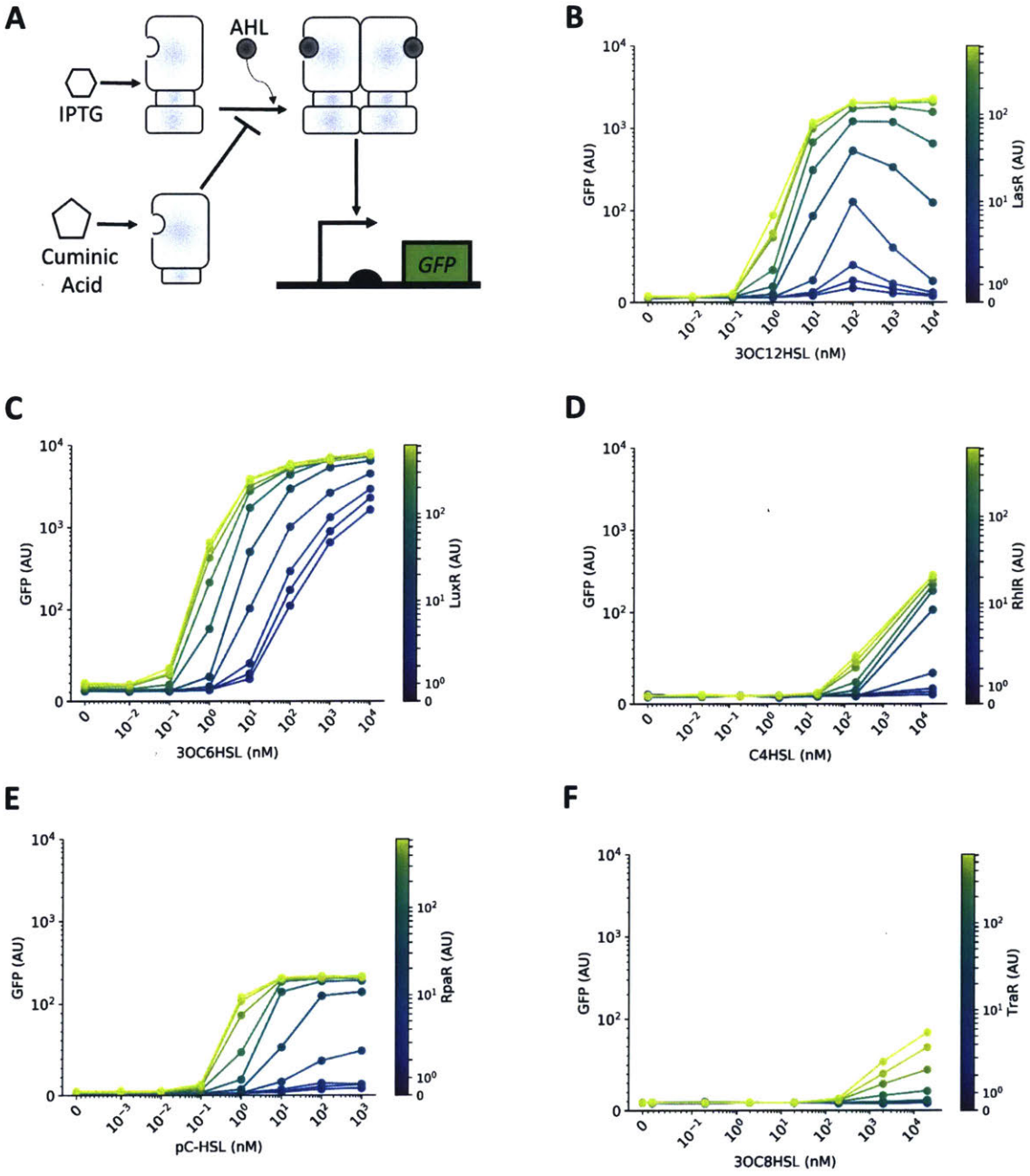

Figure 4-8: Recovery of GFP expression by induction of transcription factor over maximal induction of sequestration protein. **A.** Schematic representation of the gene circuit. **B.** LasR, **C.** LuxR, **D.** RhlR, **E.** RpaR, **F.** TraR mediated GFP expression in response to high levels of corresponding truncation protein (500 µM cuminic acid).

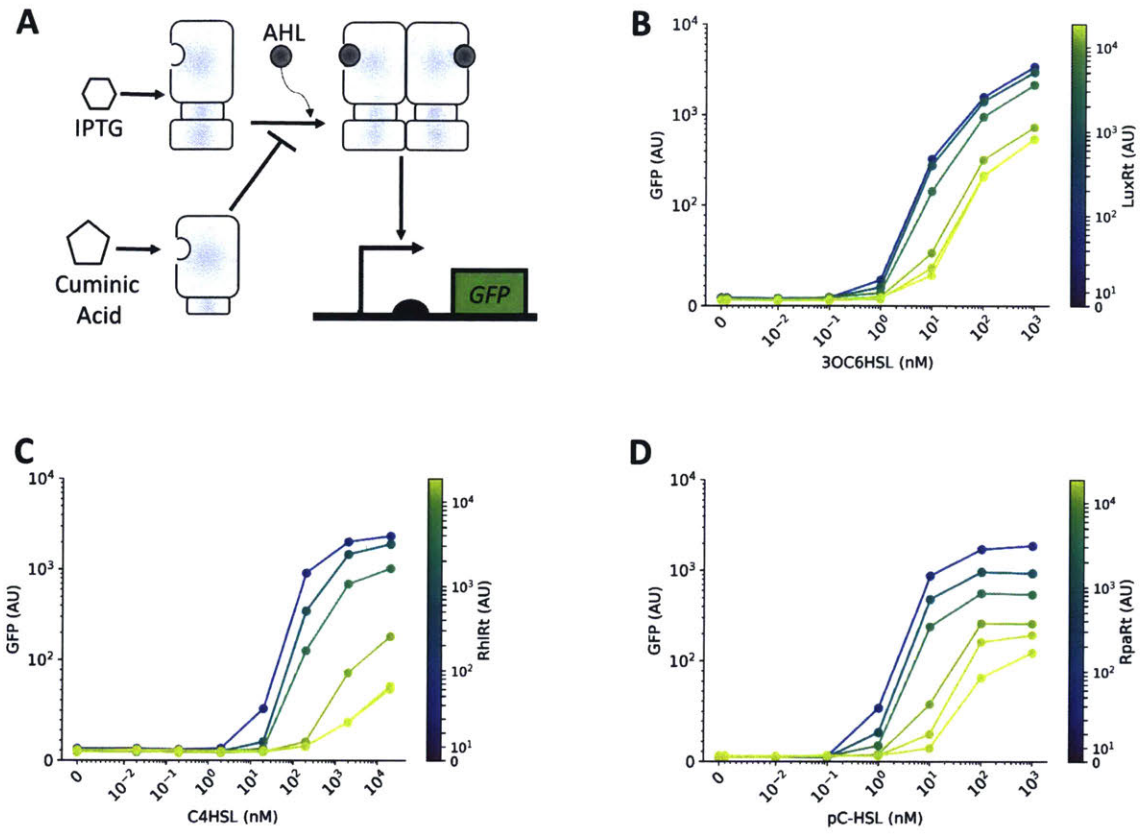

Figure 4-9: Sequestration of chimeric transcription factors by corresponding truncation product. **A.** Schematic representation of the gene circuit. **B.** Lux24lasR, **C.** Rhl24lasR, **D.** Rpa24lasR GFP expression in response to titration of corresponding truncation protein. Chimeras induced at 500 µM IPTG.

4.2.6 Sequestration of chimeric transcription factors

Chimeric transcription factors are also robustly sequestered by the corresponding truncation product (Figure 4-9). Chimeras were induced with 62.5 µM IPTG and then truncation sequester protein titrated with up to 1000 µM cuminic acid (Figure 4-9A). As previously with full-length wild type proteins, *lux* ligand-binding domain was most resistant to sequestration (Figure 4-9B) but up to 10-fold repression was still possible even at maximal AHL input.

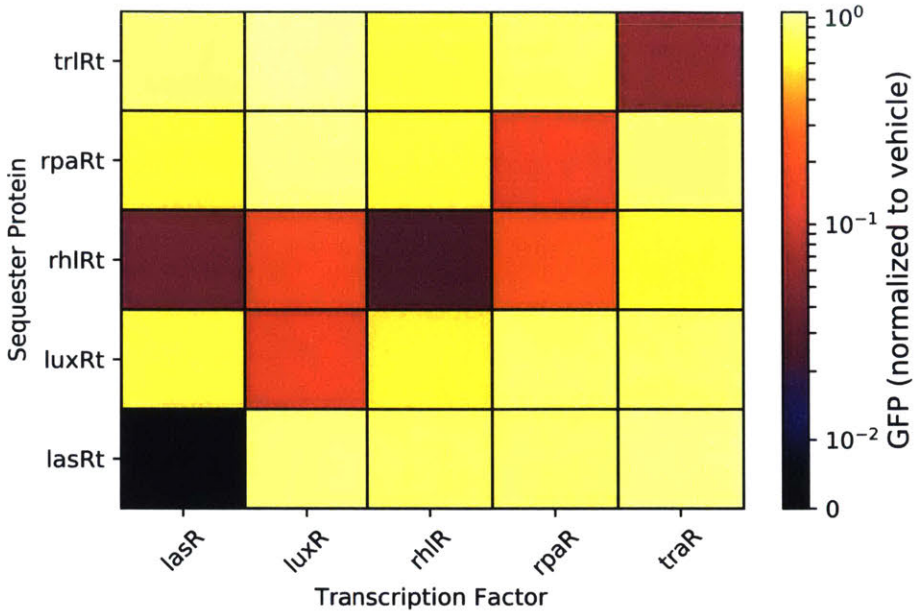

Figure 4-10: Heatmap for knockdown by truncation proteins co-expressed with wild-type five LuxR-family transcription factors with maximal AHL induction. Values are normalized to GFP expression when sequester proteins is completely uninduced. AHL concentrations are 20,000 nM for 3OC8HSL and C4HSL, 1,000 nM for 3OC12HSL, 3OC6HSL, and pC-HSL. LasR, LuxR, RhlR, RpaR: 0 µM IPTG, TraR: 500 µM IPTG.

4.2.7 Specificity of knockdown

Sequester truncation protein specificity matches to their full-length protein product with the exception of RhlRt (Figure 4-10). RhlRt shows moderate to severe off-target knockdown to LasR, LuxR, and RpaR in addition to it's strongest effect on the wild-type RhlR protein. TraR shows the most resistance to RhlRt off-target sequestration, however TraR is expressed at ~100-fold higher levels (0 µM compared to 500 µM IPTG (Figure 3-5A)); low levels of TraR result in no detectible response to 3OC8HSL (Figure 3-6). These trends are mirrored when examining the specificity of truncation sequester proteins on the X-lasR chimeras (Figure 4-11).

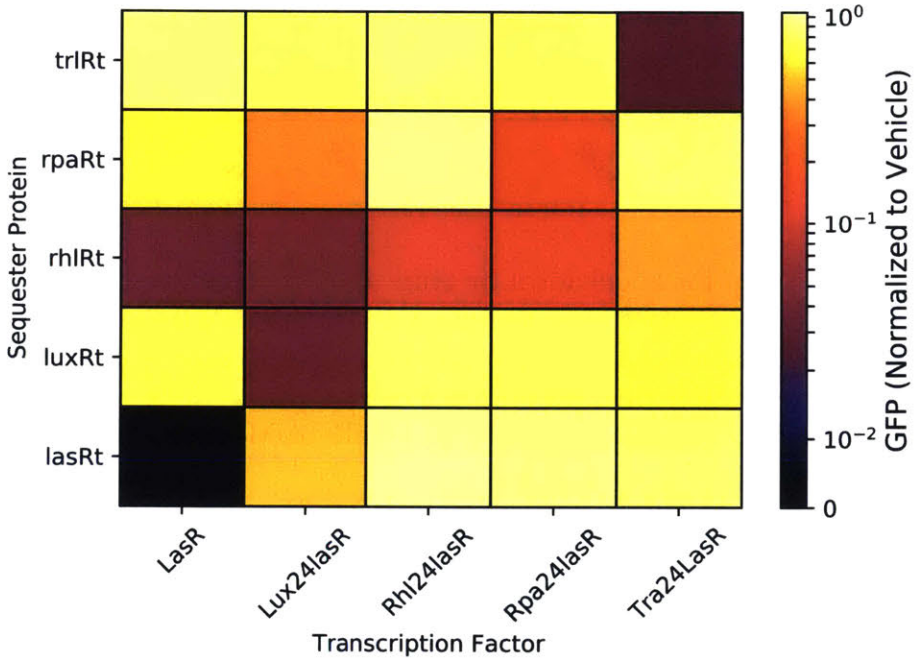

Figure 4-11: Heatmap for knockdown by truncation proteins co-expressed with chimeric transcription factors with maximal AHL induction. Values are normalized to GFP expression when sequester proteins is completely uninduced. AHL concentrations are 20,000 nM for 3OC8HSL and C4HSL, 1,000 nM for 3OC12HSL, 3OC6HSL, and pC-HSL. Lux24lasR: 0 µM IPTG, Rhl24lasR, Rpa24lasR, Tra24lasR: 500 µM IPTG.

4.2.8 Linearization and Speed

Feedback control of transcription factors underlies natural gene regulation[180, 181, 182]. Negative feedback in closed loop circuits attenuates gene expression lowering variance and increasing robustness against exogenous perturbation[50, 183, 184]. To demonstrate our circuits utilizing molecular sequestration can take advantage of classic feedback mechanisms, we demonstrate the linearization of input-ouput response curves by negative feedback also known as auto-regulation[185, 186].

The gene for *qslA* was put under either inducible control (Open Loop) or *las* control (Closed Loop)(Figure 4-12A-B). LasR is titrated by addition of IPTG. As levels of LasR increase, so do GFP levels which is under pLas control. In the Open Loop system this response can be modulated by expression of QslA by and only by exogenous control (here, cuminic acid) and gives a characteristic response curve that rises sharply before leveling off to an asymptotic maximal. When the expression of QslA is controlled by LasR concentrations this completes the feedback and the resulting auto-regulation results in a more linear response (Figure 4-12C) as QslA modulates both it's own levels and LasR's.

To demonstrate the improved properties of using molecular sequestration, we examined the temporal properties of GFP expression when mediating TraR activity by competing paradigms (Figure 4-13). An open-loop induction circuit of TraR was put into the "ON" state by additional of 20,000 nM 3OC8HSL. To track molecular sequestration, TraM was induced by addition of 500 µM cuminic acid, while retaining full AHL. The rest of the culture was thoroughly washed of any IPTG. The presence of IPTG relieves repression of pTAC by LacI, with the removal of IPTG LacI represses transcription from the pTAC promoter driving TraR.

Figure 4-13 demonstrates that the delay in GFP signal loss is greater with traditional transcriptional repression than molecular sequestration. Transcriptional control depends on the kinetics of dilution and degradation as the current pool of transcription factor complexes are still active even when no more are being produced. In contrast, using molecular sequestration to shut off expression does not require the

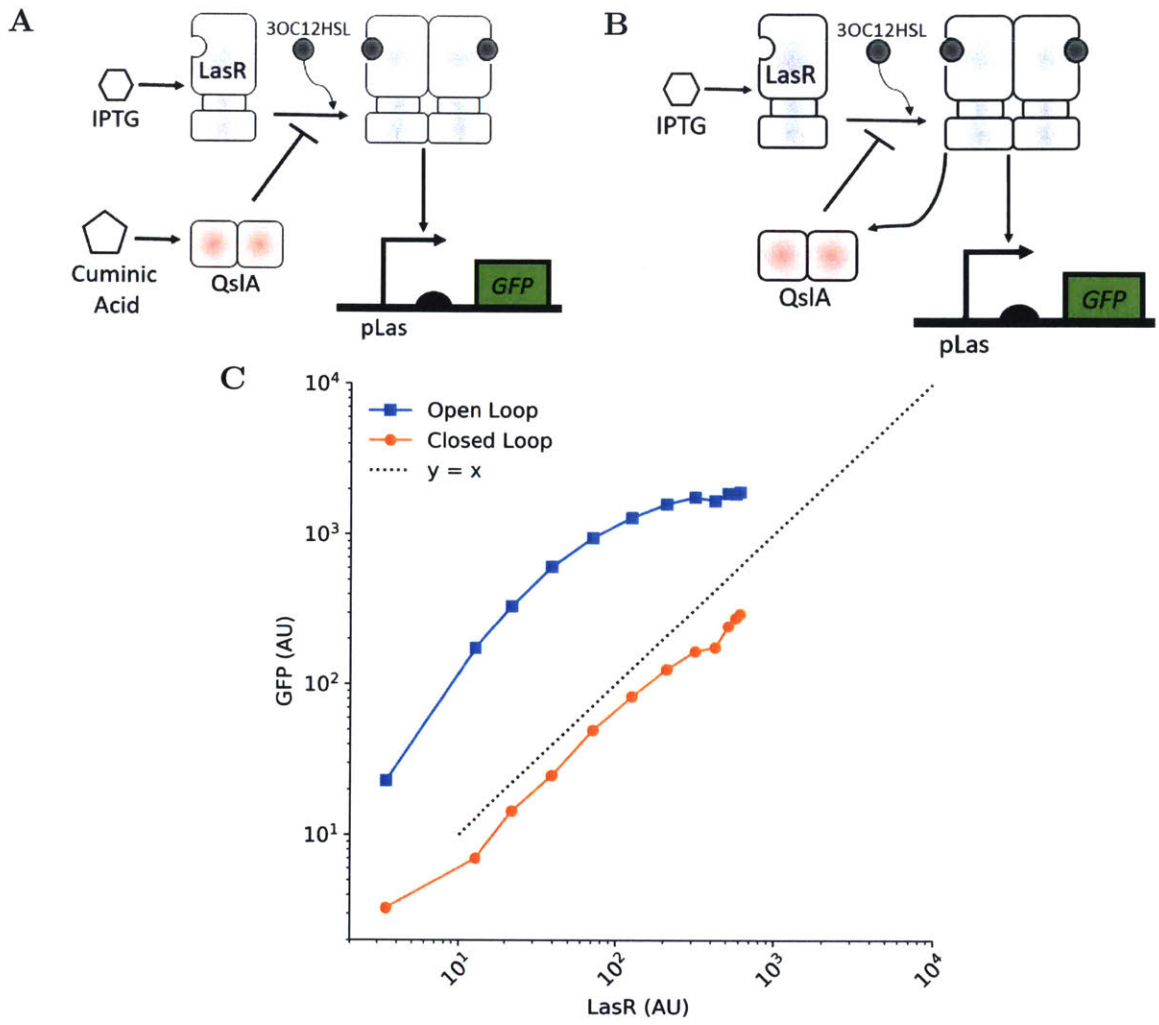

Figure 4-12: **A.** Closed loop vs Open loop genetic circuit schematic. QslA expression is controlled by exogenous cuminic acid (Open Loop) or LasR driving pLas (Closed Loop). **B.** Closing the loop results in feedback control that aligns expression along the y=x line between transcription factor and output.

dilution and degradation of the current transcription factor pool resulting in a faster update to the internal state of the cell[183, 184, 187].

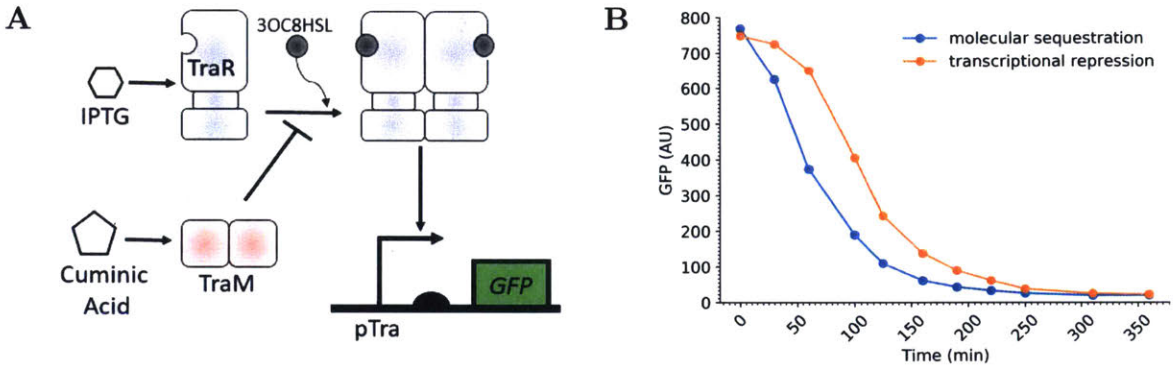

Figure 4-13: **A.** Genetic circuit schematic. TraR expression can be derepressed by IPTG (transcriptional repression, orange) and sequestered by induction of TraM by cuminic acid (molecular sequestration, blue). **B.** Temporal dynamics. Both populations started at 500 500 µM IPTG and 20,000 nM 3OC8HSL; for transcriptional repression the IPTG was removed, for molecular sequestration 50 µM cuminic acid was introduced.

4.3 Conclusions and Future Directions

Quorum sensing systems are ubiquitous in the field of synthetic biology and in particular complex genetic circuits that require cell-cell signalling. As the use of quorum sensing is integrated into logic behavior requiring more "wires" and gates, the need for direct and robust control of downstream gene expression increases. In this chapter I show the lack of tools to perform molecular sequestration at a protein-protein interaction level in the field currently for either wild-type transcription factors or the new chimeras developed in Chapter 3. I then develop a rational design protein engineering strategy to co-express truncated protein products and show that they knock down expression of their cognate full-length protein as expected.

Future work to optimize the system may include looking at additional truncation sites to either increase potency or reduce promiscuity of RhlRt. Another direction would be to attempt changing the specificity of QteE or TraM sequester proteins to harness their more powerful sequestration profiles. Due to the significant problems in mining homologs to target other transcription factors such as RpaR, one possible approach would be to leverage a directed evolution scheme.

Currently molecular sequestration modeling is confined to systems that do not involve small-molecule mediated activation, such as σ-anti*sigma*[183]; expanding computational theory to include LuxR-like transcription factors is an ongoing effort that could help uncover further circuit design principles.

Outside the promiscuity of RhlRt, any genetic circuit which wishes to (A) increase the ultra sensitivity of the response curve, (B) control the activation threshold, or (C) add another layer of control on top of transcriptional regulation for LuxR-family proteins will be made more tunable by adopting the proteins and design principles laid out in this chapter.

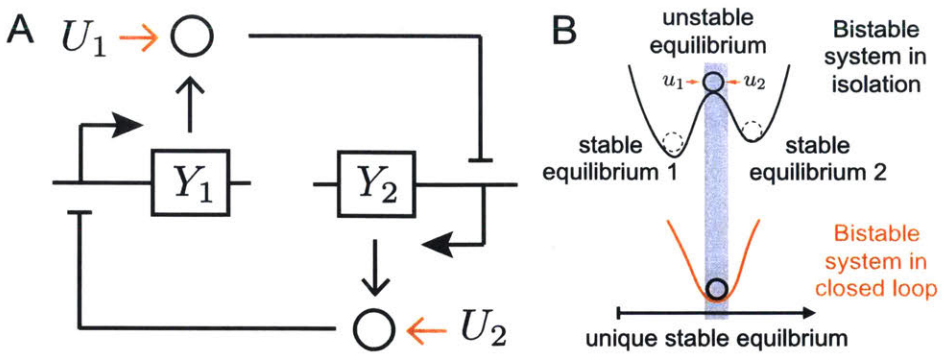

Figure 4-14: **A**. A canonical bistable gene network controlled using a molecular controller that provides two inputs U_1 and U_2. **B.** By introducing a molecular controller, we force the equilibrium landscape of the closed loop system to present a single, stable equilibrium in a neighborhood of the unstable equilibrium of the toggle switch in isolation.

One direction we are particularly interested in is the concept of stabilizing an unstable state (Figure 4-14). In engineering, feedback control is critical to regulating processes dynamically for the desired behavior under uncertainties and external disturbances. Also, feedback regulation can stabilize many unstable processes[183]. This meta-circuit which acts upon an already existing topology (in this case a classic Collins-Gardner toggle switch) is most useful when it does not require changes to the coding sequence of the circuit of interest; by applying sequestration at the protein level we need not modify the underlying system we wish to regulate.

4.4 Experimental Details

4.4.1 Primer Design and Cloning

All genetic circuits in this work were constructed by GoldenGate [143] construction using MoClo empty vectors [144]. Full circuits were generated into one of two level 2 expression vectors. pL2f1A is the canonical pL2f1 with the pVS1 origin of replication[144](Addgene kit #1000000044) removed. pL2F was assembled by InFusion (Takara #638920) fusing a lacZ negative selection marker from pL1f1[144](Addgene kit #1000000044), p15a origin of replication from pTHSS1025 (A gift from Thomas Segall-Shapiro), and chloramphenicol resistance marker from pFNK512[88].

For chimeric proteins, designed primers amplify the ligand-binding domain and DNA-binding domain with additional BbsI restriction enzyme recognition sites at the 3' and 5' respectively. Since the standard MoClo overhangs for a level 0 coding sequence empty vector are AATG at the 5' and GCTT at the 3', so the scarless junction connecting the LBD and DBD must be orthogonal. These 2 sub-level-0 amplicons were then inserted into the pL0SC entry vector by goldengate with BbsI.

4.4.2 Steady State Induction and Flow Cytometry

M9 media was prepared as 1X M9 Salts (6.78 g/L Na_2HPO_4, 3 g/L KH2PO4, 1 g/L NH_4Cl, 0.5 g/L NaCl (Sigma-Aldrich #M6030), 0.34 g/L thiamine hydrochloride (Sigma-Aldrich #T4625), 0.2% casamino acids (Acros #61204), 2 mM $MgSO_4$ (Sigma-Aldrich #63138), 0.1 mM $CaCl_2$ (Sigma-Aldrich #3000-OP), 0.4% D-glucose (Sigma-Aldrich #G8270), with 50 µg/mL kanamycin (IBI Scientific #IBI2120) and/or 20 µg/mL chloramphenicol (IBI Scientific #IBI2080) and sterile filtered.

AHL was prepared by dissolving in DMSO, diluted to 0.5 µg/mL in DMSO (Sigma-Aldrich #D8418), and then further diluted to a working concentration in M9 media. Cuminic acid (Sigma-Aldrich #268402) was prepared by dissolving to 100 mM in ethanol. IPTG (TermoFisher #R1171) and cuminic acid were then diluted to a working concentration in M9 media.

Plasmids were transformed into NEB10-beta commercial competent cells ((New England BioLabs #C3019I)) according to manufacture's recommendations on selective LB-Agar. A single colony was picked and used to inoculate 200 uL of M9 media with antibiotics overnight in a 96-well U-bottom microplate (ELMI North America #DTS-4) at 900 RPM and 37 °C. Samples were then diluted 10 µL into 190 µL M9 media, and subsequently 10 µL into 190 µL M9 media. Following 3 hours of subculture at 900 RPM and 37 °C each well was diluted 180 µL into 1620 µL M9 media and then distributed 10 µL into a well of total 200 µL containing M9 media and inducer chemical, and then were induced for 5 hours at 900 RPM and 37 °C.

Samples were stored in 2 mg/mL Kanamycin until ran on a BD LSR Fortessa flow cytometer with HTS attachment (BD, Franklin Lakes, NJ, USA). Raw .fcs data were processed with Cytoflow[145]. Morphology gating to remove debris was performed on FSC-A vs FSC-H, and then data reported as geometric mean FITC-A (488 nm laser, 350 V, 530/30 nm filter) or geometric mean PE-Texas-Red-A (561 nm laser, 600 V, 610/20 nm filter) of cellular events. Auto-fluorescent subtraction is performed by cells containing a corresponding empty vector plasmid.

4.4.3 Plasmids

Figure	Circuit	Plasmid
	IPTG reference	pL2f1768
	Cuminic reference	pL2f1773
4-1	LasR vs QslA	pL2f1801
4-1	LasR vs QteE	pL2f1802
4-2	TraR vs TraM	pL2f1803
4-2	TraR vs TraM2	pL2f1804
4-6	TraR vs TrlR	pL2f1836
4-6	TraR vs TrlR181	pL2f1805
4-7, 4-8	LasR vs LasRt	pL2f1800
4-7, 4-8	LuxR vs LuxRt	pL2f1806

Figure	Circuit	Plasmid
4-7, 4-8	RhlR vs RhlRt	pL2f1809
4-7, 4-8	RpaR vs RpaRt	pL2f1811
4-7, 4-8	TraR vs TrlR181	pL2f1805
4-9	Lux24lasR vs LuxRt	pL2f1957
4-9	Rhl24lasR vs RhlRt	pL2f1951
4-9	Rpa24lasR vs RpaRt	pL2f1954
4-3, 4-10	Inducible LasR	pL2f1787
4-3, 4-10	Inducible LuxR	pL2f1826
4-3, 4-10	Inducible RhlR	pL2f1829
4-3, 4-10	Inducible RpaR	pL2f1817
4-3, 4-10	Inducible TraR	pL2f1893
4-11, 4-4	Inducible Lux24lasR	pL2f1941
4-11, 4-4	Inducible Rhl24lasR	pL2f1942
4-11, 4-4	Inducible Rpa24lasR	pL2f1943
4-11, 4-4	Inducible Tra24lasR	pL2f1982
4-3, 4-4	Inducible QslA	pL2f1971
4-3, 4-4	Inducible QteE	pL2f1974
4-3, 4-4	Inducible TraM	pL2f1972
4-3, 4-4	Inducible TraM2	pL2f1973
4-11, 4-10	Inducible LasRt	pL2f1970
4-11, 4-10	Inducible LuxRt	pL2f1976
4-11, 4-10	Inducible RhlRt	pL2f1977
4-11, 4-10	Inducible RpaRt	pL2f1978
4-11, 4-10	Inducible TrlRt	pL2f1975
4-13	TraR vs TraM	pL2f1803
4-12	QslA Open Loop	pL2f1801
4-12	QslA Closed Loop	pL2f1839

Table 4.2: Plasmids used in this chapter

Chapter 5

Flow Cytometry Interlab

All models are wrong, but some are useful

George E. P. Box

This work was done in collaboration with many others including Brian Teague, Jacob Beal, John Sexton, Sebastian M. Castillo-Hair, David Ross, Ariel Hecht, and Peter McLean. A portion of it was presented at IWBDA 2017 as an abstract and is adapted here[188]. I developed the freezing protocol, prepared and shipped samples, measured samples, and helped analyze the results. John Sexton designed and shared 5-2, 5-3, and 5-4. Jacob Beal processed the data of the interlab, and shared figures 5-5, 5-6 and 5-7.

5.1 Motivation

As synthetic biology matures as a discipline, reproducibility and common measurement standards emerge as increasingly important problems for the field to tackle[189]. Flow cytometry, while being one of the most powerful techniques available to measure distributions of gene expression in cells, remains particularly recalcitrant to shared physical units and best practices.

Flow cytometry traditionally accomplishes boolean delineation between mammalian cell sub-populations[190]. However increased capacity and sensitivity in mod-

ern instruments allow for thousands of cells per second to be analyzed, including bacteria cells. The distribution of signal from GFP among a population has allowed for quantification of gene expression at a single cell and population level, in a way strictly more informative than traditional bulk measurement (such as plate readers).

There are few, but non trivial, drawbacks to using flow cytometry for quantitative single cell analysis of gene expression. First, without expensive and complicated additional sorting machinery post-interrogation the cells are destroyed and thus additional effort is required for time-varying experiments. Second, flow cytometers interrogate cells by exciting fluorophores with a laser of defined wavelength and collecting light in various channels with filters to select for only a given spectrum. Each channel is named after the dye they were first used for, thus the "Green" channel is often referred to as "FITC" (Fluorescein isothiocyanate) and the "Red" channel referred to as "PE-Texas-Red". These filters are not uniformly standardized among research labs, see Table 5.2, 5.3. Third, the emitted light from the cellular fluorescence, which represents the nexus of our interest in measuring, is processed after filtering and before being recorded by a photomultiplier tube (PMT) which amplifies the (weak) signal based on a user-set voltage. This signal is converted to a digital trace and each peak assigned Area, Height, and Width values. Thus the final reported raw data is in arbitrary units (AU) in a way that should be proportional to the original photonic output. Arbitrary units make the comparison and standardization of data difficult[189, 191, 192].

Previous Work on Physical Units

The first and foremost attempt to remove the arbitrariness from flow cytometry data is to perform a fold-change calculation. For example, by dividing maximally-induced sample by a non-induced sample population statistic. However this method suffers numerous problems.

Dividing an arbitrary unit by another arbitrary unit of the same source does not stop the unit from being arbitrary. The fold-change will still be affected by the voltage of the PMT, and not necessarily proportionally for low and high volt-

ages. Importantly, fold-change normalization destroys information that is essential for downstream circuit design. A module which has a basal expression of 1,000 AU and can be induced to a maximal expression of 10,000 AU is, in both theory and practice, not equivalent to a module which has a basal expression of 1 AU and a maximally induced expression of 10 AU using the same growth conditions and voltages. Fold-change reporting would give these two hypothetical modules the same characterization.

In contrast, stable reference materials have been developed, in the form of beads with a defined fluorescence quantified in terms of molecules of equivalent reference fluorophores (ERF; alternately MEF or ME[fluorophore])[193, 192]. There are now numerous open software packages to convert arbitrary units to MEF units available, such as Flowcal[194], TASBE[191], and Cytoflow[145]

5.2 Interlab

To study the variance in measuring and reporting the distribution of fluorescence in bacterial cell populations among research institutions, we designed and carried out an Interlab Study.

5.2.1 Initial Constraints

There were both scientific and logistical constraints to the Interlab project when developing a protocol. Initially we hypothesized that sending plasmid DNA would be most economical and easy to ship. However the protocol that is used at the Synthetic Biology Center for consistent exponential-phase *E. coli* takes 8 hours or more (3 hours subculture, 5 hours induction, and then actual run time). This is incompatible with those working more rigid schedules such as those at NIST. Other labs did not have the facilities to grow microplates at 37 °C and or at 900 RPM.

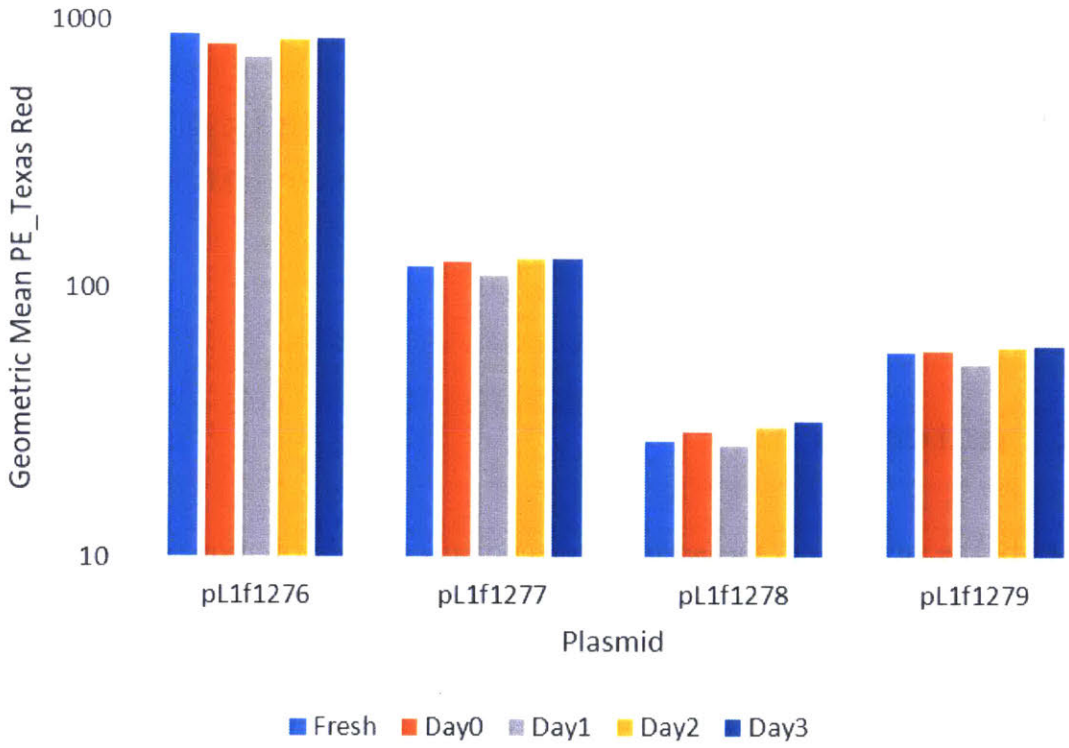

Figure 5-1: Freeze-thawing time-course for 4 different constitutive expressions of mCherry.

5.2.2 Stability

Since the central aim of the project was to examine differences in measurements for the same sample any kind of drift of the bacteria over time would be unacceptable. However even with overnight shipping not all participants would receive, much less measure, their samples at the same time. To alleviate this problem we developed a protocol that was (1) simple and (2) consistent for the preservation of *E. coli* samples for flow cytometry analysis.

Plasmids were transformed into 10-beta competent *E. coli* cells (New England Biolabs cat. #C3019H) according to the manufactures recommendation. Single colonies were struck out on selective media and then grown overnight in 100 µL of M9 minimal media supplemented with glycerol[120] and carbenicillin (100 µg mL^{-1}) at 900 RPM and 37 °C. After 16 hours each strain was diluted 15 µL into 185 µL of media twice successively and grown at 900 RPM and 37 °C. After 3 hours each strain was diluted 15 µL into 185 µL of media twice successively and grown at 900 RPM and 37 °C for another 5 hours. At this point all strains had an OD_{600} of 0.5 or less and were concentrated to an OD_{600} of 0.5; 150 µL of this culture was combined with 90 µL of 0.45 µm filter-sterilized 50% glycerol and mixed gently, then kept on ice. Pre-chilled, pre-labelled 2 mL labelled Eppendorf tubes to −80 °C were then used to aliquot 10 µL of culture and immediately placed back at −80 °C until distribution.

Aliquots were tested the day-of without freezing ("Fresh"), day-of with a freeze cycle ("Day0") and then for 3 more subsequent days for four different levels of constitutive expression of mCherry. Figure 5-1 shows the consistent expression over time suggesting this protocol retains cell morphology and fluorescence.

5.2.3 Instructions

Each participant was sent 5 samples with instructions to use one for prototyping the protocol, three for replicates each of which should be done on separate days, and finally one back up.

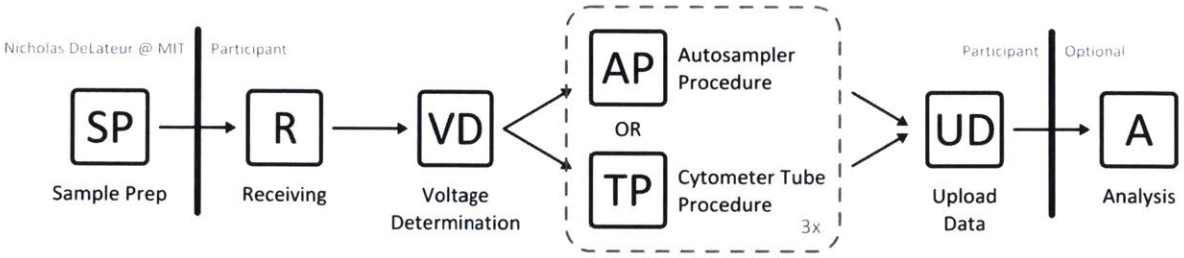

Figure 5-2: Interlab work flow. All sample culturing and preparation is done on-site at MIT. The samples are then shipped on dry-ice to participants. Each instrument at each facility must then undergo voltage determination and thresholding (Figure 5-3. Once the hardware and software have been configured each team performed measurements on three separate days and uploaded the data back to the interlab admins which then performed the data analysis.

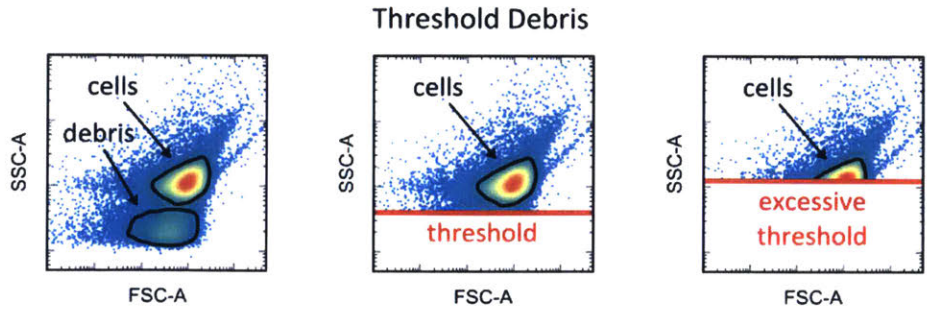

Figure 5-3: Thresholding debris from bacterial cells based on SSC-A and FSC-A.

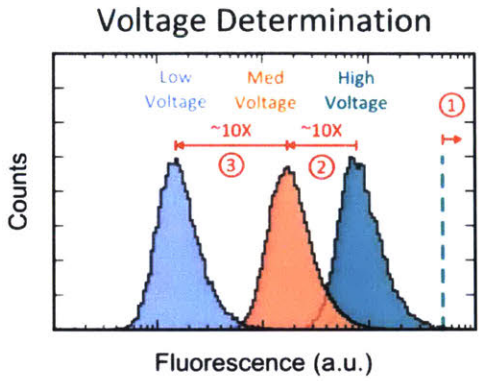

Figure 5-4: Diagram for determining low, medium, and high voltages. The user should first find the highest voltage that does not clip, then adjust voltage down until they arrive to approximately 10-fold and then 100-fold lower geometric mean population FITC-A or PE-Texas-Red-A for GFP and mCherry respectively

Determining Instrument Gating Each recipient was instructed to set FSC and SSC voltages (if permitted by their instrument) such that the peak density of cells was centered in the range of their detector. As pre-collection gating options can vary significantly by instrument and software, recipients were instructed to set gating to retain as many cell events as possible, even if this would result in more non-cell events being captured in the same.

Determining High, Medium, and Low Color Voltages Each recipient was instructed to take the brightest strain for red and green and raise the corresponding channel's voltage until the distribution was as high as possible without clipping the sample. This would be used as the High voltage; the process was repeated with targeting voltages for 10- and 100- fold less AU for Medium and Low voltage settings respectively, not to be exceeded by 10^1 geometric mean AU For instruments with low maximum values, recipients were instructed to still space the Medium and Low voltages evenly, but to lower the overall separation so that the sample was not clipped significantly on the low end. For instruments without a variable voltage setting, this step was necessarily omitted.

Sample Preparation Bacterial cultures were prepared for flow cytometry as follows: Remove one replicate of samples from $-80\,^{\circ}\mathrm{C}$ and transfer to $42\,^{\circ}\mathrm{C}$ heat bath

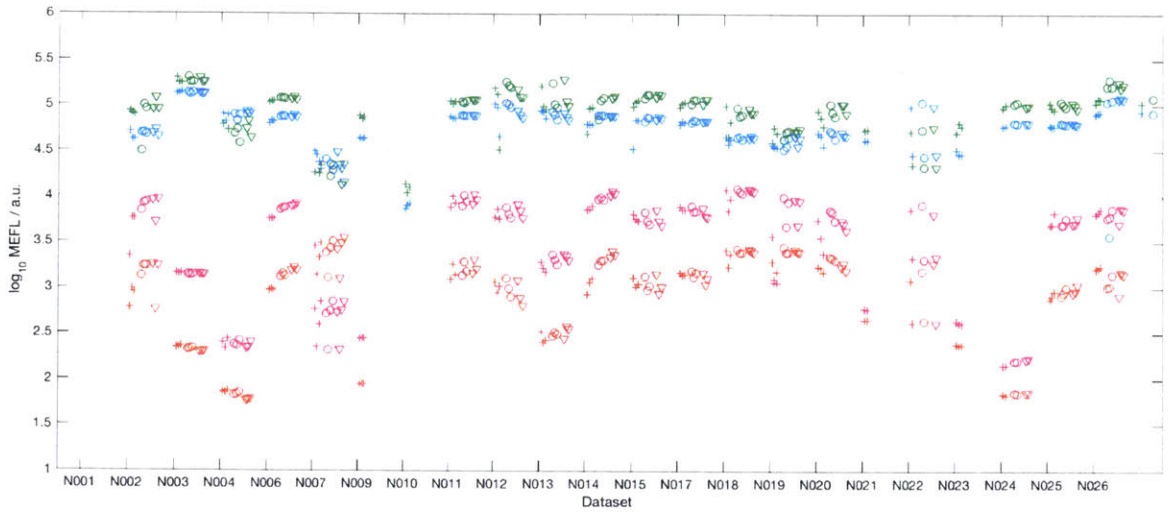

Figure 5-5: Raw results reported back as part of the interlab study. Each dataset corresponds to a single instrument. Strains are given by color; Green: T06, Cyan: T07, Red: T08, Purple:T09. Each day given by separate shape.

for 60 sec. 990 µL of sterile filtered 1X PBS to bacterial culture, or 75 µL for calibration beads, is added to bring it up to concentration for running on the flow cytometer. Samples are then run immediately. This procedure is repeated independently for each replicate.

Event Collection Samples were run as close to these conditions as possible based on local instrument and software: Each sample 1 µL s^{-1} for either 150 µL or 10^5 total events, whichever was achieved first.

5.2.4 Results

In total 25 flow cytometers between 19 institutions across the United States participated in our Interlab experiment. Figure 5-5 shows minimally processed results for each instrument that could be analyzed.

Not all cytometers are equipped with identical filters, even if the output is labelled identically as "FITC". Tables 5.2 and 5.3 show some of the heterogeneity found in cytometer hardware configurations among participants. This information is rarely reported in method sections (as opposed to wavelengths and voltages).

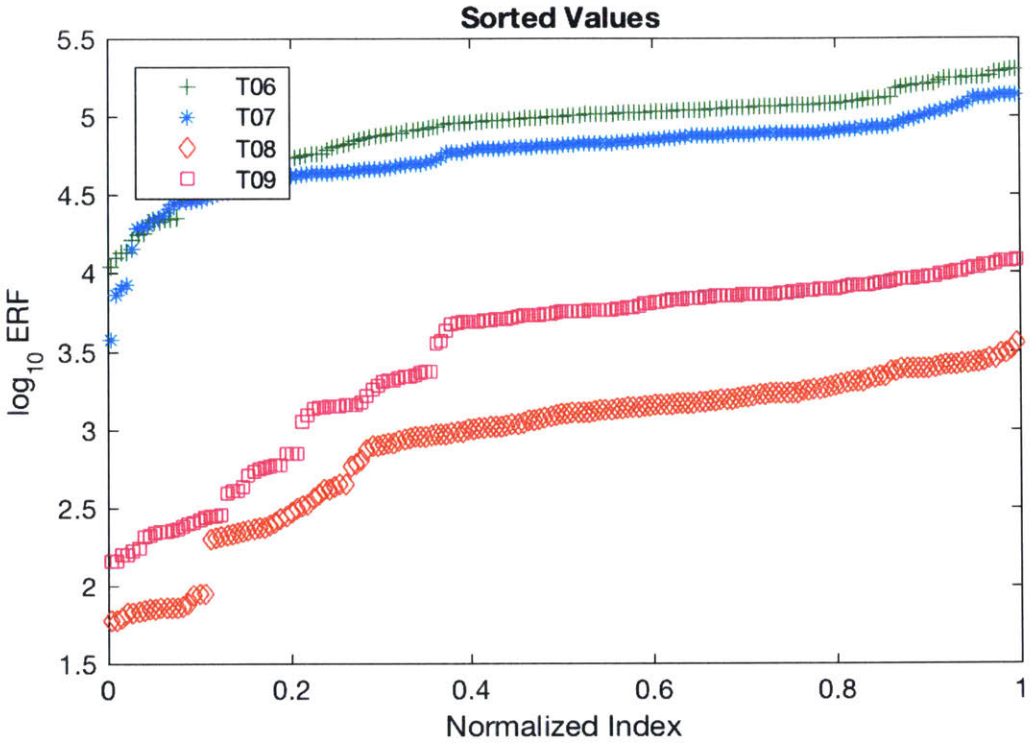

Figure 5-6: Sorted results reported back as part of the interlab study. Each dataset corresponds to a single instrument. Strains are given by color; Green: T06, Cyan: T07, Red: T08, Purple:T09.

Sample	Description	Standard Deviation
T06	Strong Green	1.90
T07	Medium Green	1.80
T08	Medium Red	3.01
T09	Weak Red	3.69

Table 5.1: Standard Deviation in ERF measurements between flow cytometers in the interlab with all results.

Owner	Place	Wavelength (nm)	Filter (nm; "center/width")
SBC	MIT	488	530/30
Medford Lab	Colorodo State	488	525/30
Moake Lab	Rice	488	510/21
SEA	Rice	488	525/50

Table 5.2: A reduced set of laser and filter combinations among cytometers in our interlab study with varying parameters all meant to measure in the FITC channel.

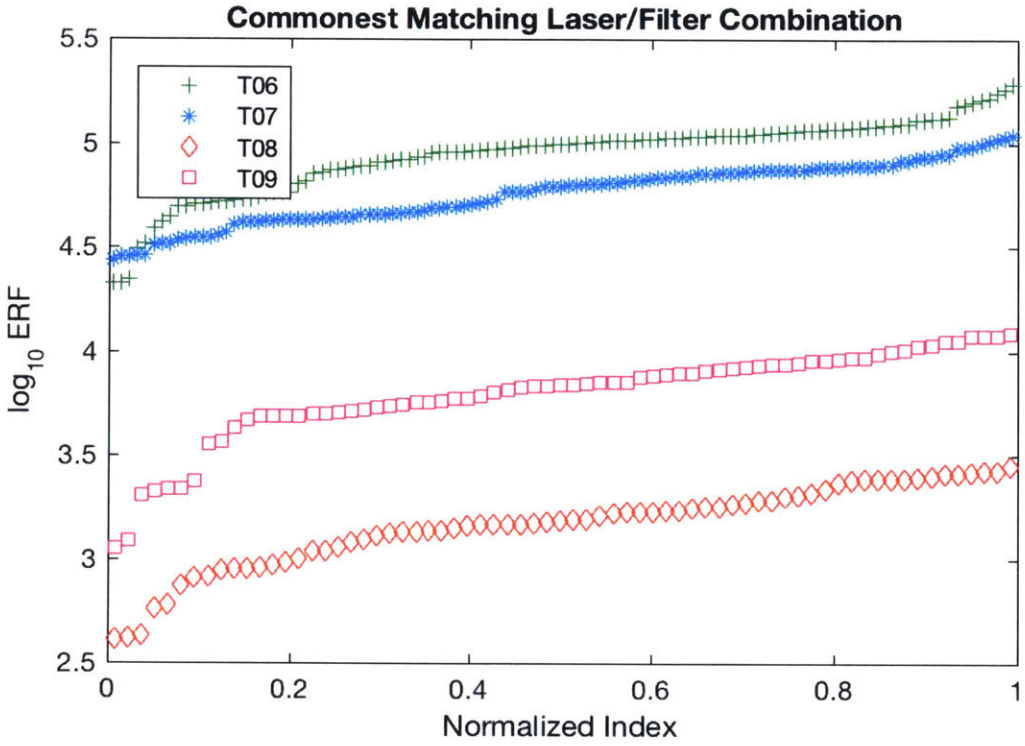

Figure 5-7: Sorted results reported back as part of the interlab study with only the most common matching laser/filter combination. Each dataset corresponds to a single instrument. Strains are given by color; Green: T06, Cyan: T07, Red: T08, Purple:T09.

Owner	Place	Wavelength (nm)	Filter (nm; "center/width")
SBC	MIT	561	610/20
Medford Lab	Colorodo State	561	655 LP
Moake Lab	Rice	561	650 LP
SEA	Rice	561	605/40

Table 5.3: A reduced set of laser and filter combinations among cytometers in our interlab study with varying parameters all meant to measure in the PE-Texas-Red channel. LP: Low Pass

Sample	Description	Standard Deviation
T06	Strong Green	1.64
T07	Medium Green	1.62
T08	Medium Red	1.59
T09	Weak Red	1.67

Table 5.4: Standard Deviation in ERF measurements between flow cytometers in the interlab using only the most common filter combinations.

Lasers and Filters

5.3 Conclusions and Future Directions

Flow cytometry remains the gold standard for reporting fluorescent activity inside the cell, whether bacterial or mammalian or in between. However it is still plagued with the issues of arbitrary units, a myriad of different software and hardware, and a lack of full reporting in the literature. Recent developments of free, open software packages such as Cytoflow[145], Flowcal[194], and TASBE Flow Analytics[191] help the field move to more reproducible data processing. At the conclusion of this interlab study we recommend the following best practices for the characterization and sharing of flow cytometry data:

1. Report the laser wavelength and filters for any channel used
2. Run calibration beads both to check the health of the instrument before sample collecting and for MEF conversion in processing
3. Process flow data with open and reproducible software

Bibliography

[1] Irene A. Chen, Richard W. Roberts, and Jack W. Szostak. The emergence of competition between model protocells. *Science*, 2004.

[2] Katarzyna Adamala and Jack W. Szostak. Nonenzymatic template-directed RNA synthesis inside model protocells. *Science*, 2013.

[3] Daniel G. Gibson, John I. Glass, Carole Lartigue, Vladimir N. Noskov, Ray Yuan Chuang, Mikkel A. Algire, Gwynedd A. Benders, Michael G. Montague, Li Ma, Monzia M. Moodie, Chuck Merryman, Sanjay Vashee, Radha Krishnakumar, Nacyra Assad-Garcia, Cynthia Andrews-Pfannkoch, Evgeniya A. Denisova, Lei Young, Zhi Ng Qi, Thomas H. Segall-Shapiro, Christopher H. Calvey, Prashanth P. Parmar, Clyde A. Hutchison, Hamilton O. Smith, and J. Craig Venter. Creation of a bacterial cell controlled by a chemically synthesized genome. *Science*, 2010.

[4] Clyde A. Hutchison, Ray Yuan Chuang, Vladimir N. Noskov, Nacyra Assad-Garcia, Thomas J. Deerinck, Mark H. Ellisman, John Gill, Krishna Kannan, Bogumil J. Karas, Li Ma, James F. Pelletier, Zhi Qing Qi, R. Alexander Richter, Elizabeth A. Strychalski, Lijie Sun, Yo Suzuki, Billyana Tsvetanova, Kim S. Wise, Hamilton O. Smith, John I. Glass, Chuck Merryman, Daniel G. Gibson, and J. Craig Venter. Design and synthesis of a minimal bacterial genome. *Science*, 2016.

[5] Geng Min Lin, Robert Warden-Rothman, and Christopher A. Voigt. Retrosynthetic design of metabolic pathways to chemicals not found in nature, 2019.

[6] Victoria L. Challinor and Helge B. Bode. Bioactive natural products from novel microbial sources. *Annals of the New York Academy of Sciences*, 2015.

[7] Dae Kyun Ro, Eric M. Paradise, Mario Quellet, Karl J. Fisher, Karyn L. Newman, John M. Ndungu, Kimberly A. Ho, Rachel A. Eachus, Timothy S. Ham, James Kirby, Michelle C.Y. Chang, Sydnor T. Withers, Yoichiro Shiba, Richmond Sarpong, and Jay D. Keasling. Production of the antimalarial drug precursor artemisinic acid in engineered yeast. *Nature*, 2006.

[8] Mark Mimee, Alex C. Tucker, Christopher A. Voigt, and Timothy K. Lu. Programming a Human Commensal Bacterium, Bacteroides thetaiotaomicron, to

Sense and Respond to Stimuli in the Murine Gut Microbiota. *Cell Systems*, 2015.

[9] Mark Mimee, Phillip Nadeau, Alison Hayward, Sean Carim, Sarah Flanagan, Logan Jerger, Joy Collins, Shane McDonnell, Richard Swartwout, Robert J. Citorik, Vladimir Bulović, Robert Langer, Giovanni Traverso, Anantha P. Chandrakasan, and Timothy K. Lu. An ingestible bacterial-electronic system to monitor gastrointestinal health. *Science*, 2018.

[10] David T. Riglar and Pamela A. Silver. Engineering bacteria for diagnostic and therapeutic applications, 2018.

[11] Fahim Farzadfard and Timothy K. Lu. Genomically encoded analog memory with precise in vivo dna writing in living cell populations. *Science*, 2014.

[12] Nathaniel Roquet, Ava P. Soleimany, Alyssa C. Ferris, Scott Aaronson, and Timothy K. Lu. Synthetic recombinase-based State machines in living cells. *Science*, 2016.

[13] Lulu Qian and Erik Winfree. Scaling up digital circuit computation with DNA strand displacement cascades. *Science*, 2011.

[14] Ahmad S. Khalil and James J. Collins. Synthetic biology: Applications come of age, 2010.

[15] D. Ewen Cameron, Caleb J. Bashor, and James J. Collins. A brief history of synthetic biology, 2014.

[16] Christopher A. Voigt. Genetic parts to program bacteria, 2006.

[17] R. Weiss and S. Basu. The device physics of cellular logic gates. In *NSC-1: The First Workshop on NonSilicon Computing*, pages 54–61, 2002.

[18] R. Weiss and T.F. Knight. Engineered communications for microbial robotics. *Lect. Notes. Comput. Sc.*, 2054:1–16, 2001.

[19] R. Weiss. *Cellular computation and communications using engineered genetic regulatory networks.* PhD thesis, Massachusetts Institute of Techonology, Cambridge, MA, 2001.

[20] Eric L Haseltine and Frances H Arnold. Synthetic gene circuits: design with directed evolution. *Annual review of biophysics and biomolecular structure*, 36:1–19, jan 2007.

[21] Susana K Checa, Matias D Zurbriggen, and Fernando C Soncini. Bacterial signaling systems as platforms for rational design of new generations of biosensors. *Current Opinion in Biotechnology*, 23(5):766–772, 2012.

[22] Jason W Chin, Lingchong You, Shana O Kelley, Petra S Dittrich, Ryan E Cobb, Tong Si, and Huimin Zhao. Directed evolution: an evolving and enabling synthetic biology tool. *Current Opinion in Chemical Biology*, 16(3):285–291, 2012.

[23] Alec A.K. Nielsen, Thomas H. Segall-Shapiro, and Christopher A. Voigt. Advances in genetic circuit design: Novel biochemistries, deep part mining, and precision gene expression, 2013.

[24] Keith V Wood, Dan S Tawfik, Ron Weiss, Sven Panke, Anand Pai, Yu Tanouchi, Cynthia H Collins, and Lingchong You. Engineering multicellular systems by cellcell communication. *Current Opinion in Biotechnology*, 20(4):461–470, 2009.

[25] Ellen C O'Shaughnessy and Casim A Sarkar. Analyzing and engineering cell signaling modules with synthetic biology. *Current Opinion in Biotechnology*, 23(5):785–790, 2012.

[26] Chen-Yu Tsao, David N Quan, and William E Bentley. Development of the quorum sensing biotechnological toolbox. *Current Opinion in Chemical Engineering*, 1(4):396–402, nov 2012.

[27] René Michele Davis, Ryan Yue Muller, and Karmella Ann Haynes. Can the natural diversity of quorum-sensing advance synthetic biology? *Frontiers in bioengineering and biotechnology*, 3:30, 2015.

[28] J A Shapiro. Thinking about bacterial populations as multicellular organisms. *Annual review of microbiology*, 52:81–104, jan 1998.

[29] Huimin Zhao, Wilfred Chen, David Payne, Karen Bush, Sara Hooshangi, and William E Bentley. From unicellular properties to multicellular behavior: bacteria quorum sensing circuitry and applications. *Current Opinion in Biotechnology*, 19(6):550–555, 2008.

[30] Margaret J. McFall-Ngai and Edward G. Ruby. Symbiont recognition and subsequent morphogenesis as early events in an animal-bacterial mutualism. *Science*, 1991.

[31] J. Engebrecht and M. Silverman. Identification of genes and gene products necessary for bacterial bioluminescence. *Proceedings of the National Academy of Sciences*, 1984.

[32] Joanne Engebrecht, Kenneth Nealson, and Michael Silverman. Bacterial bioluminescence: Isolation and genetic analysis of functions from Vibrio fischeri. *Cell*, 1983.

[33] W C Fuqua, S C Winans, and E P Greenberg. Quorum sensing in bacteria: the LuxR-LuxI family of cell density-responsive transcriptional regulators. *Journal of bacteriology*, 176(2):269–75, jan 1994.

[34] James C. Charlesworth, Charlotte Beloe, Cara Watters, and Brendan P. Burns. Quorum sensing in archaea: Recent advances and emerging directions. In *Biocommunication of Archaea*. 2017.

[35] Jorge Barriuso, Deborah A. Hogan, Tajalli Keshavarz, and María Jesús Martínez. Role of quorum sensing and chemical communication in fungal biotechnology and pathogenesis, 2018.

[36] Ming-Tang Chen and Ron Weiss. Artificial cell-cell communication in yeast Saccharomyces cerevisiae using signaling elements from Arabidopsis thaliana. *Nature biotechnology*, 23(12):1551–5, dec 2005.

[37] Lisa A. Hawver, Sarah A. Jung, and Wai Leung Ng. Specificity and complexity in bacterial quorum-sensing systemsa, 2016.

[38] Justin E. Silpe and Bonnie L. Bassler. A Host-Produced Quorum-Sensing Autoinducer Controls a Phage Lysis-Lysogeny Decision. *Cell*, 2019.

[39] Stuart A. West, Klaus Winzer, Andy Gardner, and Stephen P. Diggle. Quorum sensing and the confusion about diffusion, 2012.

[40] Melissa B. Miller and Bonnie L. Bassler. Quorum Sensing in Bacteria. *Annual Review of Microbiology*, 2001.

[41] Christopher M. Waters and Bonnie L. Bassler. QUORUM SENSING: Cell-to-Cell Communication in Bacteria. *Annual Review of Cell and Developmental Biology*, 2005.

[42] Tal Danino, Octavio Mondragón-Palomino, Lev Tsimring, and Jeff Hasty. A synchronized quorum of genetic clocks. *Nature*, 2010.

[43] Jeffrey J. Tabor, Howard M. Salis, Zachary Booth Simpson, Aaron A. Chevalier, Anselm Levskaya, Edward M. Marcotte, Christopher A. Voigt, and Andrew D. Ellington. A Synthetic Genetic Edge Detection Program. *Cell*, 2009.

[44] S. Basu, R. Mehreja, S. Thiberge, M.T. Chen, and R. Weiss. Spatiotemporal control of gene expression with pulse-generating networks. *Proc. Natl. Acad. Sci. U.S.A.*, 101(17):6355–6360, 2004.

[45] Ekaterina Osmekhina, Christopher Jonkergouw, Georg Schmidt, Farzin Jahangiri, Ville Jokinen, Sami Franssila, and Markus B. Linder. Controlled communication between physically separated bacterial populations in a microfluidic device. *Communications Biology*, 2018.

[46] Alvin Tamsir, Jeffrey J. Tabor, and Christopher A. Voigt. Robust multicellular computing using genetically encoded NOR gates and chemical 'wiresg'. *Nature*, 2011.

[47] Frederick K. Balagaddé, Hao Song, Jun Ozaki, Cynthia H. Collins, Matthew Barnet, Frances H. Arnold, Stephen R. Quake, and Lingchong You. A synthetic Escherichia coli predator-prey ecosystem. *Molecular Systems Biology*, 2008.

[48] Ye Chen, Jae Kyoung Kim, Andrew J. Hirning, Krešimir Josić, and Matthew R. Bennett. Emergent genetic oscillations in a synthetic microbial consortium. *Science*, 2015.

[49] Adam J. Meyer, Thomas H. Segall-Shapiro, Emerson Glassey, Jing Zhang, and Christopher A. Voigt. Escherichia coli Marionette strains with 12 highly optimized small-molecule sensors. *Nature Chemical Biology*, 2019.

[50] Stephanie K. Aoki, Gabriele Lillacci, Ankit Gupta, Armin Baumschlager, David Schweingruber, and Mustafa Khammash. A universal biomolecular integral feedback controller for robust perfect adaptation, 2019.

[51] H. M.H.N. Bandara, O. L.T. Lam, L. J. Jin, and Lakshman Samaranayake. Microbial chemical signaling: A current perspective, 2012.

[52] A. Eberhard, A. L. Burlingame, C. Eberhard, G. L. Kenyon, K. H. Nealson, and N. J. Oppenheimer. Structural Identification of Autoinducer of Photobacterium fischeri Luciferase. *Biochemistry*, 1981.

[53] H. B. Kaplan and E. P. Greenberg. Diffusion of autoinducer is involved in regulation of the Vibrio fischeri luminescence system. *Journal of Bacteriology*, 1985.

[54] James P. Pearson, Christian Van Delden, and Barbara H. Iglewski. Active efflux and diffusion are involved in transport of Pseudomonas aeruginosa cell-to-cell signals. *Journal of Bacteriology*, 1999.

[55] Amy L. Schaefer, E. P. Greenberg, Colin M. Oliver, Yasuhiro Oda, Jean J. Huang, Gili Bittan-Banin, Caroline M. Peres, Silke Schmidt, Katarina Juhaszova, Janice R. Sufrin, and Caroline S. Harwood. A new class of homoserine lactone quorum-sensing signals. *Nature*, 2008.

[56] Spencer R Scott and Jeff Hasty. Quorum Sensing Communication Modules for Microbial Consortia. *ACS Synthetic Biology*, 5(9):969–977, 2016.

[57] Nicolas Kylilis, Zoltan A. Tuza, Guy Bart Stan, and Karen M. Polizzi. Tools for engineering coordinated system behaviour in synthetic microbial consortia. *Nature Communications*, 2018.

[58] Quorum sensing: How bacteria can coordinate activity and synchronize their response to external signals?, 2012.

[59] Mair E A Churchill and Lingling Chen. Structural basis of acyl-homoserine lactone-dependent signaling. *Chemical reviews*, 111(1):68–85, jan 2011.

[60] D. Karig and R. Weiss. Signal-amplifying genetic circuit enables in vivo observation of weak promoter activation in the Rhl quorum sensing system. *Biotechnol Bioeng*, 89(6):709–18, 2005.

[61] D. A. Siegele and J. C. Hu. Gene expression from plasmids containing the araBAD promoter at subsaturating inducer concentrations represents mixed populations. *Proceedings of the National Academy of Sciences*, 1997.

[62] Rolf Lutz and Hermann Bujard. Independent and tight regulation of transcriptional units in escherichia coli via the LacR/O, the TetR/O and AraC/I1-I2 regulatory elements. *Nucleic Acids Research*, 1997.

[63] D. Karig. *Engineering Multi-Signal Synthetic Biological Systems.* PhD thesis, Princeton University, Princeton, NJ, 2007.

[64] Janet R. Lamb, Hetal Patel, Timothy Montminy, Victoria E. Wagner, and Barbara H. Iglewski. Functional Domains of the RhlR Transcriptional Regulator of Pseudomonas aeruginosa. *Journal of Bacteriology*, 2003.

[65] Kaia J. Sappington, Ajai A. Dandekar, Ken Ichi Oinuma, and E. Peter Greenberg. Reversible signal binding by the Pseudomonas aeruginosa quorum-sensing signal receptor LasR. *mBio*, 2011.

[66] Sung Kuk Lee, Howard H Chou, Brian F Pfleger, Jack D Newman, Yasuo Yoshikuni, and Jay D Keasling. Directed evolution of AraC for improved compatibility of arabinose- and lactose-inducible promoters. *Applied and environmental microbiology*, 73(18):5711–5, sep 2007.

[67] Yinping Qin, Carrie Keenan, and Stephen K. Farrand. N- and C-terminal regions of the quorum-sensing activator TraR cooperate in interactions with the alpha and sigma-70 components of RNA polymerase. *Molecular Microbiology*, 74(2):330–346, oct 2009.

[68] B. Koch, T. Liljefors, T. Persson, J. Nielsen, S. Kjelleberg, and Michael Givskov. The LuxR receptor: The sites of interaction with quorum-sensing signals and inhibitors. *Microbiology*, 2005.

[69] William Nasser and Sylvie Reverchon. New insights into the regulatory mechanisms of the LuxR family of quorum sensing regulators. *Analytical and Bioanalytical Chemistry*, 2007.

[70] M Schuster, M L Urbanowski, and E P Greenberg. Promoter specificity in Pseudomonas aeruginosa quorum sensing revealed by DNA binding of purified LasR. *Proceedings of the National Academy of Sciences of the United States of America*, 101(45):15833–9, nov 2004.

[71] J. Zhu and S. C. Winans. Autoinducer binding by the quorum-sensing regulator TraR increases affinity for target promoters in vitro and decreases TraR turnover rates in whole cells. *Proceedings of the National Academy of Sciences*, 2002.

[72] Jon E. Paczkowski, Amelia R. McCready, Jian Ping Cong, Zhijie Li, Philip D. Jeffrey, Chari D. Smith, Brad R. Henke, Frederick M. Hughson, and Bonnie L. Bassler. An Autoinducer Analogue Reveals an Alternative Mode of Ligand Binding for the LasR Quorum-Sensing Receptor. *ACS Chemical Biology*, 2019.

[73] Andrés Corral-Lugo, Abdelali Daddaoua, Alvaro Ortega, Manuel Espinosa-Urgel, and Tino Krell. Rosmarinic acid is a homoserine lactone mimic produced by plants that activates a bacterial quorum-sensing regulator. *Science Signaling*, 2016.

[74] Andrés Corral Lugo, Abdelali Daddaoua, Alvaro Ortega, Bertrand Morel, Ana Isabel Díez Peña, Manuel Espinosa-Urgel, and Tino Krell. Purification and characterization of Pseudomonas aeruginosa LasR expressed in acyl-homoserine lactone free Escherichia coli cultures. *Protein Expression and Purification*, 2017.

[75] Carolina Lixa, Adriana F. Marques, Juliana R. Cortines, Bianca C. Neves, Danielle M.P. Oliveira, Cristiane D. Anobom, Luís Maurício T.R. Lima, and Anderson S. Pinheiro. Refolding, purification, and preliminary structural characterization of the DNA-binding domain of the quorum sensing receptor RhlR from Pseudomonas aeruginosa. *Protein Expression and Purification*, 2016.

[76] Amelia R McCready, Jon E Paczkowski, Jian-Ping Cong, and Bonnie L Bassler. An autoinducer-independent RhlR quorum-sensing receptor enables analysis of RhlR regulation. *PLOS Pathogens*, 15(6):e1007820, jun 2019.

[77] Helen M. Berman, Tammy Battistuz, T. N. Bhat, Wolfgang F. Bluhm, Philip E. Bourne, Kyle Burkhardt, Zukang Feng, Gary L. Gilliland, Lisa Iype, Shri Jain, Phoebe Fagan, Jessica Marvin, David Padilla, Veerasamy Ravichandran, Bohdan Schneider, Narmada Thanki, Helge Weissig, John D. Westbrook, and Christine Zardecki. The protein data bank. *Acta Crystallographica Section D: Biological Crystallography*, 2002.

[78] Yaozhong Zou and Satish K. Nair. Molecular Basis for the Recognition of Structurally Distinct Autoinducer Mimics by the Pseudomonas aeruginosa LasR Quorum-Sensing Signaling Receptor. *Chemistry and Biology*, 2009.

[79] Matthew J. Bottomley, Ester Muraglia, Renzo Bazzo, and Andrea Carfi. Molecular insights into quorum sensing in the human pathogen Pseudomonas aeruginosa from the structure of the virulence regulator LasR bound to its autoinducer. *Journal of Biological Chemistry*, 2007.

[80] Joseph P. Gerdt, Christine E. McInnis, Trevor L. Schell, Francis M. Rossi, and Helen E. Blackwell. Mutational analysis of the quorum-sensing receptor LasR reveals interactions that govern activation and inhibition by nonlactone ligands. *Chemistry and Biology*, 2014.

[81] Amelia R. McCready, Jon E. Paczkowski, Brad R. Henke, and Bonnie L. Bassler. Structural determinants driving homoserine lactone ligand selection in the Pseudomonas aeruginosa LasR quorum-sensing receptor . *Proceedings of the National Academy of Sciences*, 2019.

[82] Matthew C. O'Reilly, Shi Hui Dong, Francis M. Rossi, Kaleigh M. Karlen, Rohan S. Kumar, Satish K. Nair, and Helen E. Blackwell. Structural and Biochemical Studies of Non-native Agonists of the LasR Quorum-Sensing Receptor Reveal an L3 Loop Out Conformation for LasR. *Cell Chemical Biology*, 2018.

[83] Sudha Chugani and Everett P. Greenberg. Corrigendum: An evolving perspective on the Pseudomonas aeruginosa orphan quorum sensing regulator QscR. *Frontiers in Cellular and Infection Microbiology*, 2015.

[84] A. Vannini, Cinzia Volpari, Cesare Gargioli, Ester Muraglia, Riccardo Cortese, Raffaele De Francesco, Petra Neddermann, Stefania Di Marco, AK. Aggarwal, DW. Rodgers, M. Drottar, M. Ptashne, SC. Harrison, V. Anantharaman, EV. Koonin, L. Aravind, I. Baikalov, I. Schroder, M. KaczorGrzeskowiak, D. Cascio, RP. Gunsalus, RE. Dickerson, BL. Bassler, RH. Blessing, DY. Guo, DA. Langs, GE. Borgstahl, DR. Williams, ED. Getzoff, Y. Chai, J. Zhu, SC. Winans, SH. Choi, EP. Greenberg, SH. Choi, EP. Greenberg, E. de La Fortelle, G. Bricogne, VMA. Ducros, RJ. Lewis, CS. Verma, EJ. Dodson, G. Leonard, GP. Turkenburg, GN. Murshudov, AJ. Wilkinson, JA. Brannigan, KA. Egland, EP. Greenberg, RM. Esnouf, C. Fuqua, EP. Greenberg, C. Fuqua, SC. Winans, EP. Greenberg, P. Gouet, E. Courcelle, DI. Stuart, F. Metoz, BL. Hanzelka, EP. Greenberg, YS. Ho, LM. Burden, JH. Hurley, L. Holm, C. Sander, SR. Jordan, CO. Pabo, T. Kawabata, K. Nishikawa, GJ. Kleywegt, GJ. Kleywegt, TA. Jones, PJ. Kraulis, RA. Laskowski, MW. MacArthur, DS. Moss, JM. Thornton, ZQ. Luo, SK. Farrand, ZQ. Luo, Y. Qin, SK. Farrand, EA. Merritt, DJ. Bacon, MB. Miller, BL. Bassler, A. MuellerFahrnow, U. Egner, KH. Nelson, JW. Hastings, A. Nicholls, K. Sharp, B. Honig, K. Pervushin, M. Billeter, G. Siegal, K. Wuthrich, HR. Powell, Y. Qin, ZQ. Luo, AJ. Smyth, P. Gao, S. Beck von Bodman, SK. Farrand, M. Suzuki, A. Swiderska, AK. Berndtson, MR. Cha, L. Li, GM. Beaudoin, J. Zhu, C. Fuqua, JD. Thompson, TJ. Gibson, F. Plewniak, DG. Higgins, CM. Weeks, R. Miller, L. Zhang, PJ. Murphy, A. Kerr, ME. Tate, J. Zhu, SC. Winans, J. Zhu, SC. Winans, J. Zhu, SC. Winans, J. Zhu, PM. Oger, B. Schrammeijer, PJ. Hooykaas, SK. Farrand, and SC. Winans. The crystal structure of the quorum sensing protein TraR bound to its autoinducer and target DNA. *The EMBO Journal*, 21(17):4393–4401, sep 2002.

[85] Guozhou Chen, James W. Malenkos, Mee Rye Cha, Clay Fuqua, and Lingling Chen. Quorum-sensing antiactivator TraM forms a dimer that dissociates to inhibit TraR. *Molecular Microbiology*, 2004.

[86] G. Chen, P. D. Jeffrey, C. Fuqua, Y. Shi, and L. Chen. Structural basis for antiactivation in bacterial quorum sensing. *Proceedings of the National Academy of Sciences*, 2007.

[87] A. M. Turing. The chemical basis of morphogenesis. *Bulletin of Mathematical Biology*, 1952.

[88] David Karig, K. Michael Martini, Ting Lu, Nicholas A. DeLateur, Nigel Goldenfeld, and Ron Weiss. Stochastic Turing patterns in a synthetic bacterial population. *Proceedings of the National Academy of Sciences*, 2018.

[89] E. Andrianantoandro, S. Basu, D.K. Karig, and R. Weiss. Synthetic biology: new engineering rules for an emerging discipline. *Mol. Syst. Biol.*, 2(1), 2006.

[90] S. Basu, Y. Gerchman, C.H. Collins, F.H. Arnold, and R. Weiss. A synthetic multicellular system for programmed pattern formation. *Nature*, 434(7037):1130–1134, 2005.

[91] L. You, R.S. Cox, R. Weiss, and F.H. Arnold. Programmed population control by cell–cell communication and regulated killing. *Nature*, 428(6985):868–871, 2004.

[92] J. Stricker, S. Cookson, M.R. Bennett, W.H. Mather, L.S. Tsimring, and J. Hasty. A fast, robust and tunable synthetic gene oscillator. *Nature*, 456(7221):516–519, 2008.

[93] M.B. Elowitz and S. Leibler. A synthetic oscillatory network of transcriptional regulators. *Nature*, 403(6767):335–338, 2000.

[94] N.J. Guido, X. Wang, D. Adalsteinsson, D. McMillen, J. Hasty, C.R. Cantor, T.C. Elston, and JJ Collins. A bottom-up approach to gene regulation. *Nature*, 439(7078):856–860, 2006.

[95] A. Levskaya, A.A. Chevalier, J.J. Tabor, Z.B. Simpson, L.A. Lavery, M. Levy, E.A. Davidson, A. Scouras, A.D. Ellington, E.M. Marcotte, et al. Synthetic biology: engineering Escherichia coli to see light. *Nature*, 438(7067):441–442, 2005.

[96] G. Theraulaz, E. Bonabeau, S.C. Nicolis, R.V. Solé, V. Fourcassié, S. Blanco, R. Fournier, J.L. Joly, P. Fernández, A. Grimal, et al. Spatial patterns in ant colonies. *Proc. Natl. Acad. Sci. U.S.A.*, 99(15):9645, 2002.

[97] A.M. Turing. The chemical basis of morphogenesis. *Philos. Trans. R. Soc. London, Ser. B*, 237(641):37–72, 1952.

[98] A. Gierer and H. Meinhardt. A theory of biological pattern formation. *Biol. Cybern.*, 12(1):30–39, 1972.

[99] Thomas Butler and Nigel Goldenfeld. Fluctuation-driven turing patterns. *Physical Review E*, 84(1):011112, 2011.

[100] Tommaso Biancalani, Duccio Fanelli, and Francesca Di Patti. Stochastic turing patterns in the brusselator model. *Physical Review E*, 81(4):046215, 2010.

[101] Tal Danino, Octavio Mondragón-Palomino, Lev Tsimring, and Jeff Hasty. A synchronized quorum of genetic clocks. *Nature*, 463(7279):326–330, 2010.

[102] Ye Chen, Jae Kyoung Kim, Andrew J Hirning, Krešimir Josić, and Matthew R Bennett. Emergent genetic oscillations in a synthetic microbial consortium. *Science*, 349(6251):986–989, 2015.

[103] Mehdi Sadeghpour, Alan Veliz-Cuba, Gábor Orosz, Krešimir Josić, and Matthew R. Bennett. Bistability and oscillations in co-repressive synthetic microbial consortia. *Quantitative Biology*, 5(1):55–66, mar 2017.

[104] Takayuki Sohka, Richard A Heins, Ryan M Phelan, Jennifer M Greisler, Craig A Townsend, and Marc Ostermeier. An externally tunable bacterial band-pass filter. *Proceedings of the National Academy of Sciences*, 106(25):10135–10140, 2009.

[105] Jesus Fernandez-Rodriguez, Felix Moser, Miryoung Song, and Christopher A Voigt. Engineering RGB color vision into Escherichia coli. *Nat Chem Biol*, 13(7):706–708, jul 2017.

[106] Chenli Liu, Xiongfei Fu, Lizhong Liu, Xiaojing Ren, Carlos KL Chau, Sihong Li, Lu Xiang, Hualing Zeng, Guanhua Chen, Lei-Han Tang, et al. Sequential establishment of stripe patterns in an expanding cell population. *Science*, 334(6053):238–241, 2011.

[107] Natalie S. Scholes and Mark Isalan. A three-step framework for programming pattern formation. *Current Opinion in Chemical Biology*, 40:1–7, oct 2017.

[108] Han-Sung Jung, Philippa H Francis-West, Randall B Widelitz, Ting-Xin Jiang, Sheree Ting-Berreth, Cheryll Tickle, Lewis Wolpert, and Cheng-Ming Chuong. Local Inhibitory Action of BMPs and Their Relationships with Activators in Feather Formation: Implications for Periodic Patterning. *Developmental Biology*, 196(1):11–23, apr 1998.

[109] Akiko Nakamasu, Go Takahashi, Akio Kanbe, and Shigeru Kondo. Interactions between zebrafish pigment cells responsible for the generation of Turing patterns. *Proceedings of the National Academy of Sciences of the United States of America*, 106(21):8429–34, may 2009.

[110] A.D. Economou, A. Ohazama, T. Pornaveetus, P.T. Sharpe, S. Kondo, M.A. Basson, A. Gritli-Linde, M.T. Cobourne, and J.B.A. Green. Periodic stripe formation by a Turing mechanism operating at growth zones in the mammalian palate. *Nature Genetics*, 44(3):348–351, 2012.

[111] Patrick Müller, Katherine W Rogers, Ben M Jordan, Joon S Lee, Drew Robson, Sharad Ramanathan, and Alexander F Schier. Differential diffusivity of nodal and lefty underlies a reaction-diffusion patterning system. *Science*, 336(6082):721–724, 2012.

[112] J. Raspopovic, L. Marcon, L. Russo, and J. Sharpe. Digit patterning is controlled by a Bmp-Sox9-Wnt Turing network modulated by morphogen gradients. *Science*, 345(6196):566–570, 2014.

[113] E.C. Pesci and B.H. Iglewski. The chain of command in Pseudomonas quorum sensing. *Trends Microbiol.*, 5(4):132–134, 1997.

[114] E.C. Pesci, J.P. Pearson, P.C. Seed, and B.H. Iglewski. Regulation of las and rhl quorum sensing in Pseudomonas aeruginosa. *J. Bacteriol.*, 179(10):3127–3132, 1997.

[115] J.P. Pearson, C. Van Delden, and B.H. Iglewski. Active efflux and diffusion are involved in transport of Pseudomonas aeruginosa cell-to-cell signals. *Journal of bacteriology*, 181(4):1203–1210, 1999.

[116] Matthew R Parsek and Tim Tolker-Nielsen. Pattern formation in pseudomonas aeruginosa biofilms. *Current opinion in microbiology*, 11(6):560–566, 2008.

[117] Xu Huang, Yuqing Dong, and Jindong Zhao. Hetr homodimer is a dna-binding protein required for heterocyst differentiation, and the dna-binding activity is inhibited by pats. *Proceedings of the National Academy of Sciences of the United States of America*, 101(14):4848–4853, 2004.

[118] David Sprinzak, Amit Lakhanpal, Lauren LeBon, Jordi Garcia-Ojalvo, and Michael B. Elowitz. Mutual Inactivation of Notch Receptors and Ligands Facilitates Developmental Patterning. *PLoS Computational Biology*, 7(6):e1002069, jun 2011.

[119] Allen Y Chen, Zhengtao Deng, Amanda N Billings, Urartu OS Seker, Michelle Y Lu, Robert J Citorik, Bijan Zakeri, and Timothy K Lu. Synthesis and patterning of tunable multiscale materials with engineered cells. *Nature materials*, 13(5):515–523, 2014.

[120] K. Brenner, D.K. Karig, R. Weiss, and F.H. Arnold. Engineered bidirectional communication mediates a consensus in a microbial biofilm consortium. *Proc. Natl. Acad. Sci. U.S.A.*, 104(44):17300, 2007.

[121] Jordan Ang, Edouard Harris, Brendan J Hussey, Richard Kil, and David R McMillen. Tuning Response Curves for Synthetic Biology. *ACS synthetic biology*, 2(10):547–567, sep 2013.

[122] George B. Cohen, Ruibao Ren, and David Baltimore. Modular binding domains in signal transduction proteins, 1995.

[123] Roby P. Bhattacharyya, Attila Reményi, Brian J. Yeh, and Wendell A. Lim. Domains, Motifs, and Scaffolds: The Role of Modular Interactions in the Evolution and Wiring of Cell Signaling Circuits. *Annual Review of Biochemistry*, 2006.

[124] James A. Davey and Corey J. Wilson. Deconstruction of complex protein signaling switches: a roadmap toward engineering higher-order gene regulators, 2017.

[125] Abigail J. Smith, Franziska Thomas, Deborah Shoemark, Derek N. Woolfson, and Nigel J. Savery. Guiding Biomolecular Interactions in Cells Using de Novo Protein-Protein Interfaces. *ACS Synthetic Biology*, 2019.

[126] Sarah Meinhardt, Michael W. Manley, Daniel J. Parente, and Liskin Swint-Kruse. Rheostats and toggle switches for modulating protein function. *PLoS ONE*, 2013.

[127] David L. Shis, Faiza Hussain, Sarah Meinhardt, Liskin Swint-Kruse, and Matthew R. Bennett. Modular, Multi-Input Transcriptional Logic Gating with Orthogonal LacI/GalR Family Chimeras. *ACS Synthetic Biology*, 2014.

[128] Ronald E. Rondon and Corey J. Wilson. Engineering a New Class of Anti-LacI Transcription Factors with Alternate DNA Recognition. *ACS Synthetic Biology*, 2019.

[129] Sebastian R. Schmidl, Felix Ekness, Katri Sofjan, Kristina N.M. Daeffler, Kathryn R. Brink, Brian P. Landry, Karl P. Gerhardt, Nikola Dyulgyarov, Ravi U. Sheth, and Jeffrey J. Tabor. Rewiring bacterial two-component systems by modular DNA-binding domain swapping. *Nature Chemical Biology*, 2019.

[130] Karsten Temme, Rena Hill, Thomas H. Segall-Shapiro, Felix Moser, and Christopher A. Voigt. Modular control of multiple pathways using engineered orthogonal T7 polymerases. *Nucleic Acids Research*, 2012.

[131] John E. Dueber, Brian J. Yeh, Kayam Chak, and Wendell A. Lim. Reprogramming control of an allosteric signaling switch through modular recombination. *Science*, 2003.

[132] Sarah Meinhardt, Michael W. Manley, Nicole A. Becker, Jacob A. Hessman, L. James Maher, and Liskin Swint-Kruse. Novel insights from hybrid LacI/GalR proteins: Family-wide functional attributes and biologically significant variation in transcription repression. *Nucleic Acids Research*, 2012.

[133] Kelly A. Schwarz, Nichole M. Daringer, Taylor B. Dolberg, and Joshua N. Leonard. Rewiring human cellular input-output using modular extracellular sensors. *Nature Chemical Biology*, 2017.

[134] Androulla N. Miliotou and Lefkothea C. Papadopoulou. CAR T-cell Therapy: A New Era in Cancer Immunotherapy. *Current Pharmaceutical Biotechnology*, 2018.

[135] Hollie J. Jackson, Sarwish Rafiq, and Renier J. Brentjens. Driving CAR T-cells forward, 2016.

[136] Fábio Madeira, Young mi Park, Joon Lee, Nicola Buso, Tamer Gur, Nandana Madhusoodanan, Prasad Basutkar, Adrian R N Tivey, Simon C Potter, Robert D Finn, and Rodrigo Lopez. The EMBL-EBI search and sequence analysis tools APIs in 2019. *Nucleic Acids Research*, 2019.

[137] M Whiteley and E P Greenberg. Promoter specificity elements in Pseudomonas aeruginosa quorum-sensing-controlled genes. *Journal of bacteriology*, 183(19):5529–34, oct 2001.

[138] Daniel Passos da Silva, Hitendra K. Patel, Juan F. González, Giulia Devescovi, Xianfa Meng, Sonia Covaceuszach, Doriano Lamba, Sujatha Subramoni, and Vittorio Venturi. Studies on synthetic LuxR solo hybrids. *Frontiers in Cellular and Infection Microbiology*, 2015.

[139] Carolyn A. Brotherton, Marnix H. Medema, and E. Peter Greenberg. luxR Homolog-Linked Biosynthetic Gene Clusters in Proteobacteria . *mSystems*, 2018.

[140] Ruchira Mukherji, Somak Chowdhury, and Pierre Stallforth. Chimeric luxr transcription factors rewire natural product regulation. *bioRxiv*, 2019.

[141] Wentao Kong, Venhar Celik, Chen Liao, Qiang Hua, and Ting Lu. Programming the group behaviors of bacterial communities with synthetic cellular communication. *Bioresources and Bioprocessing*, 1(1):24, nov 2014.

[142] Yohei Tashiro, Yuki Kimura, Maiko Furubayashi, Akira Tanaka, Kei Terakubo, Kyoichi Saito, Shigeko Kawai-Noma, and Daisuke Umeno. Directed evolution of the autoinducer selectivity of Vibrio fischeri LuxR. *The Journal of General and Applied Microbiology*, 2016.

[143] Carola Engler, Romy Kandzia, and Sylvestre Marillonnet. A one pot, one step, precision cloning method with high throughput capability. *PLoS ONE*, 2008.

[144] Ernst Weber, Carola Engler, Ramona Gruetzner, Stefan Werner, and Sylvestre Marillonnet. A modular cloning system for standardized assembly of multigene constructs. *PLoS ONE*, 2011.

[145] Cytoflow. https://github.com/bpteague/cytoflow.

[146] Jennifer A.N. Brophy and Christopher A. Voigt. Principles of genetic circuit design, 2014.

[147] Patrick M. Boyle and Pamela A. Silver. Harnessing nature's toolbox: Regulatory elements for synthetic biology, 2009.

[148] Alec A.K. Nielsen, Bryan S. Der, Jonghyeon Shin, Prashant Vaidyanathan, Vanya Paralanov, Elizabeth A. Strychalski, David Ross, Douglas Densmore, and Christopher A. Voigt. Genetic circuit design automation. *Science*, 2016.

[149] Timothy D. Minogue, Markus Wehland-Von Trebra, Frank Bernhard, and Susanne B. Von Bodman. The autoregulatory role of EsaR, a quorum-sensing regulator in Pantoea stewartii ssp. stewartii: Evidence for a repressor function. *Molecular Microbiology*, 2002.

[150] Jasmine Shong and Cynthia H. Collins. Engineering the esaR promoter for tunable quorum sensing-dependent gene expression. *ACS Synthetic Biology*, 2013.

[151] Deepak Mishra, Phillip M. Rivera, Allen Lin, Domitilla Del Vecchio, and Ron Weiss. A load driver device for engineering modularity in biological networks. *Nature Biotechnology*, 2014.

[152] Hsin Ho Huang, Yili Qian, and Domitilla Del Vecchio. A quasi-integral controller for adaptation of genetic modules to variable ribosome demand. *Nature Communications*, 2018.

[153] Tom Defoirdt, Gilles Brackman, and Tom Coenye. Quorum sensing inhibitors: how strong is the evidence? *Trends in Microbiology*, 21(12):619–624, 2013.

[154] Susanne Fetzner. Quorum quenching enzymes. *Journal of Biotechnology*, 2014.

[155] Tom Defoirdt. Quorum-Sensing Systems as Targets for Antivirulence Therapy, 2018.

[156] Walter Fast and Peter A. Tipton. The enzymes of bacterial census and censorship. *Trends in Biochemical Sciences*, 37(1):7–14, 2012.

[157] S R Khan, S Su, and S K Farrand. Degradation of acyl-HSLs by AttM lactonase and its role in controlling the conjugative transfer of Ti-plasmids in Agrobacterium tumefaciens. *Plasmid*, 2007.

[158] Bartłomiej Borek, Jeff Hasty, and Lev Tsimring. Turing Patterning Using Gene Circuits with Gas-Induced Degradation of Quorum Sensing Molecules. *PloS one*, 2016.

[159] Hidetada Hirakawa and Haruyoshi Tomita. Interference of bacterial cell-to-cell communication: A new concept of antimicrobial chemotherapy breaks antibiotic resistance, 2013.

[160] Kyle L. Asfahl and Martin Schuster. Social interactions in bacterial cell-cell signaling, 2017.

[161] Kyle L. Asfahl and Martin Schuster. Additive effects of quorum sensing anti-activators on Pseudomonas aeruginosa virulence traits and transcriptome. *Frontiers in Microbiology*, 2018.

[162] Jasmine Lee and Lianhui Zhang. The hierarchy quorum sensing network in Pseudomonas aeruginosa. *Protein and Cell*, 2014.

[163] Mario J Lintz, Ken-ichi Oinuma, Christina L Wysoczynski, Everett Peter Greenberg, and Mair E A Churchill. Crystal structure of QscR, a Pseudomonas aeruginosa quorum sensing signal receptor. *Proceedings of the National Academy of Sciences of the United States of America*, 108(38):15763–8, sep 2011.

[164] Sujatha Subramoni and Vittorio Venturi. LuxR-family 'solos': Bachelor sensors/regulators of signalling molecules, 2009.

[165] Sanjarbek Hudaiberdiev, Kumari S. Choudhary, Roberto Vera Alvarez, Zsolt Gelencsér, Balázs Ligeti, Doriano Lamba, and Sándor Pongor. Census of solo LuxR genes in prokaryotic genomes. *Frontiers in Cellular and Infection Microbiology*, 2015.

[166] Fengming Ding, Ken-Ichi Oinuma, Nicole E Smalley, Amy L Schaefer, Omar Hamwy, E Peter Greenberg, and Ajai A Dandekar. The Pseudomonas aeruginosa Orphan Quorum Sensing Signal Receptor QscR Regulates Global Quorum Sensing Gene Expression by Activating a Single Linked Operon. *mBio*, 9(4), sep 2018.

[167] H. Fan, Y. Dong, D. Wu, M. W. Bowler, L. Zhang, and H. Song. QsIA disrupts LasR dimerization in antiactivation of bacterial quorum sensing. *Proceedings of the National Academy of Sciences*, 2013.

[168] Qihui Seet and Lian Hui Zhang. Anti-activator QslA defines the quorum sensing threshold and response in Pseudomonas aeruginosa. *Molecular Microbiology*, 2011.

[169] Richard Siehnel, Beth Traxler, Ding Ding An, Matthew R. Parsek, Amy L. Schaefer, and Pradeep K. Singh. A unique regulator controls the activation threshold of quorum-regulated genes in Pseudomonas aeruginosa. *Proceedings of the National Academy of Sciences*, 2010.

[170] Haihua Liang, Jiali Duan, Christopher D. Sibley, Michael G. Surette, and Kangmin Duan. Identification of mutants with altered phenazine production in Pseudomonas aeruginosa. *Journal of Medical Microbiology*, 2011.

[171] Julien Lang and Denis Faure. Functions and regulation of quorum-sensing in Agrobacterium tumefaciens. *Frontiers in Plant Science*, 2014.

[172] C. Fuqua, M. Burbea, and S. C. Winans. Activity of the Agrobacterium Ti plasmid conjugal transfer regulator TraR is inhibited by the product of the traM gene. *Journal of Bacteriology*, 1995.

[173] Zhao Qing Luo, Yinping Qin, and Stephen K. Farrand. The antiactivator TraM interferes with the autoinducer-dependent binding of TraR to DNA by interacting with the C-terminal region of the quorum- sensing activator. *Journal of Biological Chemistry*, 2000.

[174] Yinping Qin, Audra J. Smyth, Shengchang Su, and Stephen K. Farrand. Dimerization properties of TraM, the antiactivator that modulates TraR-mediated quorum-dependent expression of the Ti plasmid tra genes. *Molecular Microbiology*, 2004.

[175] Alessandro Vannini, Cinzia Volpari, and Stefania Di Marco. Crystal structure of the quorum-sensing protein TraM and its interaction with the transcriptional regulator TraR. *Journal of Biological Chemistry*, 2004.

[176] Yinping Qin, Shengchang Su, and Stephen K. Farrand. Molecular basis of transcriptional antiactivation: TraM disrupts the TraR-DNA complex through stepwise interactions. *Journal of Biological Chemistry*, 2007.

[177] Guozhou Chen, Chao Wang, Clay Fuqua, Lian Hui Zhang, and Lingling Chen. Crystal structure and mechanism of TraM2, a second quorum-sensing antiactivator of agrobacterium tumefaciens strain A6. *Journal of Bacteriology*, 2006.

[178] Philippe Oger, Kun Soo Kim, Rebecca L. Sackett, Kevin R. Piper, and Stephen K. Farrand. Octopine-type Ti plasmids code for a mannopine-inducible dominant-negative allele of traR, the quorum-sensing activator that regulates Ti plasmid conjugal transfer. *Molecular Microbiology*, 1998.

[179] Y. Chai, J. Zhu, and S. C. Winans. TrlR, a defective TraR-like protein of Agrobacterium tumefaciens, blocks TrafR function in vitro by forming inactive TrlR:TraR dimers. *Molecular Microbiology*, 2001.

[180] A R Asthagiri and D A Lauffenburger. Bioengineering models of cell signaling. *Annual review of biomedical engineering*, 2:31–53, jan 2000.

[181] R. Milo, S. Shen-Orr, S. Itzkovitz, N. Kashtan, D. Chklovskii, and U. Alon. Network motifs: Simple building blocks of complex networks. *Science*, 2002.

[182] Shai S. Shen-Orr, Ron Milo, Shmoolik Mangan, and Uri Alon. Network motifs in the transcriptional regulation network of Escherichia coli. *Nature Genetics*, 2002.

[183] Christian Cuba Samaniego and Elisa Franco. An ultrasensitive biomolecular network for robust feedback control. *IFAC-PapersOnLine*, 2017.

[184] Christian Cuba Samaniego and Elisa Franco. An ultrasensitive motif for robust closed loop control of biomolecular systems. In *2017 IEEE 56th Annual Conference on Decision and Control, CDC 2017*, 2018.

[185] Attila Becskei and Luis Serrano. Engineering stability in gene networks by autoregulation. *Nature*, 2000.

[186] D. W. Austin, M. S. Allen, J. M. McCollum, R. D. Dar, J. R. Wilgus, G. S. Sayler, N. F. Samatova, C. D. Cox, and M. L. Simpson. Gene network shaping of inherent noise spectra. *Nature*, 2006.

[187] Vahid Mardanlou, Christian Cuba Samaniego, and Elisa Franco. A bistable biomolecular network based on monomeric inhibition reactions. In *Proceedings of the IEEE Conference on Decision and Control*, 2015.

[188] Brian Teague Ron Weiss John Sexton Sebastian M. Castillo-Hair Jeff J. Tabor Jacob Beal, Nicholas DeLateur. Toward quantitative comparison of fluorescent protein in expression levels via fluorescent beads. *2017 8th International Workshop on Bio-Design Automation.*

[189] Jacob Beal, Traci Haddock-Angelli, Natalie Farny, and Randy Rettberg. Time to Get Serious about Measurement in Synthetic Biology. *Trends in Biotechnology*, 36(9):869–871, sep 2018.

[190] Leonore A. Herzenberg, James Tung, Wayne A. Moore, Leonard A. Herzenberg, and David R. Parks. Interpreting flow cytometry data: A guide for the perplexed. 2006.

[191] Jacob Beal, Cassandra Overney, Aaron Adler, Fusun Yaman, Lisa Tiberio, and Meher Samineni. TASBE Flow Analytics: A Package for Calibrated Flow Cytometry Analysis. *ACS Synthetic Biology*, 2019.

[192] Lili Wang, Paul DeRose, and Adolfas K. Gaigalas. Assignment of the Number of Equivalent Reference Fluorophores to Dyed Microspheres. *Journal of Research of the National Institute of Standards and Technology*, 2016.

[193] Lili Wang and Adolfas K. Gaigalas. Development of Multicolor Flow Cytometry Calibration Standards: Assignment of Equivalent Reference Fluorophores (ERF) Unit. *Journal of Research of the National Institute of Standards and Technology*, 2011.

[194] Sebastian M. Castillo-Hair, John T. Sexton, Brian P. Landry, Evan J. Olson, Oleg A. Igoshin, and Jeffrey J. Tabor. FlowCal: A User-Friendly, Open Source Software Tool for Automatically Converting Flow Cytometry Data from Arbitrary to Calibrated Units. *ACS Synthetic Biology*, 2016.